
Contents

2 Rapid X-Ray Variability	<i>page</i>
2.1 Introduction	1
2.2 Timing	3
2.3 Spectroscopy	5
2.4 Source types	7
2.5 Source states	10
2.6 Variability components	18
2.7 Frequency correlations	22
2.8 Orbital and epicyclic frequency models	27
2.9 Low magnetic-field neutron stars	38
2.10 Black holes	49
2.11 High-magnetic-field neutron stars	56
2.12 Flow-instability and non-flow models	56
2.13 Final remarks	61
References	62

2

Rapid X-Ray Variability

M. VAN DER KLIS

*Astronomical Institute “Anton Pannekoek”, University of Amsterdam,
Kruislaan 403, 1098 SJ Amsterdam*

2.1 Introduction

One of the principal motivations for studying X-ray binaries is the unique window that accretion onto neutron stars and black holes provides on the physics of strong gravity and dense matter. Our best theory of gravity, general relativity, while tested, and confirmed, with exquisite precision in weak fields ($GM/R \ll c^2$; e.g., Taylor et al. 1992) has not yet been tested by direct observation of the motion of particles in the strong gravitational field near compact objects, where the gravitational binding energy is of order the rest mass. Among the extreme predictions relativity makes for these regions are the existence of event horizons, i.e., black holes (§2.4.1), the existence of an inner radius within which no stable orbits exist, strong dragging of inertial frames, and general-relativistic precession at rates similar to the orbital motion itself, $\sim 10^{16}$ times as fast as that of Mercury.

In a neutron star the density exceeds that in an atomic nucleus. Which elementary particles occur there, and what their collective properties are, is not known well enough to predict the equation of state (EOS), or compressibility, of the matter there, and hence the mass-radius (M - R) relation of neutron stars is uncertain. Consequently, by measuring this relation, the EOS of supra-nuclear density matter is constrained. As orbital motion around a neutron star constrains both M and R (§2.8.1), measurements of such motion bear on the fundamental properties of matter. Likewise, such motion near black holes constrains the size and spin of black holes of given mass.

For addressing these issues of strong gravity and dense matter, we need to study motion under the influence of gravity within a few Schwarzschild radii¹ of compact objects and map out the strongly curved spacetime there. As the characteristic velocities near the compact object are of order $(GM/R)^{1/2} \sim 0.5c$, the dynamical time scale $(r^3/GM)^{1/2}$ for the motion through this region is short; ~ 0.1 ms at ~ 15 km, and ~ 2 ms at 10^2 km from a $1.4 M_\odot$ neutron star, and ~ 1 ms at $3R_{Schw}$ ($\sim 10^2$ km) from a $10 M_\odot$ black hole. These millisecond dynamical time scales, the shortest associated with any astrophysical object, form one of the most basic expressions of the compactness of compact objects.

The accretion flow is expected to be turbulent and may show magnetic structures. Its emission will vary in time due to the motions of inhomogeneities through, and

¹ The radius of a zero angular-momentum black hole, $R_{Schw} = 2r_g = 2GM/c^2 \approx 3$ km M/M_\odot .

2 Rapid X-Ray Variability

with, the flow. This variability can be used to probe the accretion-flow dynamics. For a 10-km object, 90% of the gravitational energy is released in the inner $\sim 10^2$ km, hence the bulk of the emission likely comes from within the strong-field region from where we expect the millisecond variability. Temperatures here are $\gtrsim 10^7$ K, so most of this emission is in X-rays.

The transfer of matter towards the compact object usually occurs by way of an accretion disk in which the matter moves in near-Keplerian orbits (Ch. 13.2). However, the geometry of the innermost part of the flow is uncertain. In many models the Keplerian disk extends down to well into the strong-field region. It is terminated at an inner radius r_{in} of a few R_{Schw} by for example relativistic effects, radiation drag, a weak magnetic field (or the neutron-star surface). Advective, or in the case of strongly magnetic neutron stars, magnetically dominated flows feature larger ($\sim 10^2 R_{Schw}$) inner disk radii. Within r_{in} the flow is no longer Keplerian, and may or may not be disk-like. Both inside and outside r_{in} matter may leave the disk plane and either flow in more radially, or be expelled. Together these flows constitute what is called the “accretion flow” in this chapter.

The radiation from the Keplerian disk and from a neutron-star surface are expected to be basically thermal, and observations indeed show such thermal X-rays. In addition there is ubiquitous evidence for non-thermal spectral components which may originate in one of the non-disk flows and/or in an energetic ‘corona’ of uncertain geometry (§2.5.1) associated with the disk.

Observations of X-ray binaries show considerable variability on a wide range of time scales in all wavelengths, and down to less than a millisecond in X-rays. The study of this variability is called ‘timing’. In this chapter we focus on aperiodic phenomena (QPOs and noise, §2.2) that are potential probes of the strong-gravity dominated flow dynamics, i.e., millisecond aperiodic phenomena in weakly magnetic compact objects, with particular attention to the potential for measuring fundamental properties of spacetime and matter. As observationally there are correlated spectral and timing phenomena covering a range of time scales, we look at longer time-scale phenomena and relations with X-ray spectral properties as well.

That millisecond variability will naturally occur in the process of accretion of matter onto a stellar-mass compact object is an insight that dates back to at least Shvartsman (1971). Sunyaev (1973) noted that clumps orbiting in an accretion disk closely around a black hole could cause quasi-periodic variability on time scales of about a millisecond. Twenty-five years after these early predictions, millisecond variability was finally discovered, with NASA’s breakthrough Rossi X-Ray Timing Explorer (RXTE; Bradt et al. 1993, see §2.9.1, §3.4, §2.10.1, §1). To this day, RXTE is providing a veritable flood of timing information that is still only partially digested. Hence, contrary to the situation ten years ago it is no longer possible to be exhaustive when reviewing X-ray binary timing (see, e.g., Lewin et al. 1988, Stella 1988, Hasinger 1988, Miyamoto 1994, van der Klis 1986, 1989a, 1995a,b, 2000 for preceding timing reviews). In this chapter §§2.2–2.7 provide a broad overview of the phenomenology. We look for common traits in the phenomena of different classes of objects indicating common physics. In §§2.8 and 2.12 we examine the ideas that have been put forward to explain the phenomena by, respectively, orbital motions and accretion-flow instabilities. Sections 2.9 and 2.10 give more detail on

individual objects and phenomena, with §§2.9.1 and 2.10.1 dealing with the most rapid (millisecond) phenomena and the remaining sections summarizing the work on slower variability.

2.2 Timing

The rapid variations diagnosing the inner accretion flow are stochastic, and most effectively dealt with using statistical (random-process) techniques. Fourier analysis is the dominant tool, and the one we focus on here. Some other techniques are mentioned as well.

Fourier analysis. The Fourier power spectrum of the X-ray flux time series provides an estimate of the variance as a function of Fourier frequency ν in terms of the *power density* $P_\nu(\nu)$ (van der Klis 1989b for details). The usual range of ν is mHz to kHz; slower variations are usually studied in the time-domain (but see Reig et al. 2002, 2003a), as on longer time scales source-state changes and data gaps cause trouble for Fourier techniques. Variations faster than those in the kHz range have not (yet) been detected.

A number of *variability components* or *power-spectral components* together make up the power spectrum (see, e.g., Fig. 2.8). An aperiodic component by definition covers several, usually many, frequency resolution elements. Broad structures are called *noise* and narrow features *quasi-periodic oscillations* (QPOs); ‘broad-band noise’ and ‘QPO peaks’ are common terms. Least-squares fitting techniques are used to measure these components. When a series of power spectra is calculated from consecutive chunks of data, usually the components change: they move through the power spectrum (change frequency from one power spectrum to the next), vary in width and strength, etc., but they remain identifiable as the changes are gradual. This is the empirical basis for the concept of a power-spectral component. The shortest time scale on which changes can typically be followed is seconds to minutes.

The signal in the time series is not completely specified by the power spectrum (and the signals are usually too weak to recover the Fourier phases). The same QPO peak could be due to, e.g., a damped harmonic oscillator, randomly occurring short wave trains, a frequency-modulated oscillation, an autoregressive signal, white noise observed through a narrow passband filter or even a closely spaced set of periodic signals. *Time lags* (delays) between signals simultaneously detected in different energy bands can be measured using the cross-correlation function (CCF; Brinkman et al. 1974, Weisskopf et al. 1975), but if the lags at different time scales differ, the *cross-spectrum* (van der Klis et al. 1987c, Miyamoto et al. 1988, Vaughan et al. 1994, Nowak et al. 1999a) performs better. This is the Fourier transform of the CCF and in a sense its frequency-domain equivalent. It measures a *phase lag* (time lag multiplied by frequency) at each frequency. The term *hard lag* means that higher energy photons lag lower energy ones, and vv. for *soft lag*. *Cross-coherence*² is a measure for the correlation between the signals (Vaughan & Nowak 1997).

Power-law noise is noise that (in the frequency range considered) follows a power law $P_\nu \propto \nu^{-\alpha}$. The power-law index (also ‘slope’) α is typically between 0 and 2; for

² Often just called ‘coherence’, a term that is also used for the sharpness of a QPO peak, below.

4 Rapid X-Ray Variability

$|\alpha| > 2$ Fourier analysis suffers from power leakage, so measurements of noise steeper than that are suspect (e.g., Bracewell 1986, Deeter 1984). '1/f noise' has $\alpha = 1$, and *white noise* is constant ($\alpha = 0$). *Red noise* is a term variously used for either $\alpha = 2$ power-law noise or any kind of noise whose P_ν decreases with ν .

Band-limited noise (BLN) is defined here as noise that steepens towards higher frequency (i.e., its local power-law slope $-d \log P_\nu / d \log \nu$ increases with ν) either abruptly (showing a "break" at *break frequency* ν_{break}) or gradually. BLN whose power density below a certain frequency is approximately constant (white) is called *flat-topped noise*. The term *peaked noise* is used for noise whose P_ν has a local maximum at $\nu > 0$). Various modified power laws (broken, cut-off) as well as broad Lorentzians are used to describe BLN. The precise value of the characteristic frequency associated with the steepening (e.g., ν_{break}) differs by factors of order unity depending on the description chosen (e.g., Belloni et al. 2002a).

A *quasi-periodic oscillation* (QPO) is a finite-width peak in the power spectrum. It can usually be described with a Lorentzian $P_\nu \propto \lambda / [(\nu - \nu_0)^2 + (\lambda/2)^2]$ with *centroid frequency* ν_0 and full width at half maximum (FWHM) λ . This is the power spectrum of an exponentially damped sinusoid $x(t) \propto e^{-t/\tau} \cos(2\pi\nu_0 t)$, but the underlying signal may well be different from this. λ is related to the *coherence time* $\tau = 1/\pi\lambda$ of the signal, and is often reported in terms of the *quality factor* $Q \equiv \nu_0/\lambda$, a measure for the *coherence* of the QPO. Conventionally, signals with $Q > 2$ are called QPOs and those with $Q < 2$ peaked noise. A *sharp* QPO peak is one with high Q .

The strength (variance) of a signal is proportional to the integrated power $P = \int P_\nu d\nu$ of its contribution to the power spectrum, and is usually reported in terms of its *fractional root-mean-squared (rms) amplitude* $r \propto P^{1/2}$, which is a measure for signal amplitude as a fraction of the total source flux. It is often expressed in percent, as in "2% (rms)".

The signal-to-noise of a weak QPO or noise component is $n_\sigma = \frac{1}{2} I_x r^2 (T/\lambda)^{1/2}$ (van der Klis 1989b, see van der Klis 1998 for more details), where I_x is the count rate and T the observing time (assumed $\gg 1/\lambda$). As n_σ is proportional to signal amplitude *squared*, if a clear power-spectral feature "suddenly disappears" it may have only decreased in amplitude by a factor of two (and gone from, say, 6 to 1.5σ).

Red and flat-topped BLN may have only one characteristic frequency (e.g., ν_{break}), but peaked noise and a QPO have two (ν_0 and λ). This leads to difficulties in describing the phenomenology when, over time, power-spectral components change in Q between noise and QPO. For this reason, defining the characteristic frequency as ν_{max} , the frequency at which power-density times frequency (νP_ν , equivalent to νS_ν in spectroscopy) reaches its maximum, has gained some popularity (Belloni et al. 2002a). This method is equally applicable to centroids of narrow peaks and breaks in broad-band noise, and smoothly deals with intermediate cases (see §2.8.6 for an interpretation). For a Lorentzian, $\nu_{max} = \sqrt{\nu_0^2 + \Delta^2}$, where $\Delta \equiv \lambda/2$, so a narrow QPO peak has $\nu_{max} \approx \nu_0$ and a BLN component described by a zero-centered Lorentzian $\nu_{max} = \Delta$.

Power spectra are in practice presented in a variety of ways, each more suitable to emphasize particular aspects (displaying either P_ν or νP_ν , linearly or logarithmically, subtracting the white Poisson background noise or not; e.g., Figs. 2.6 and 2.8).

Time-series modeling. Time-series modeling goes beyond Fourier analysis in an attempt to obtain more detailed information about what is going on in the time domain. One approach is to invent, based on physical hunches, synthetic time series that reproduce observed statistical properties of the variability. Shot noise and chaos (below) are common hunches. Another approach is to refine statistical analysis beyond Fourier analysis. Here, systematic approaches involving higher order statistics, such as skewness and bi-spectra (e.g., Priedhorsky et al. 1979, Elsner et al. 1988, Maccarone & Coppi 2002b) as well as more heuristic ones (e.g., shot alignment, below) have been tried. 'Variation functions' measuring variance as a function of time scale τ (e.g., Ogawara et al. 1977, Maejima et al. 1984, Li & Muraki 2002) do not contain additional information as is sometimes claimed; they basically provide power integrated over frequencies $< 1/\tau$. The calculation of Fourier power spectra on short time scales is a useful technique that has produced interesting results (e.g., Norris et al. 1990, Yu et al. 2001, Yu & van der Klis 2002, Uttley & McHardy 2001).

Shot noise is a time-series model of randomly occurring identical discrete finite events called shots (Terrell 1972, Weisskopf et al. 1975, Sutherland et al. 1978, Priedhorsky et al. 1979, Lochner et al. 1991). The power spectrum is that of an individual shot. Mathematically, the power spectrum of a random process can always be modeled in this way (Doi 1978), so for modeling power spectra the method has little predictive power, but it can be physically motivated in various settings (§2.12.3). Heuristic 'shot alignment' techniques (Negoro et al. 1994, 1995, 2001, Feng et al. 1999), like any 'fishing in the noise' technique must be applied with care: they can be misleading if the underlying assumption (i.e., shot noise) is incorrect. Various modifications of pure shot noise have been explored, e.g., involving distributions of different shot profiles. As pointed out by Vikhlinin et al. (1994), if the shot occurrence times are correlated (e.g., a shot is less likely to occur within a certain interval of time after the previous shot, certainly plausible in, e.g., magnetic flare scenarios; §2.12.3), then peaked noise or a QPO is produced whose Q increases as the correlation between the shot times increases. Oscillating shots, short wave trains with positive integrated flux, produce a QPO (due to the oscillation) and BLN (due to the shot envelope) in the power spectrum (Lamb et al. 1985, Alpar 1986, Shibasaki & Lamb 1987, Elsner et al. 1987, Shibasaki et al. 1987, 1988, Elsner et al. 1988), and fit well within models involving short-lived orbiting clumps (§2.8.2).

Given our limited a priori knowledge of the physical processes producing the rapid variability, mostly mathematically-motivated time-series models such as autoregressive, linear phase-state and chaos models (e.g., Lochner et al. 1989, Unno et al. 1990, Scargle et al. 1993, Pottschmidt et al. 1998, Timmer et al. 2000) usually do not sufficiently constrain the physics to conclude much from them (but see §2.12.3).

2.3 Spectroscopy

Recent work with Chandra and XMM-Newton suggests that, as previously suspected (e.g., Barr et al. 1985, White et al. 1985), relativistically broadened Fe lines near 6.5 keV similar to those inferred in AGNs (e.g., Fabian et al. 2000) occur in some neutron-star and black-hole binaries as well (e.g., Miller et al. 2002, Parmar et al. 2002; §4.2.3). The gravitational and Doppler distortions of these lines diagnose the dynamics of the same strong-field region as millisecond timing (e.g., Reynolds &

6 Rapid X-Ray Variability

Nowak 2003). Combining timing with such spectroscopic diagnostics can enormously improve the grip we have on what is going on in the inner disk, but such work is still in a very early stage, and here we concentrate on the better-explored link between timing and *broad-band spectroscopy*.

Variations in broad-band ($\Delta E/E > 0.1$, usually continuum-dominated) X-ray spectral shape usually just become detectable on the same seconds to minutes time scales on which power-spectral changes are detectable (§2.2). Two different techniques of broad-band spectroscopy are used to diagnose these changes: multi-band photometry and spectral fitting. The spectral band used varies somewhat but is usually in the 1–60 keV range and nearly always covers at least the 3–8 keV band.

Photometric method One approach to quantifying broad-band X-ray spectral shape uses *X-ray colors*. An X-ray color is a 'hardness' ratio between the photon counts in two broad bands; it is a rough measure for spectral slope. By calculating two X-ray colors (a *hard color* in a higher energy band and a *soft color* in a lower band) as a function of time, a record is obtained of the broad-band X-ray spectral variations that is well-matched to the power-spectral variations. Plotted vs. one another in a *color-color diagram* (CD), one can observe the source to move through the diagram and, nearly always, create a pattern. It is then possible to study the relation between timing and location in the CD. A *hardness-intensity diagram* (HID) or color-intensity diagram is a similar diagram with a color vs. 'intensity'; *X-ray intensity* in this context is nothing but a count rate in some broad X-ray spectral band. Figs. 2.4 and 2.5 provide examples of CD and HID patterns. Whether CD or HID presents the 'cleanest' pattern depends on source, and on the quality of the data. There are distinct advantages to working with the logarithm of colors and intensities, like magnitudes in the optical, but this is not general practice.

For distinguishing between source states (§2.5) the photometric method combined with timing performs well, and the method provides excellent sensitivity to subtle spectral variations. However, this is at the expense of detector dependence. All X-ray detectors are different and change over time, and contrary to optical photometry, in X-rays there is only one bright standard star (Crab). For the low spectral resolution detectors typically used for timing (proportional counters) it is not possible to completely correct X-ray colors for the detector response: In the absence of *a priori* knowledge of the intrinsic spectral shape all correction methods intended to derive 'intrinsic' colors (scaling by Crab colors, unfolding through the detector response matrix either directly or by fitting an arbitrary model) are mathematically imperfect (Kahn & Blisset 1980, Kuulkers et al. 1994, Kuulkers 1995, Done & Gierliński 2003).

Spectral fitting method There are considerable interpretative advantages in describing the X-ray spectral variations instead in terms of physical models fitted to the observed spectra. The drawback is that this involves a description of spectral shape in terms of more numbers (the spectral parameters) than just two X-ray colors, and that the correct models are unknown. This, plus the tendency towards spurious results related to statistical fit-parameter correlations masking true source variations, usually means that to obtain sensible results, fitting requires longer integration times than the time scale on which we see the power spectra, and the X-ray colors, change, and that measured parameter-value changes obtained are hard to in-

terpret. Nevertheless, for sufficiently long integration times, and particularly in the case of the black-hole candidates, where the X-ray spectral variations are clearer than in neutron stars, this approach has met with some success. Because both methods have limitations, in practice the interpretation of X-ray spectral variations tends to occur in a back-and-forth between CD/HIDs and spectral fitting. Techniques such as plotting the predicted colors of model spectra in CDs together with the data, fitting spectra obtained by averaging data collected at different epochs but in the same part of the CD, and approximate intrinsic colors (e.g., Belloni et al. 2000, Done & Gierliński 2003), are all being employed to make the link between the two methods.

Presentation and parametrization of CD/HIDs There is unfortunately no uniformity in either the presentation or the choice of X-ray spectral bands for CD/HIDs. In particular, there is a tendency to present the black-hole diagrams transposed as compared to the neutron-star ones. As illustrated by Jonker et al. (2002a) these differences can obscure some of the similarities between neutron-star and black-hole X-ray spectral behavior.

For sources which trace out one-dimensional *tracks* in the CD/HIDs along which a source moves smoothly, position in the track, in a single datum, summarizes its spectral state. Curve length along the track (Hertz et al. 1992, Kuulkers et al. 1994) is conventionally indicated with a symbol S (S_z , S_a ; see §2.5.2). S is defined relative to the track: if the track drifts, the colors of a point with given S_x drift along with it. The patterns observed in a CD are often also recognizable in the corresponding HID obtained by replacing soft color by intensity. Presumably this is the case because intensity is dominated by the more numerous photons in the lower bands, whose dominant thermal component(s) strongly correlate to temperature and hence, color.

2.4 Source types

Different sources exhibit similar patterns of timing and spectral properties, allowing to group them into a number of *source types*. Both spectroscopy and timing, preferably in several source states (§2.5), are necessary to reliably identify source type. The primary distinction is not between neutron stars and black holes (§2.4.1) but between high and low magnetic-field strengths. Black holes and low magnetic-field ($\lesssim 10^{10}$ G) neutron stars potentially have gravity-dominated flows down to the strong-field region (although radiative stresses can also be important, §2.8.5). It is these objects, mostly found in low-mass X-ray binaries (LMXBs, §1), that we shall be mostly concerned with. Strongly magnetic ($\gtrsim 10^{12}$ G) neutron stars are briefly discussed in §2.11.

2.4.1 *Neutron stars vs. black holes*

A neutron star is only a few times larger than its Schwarzschild radius, so accretion onto black holes and neutron stars is expected to show similarities. Indeed, based on just the inner-flow diagnostics (timing and spectrum), the distinction between neutron stars and black holes is notoriously difficult to make, with some examples of black-hole candidates turned neutron stars (e.g., Cir X-1, Jones et al. 1974, Tennant et al. 1986; V0332+53, Tanaka et al. 1983, Stella et al. 1985; GS 1826–238, Tanaka 1989, Ubertini et al. 1999; 4U0142+61, White & Marshall 1984, Israel et al.

1994), and in practice it is not easy to prove a compact object is a black hole. There are two levels of proof: (i) showing that, assuming general relativity, the compact object must be a black hole, and (ii) showing that such an object indeed has the properties general relativity predicts for a black hole. For (i) it is sufficient to prove that a mass is concentrated within its Schwarzschild radius; currently, this mostly relies on dynamical mass estimates combined with theoretical arguments about the maximum mass of a neutron star (e.g., Srinivasan 2002, §1.3.8) and not on direct, empirical measurements of radius. For (ii) it is necessary to observe the interaction of the compact object with its surroundings, empirically map out its exterior space-time, and demonstrate properties such as extreme frame dragging, the existence of an innermost stable orbit, and an event horizon.

In recent work, for well-studied sources, clear differences are discerned between the patterns of correlated spectral and timing behaviour (§2.5) of neutron stars and black holes which agree with distinctions based on X-ray bursts, pulsations, and dynamical mass estimates. In particular the most rapid variability (see §2.6.1), presumably that produced closest to the compact object and most affected by its properties, is clearly quite different between neutron stars and black-hole candidates. Evidently we are learning to distinguish between black holes and neutron stars based on the properties of the flow in the strong-field gravity region, so there is progress towards the goal of testing general relativity. On the other hand, remarkable spectral and timing similarities exist between certified neutron stars and black-hole candidates, particularly in low luminosity states (§2.6.2). To demonstrate the existence of black holes in the sense of general relativity based on an understanding of the accretion phenomena near them is a goal that has not yet been reached. The study of rapid X-ray variability of low-magnetic field compact objects in X-ray binaries is one of the programs contributing towards this end. Both the actual measurement of compact-object radius, which is part of a level (i) proof, as well as level (ii) proofs are addressed by the research described in this chapter: timing to diagnose motion very near compact objects. I shall use the term *black hole* both for objects whose black-hole candidacy is based on a measured mass as well as for those whose patterns of timing and spectral behavior put them into the same phenomenological category as these objects.

2.4.2 *Low magnetic-field object types*

The low magnetic-field neutron-star systems are subdivided into Z sources, atoll sources (Hasinger & van der Klis 1989) and what I shall call the 'weak LMXBs'. These three main sub-types are closely related (see also §2.5.2). *Z sources* are the most luminous (Fig. 2.1), and accrete at an appreciable fraction of the Eddington critical rate (perhaps 0.5–1 L_{Edd}). *Atoll sources*, many of which are X-ray burst sources, cover a much wider range in luminosities, from perhaps 0.001 L_{Edd} (much lower in transients, but below this level timing becomes difficult) all the way up to the range of the Z sources (e.g., Ford et al. 2000; L_x overlaps may well occur; distances are uncertain). Ordinary atoll sources are usually in the 0.01–0.2 L_{Edd} range, while the 'GX' atoll sources in the galactic bulge (see §2.5.2) usually hover at the upper end (perhaps 0.2–0.5 L_{Edd}), and the *weak LMXBs* (see §2.5.2) at the lower end ($<0.01 L_{Edd}$) of that range. Weak LMXBs comprise the overlapping ³

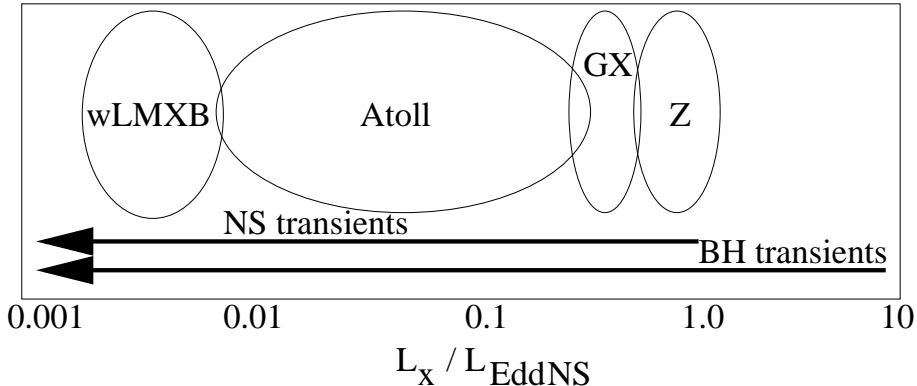


Fig. 2.1. Luminosities attained by Z sources, GX atoll sources, ordinary atoll sources and weak LMXBs, respectively, as well as by neutron-star and black-hole transients. The extent of the L_x overlaps between these source types is undecided in detail, but those shown here are likely.

groups of faint burst sources, millisecond pulsars and low-luminosity transients (§6); many of them appear to be just atoll sources stuck at low L_x . Some faint LMXBs have luminosities that are not well known due to uncertain distances or emission anisotropies (e.g., in dippers, §1), but many of these are probably weak as well.

While nearly all LMXBs whose X-ray emission is persistent contain a neutron star, nearly all with a black hole (and many with a neutron star as well) are transients, showing intermittent activity intervals called outbursts usually lasting weeks to months and separated by long quiescent intervals. The black holes have no well-defined subdivisions; although one might expect differences in spin (and hence, frame dragging, §2.8.1), accretion mode (wind or Roche-lobe overflow, §1) or between transient and persistent systems to show up, none of these lead to obvious differences in the observable properties attributable to the inner flow. Some black-hole transients remain in the low hard state (§2.5) during their entire outburst (e.g., Nowak 1995, Brocksopp 2004), but this can vary from one outburst to another (e.g., Belloni et al. 2002b).

Some accreting objects that are *not* the topic of this chapter (or even in some cases this book) notably the ultra-luminous X-ray sources observed in some external galaxies (ULX), active galactic nuclei (AGN), both of which are thought to contain black holes, and cataclysmic variables (CV), which contain white dwarfs, can have accretion geometries that are similar to those in X-ray binaries (XRB), and it is of interest to compare their variability properties. The ULX are discussed in §9.8.4, §12.3, 12.4.1 and §13.8 (see also Strohmayer & Mushotzky 2003, Cropper et al. 2004) and the CV in §10. In AGN, while QPO detections are still difficult (see

³ Since the discovery in 1998 of millisecond pulsations in the thermonuclear burster and low magnetic field neutron star SAX J1808.4–3658 (§1, §2.9.1) the old adage about the mutual exclusion between pulsations and type I X-ray bursts “pulsars don’t burst and bursters don’t pulse” (e.g., Lewin et al. 1993), which was based on the dichotomy in neutron-star B fields (§2.4), no longer holds, because low magnetic-field neutron stars now can be pulsars, too. .

10 *Rapid X-Ray Variability*

Benlloch et al. 2001 and references therein, and see also Halpern et al. 2003) the best measurements now clearly show band-limited noise with characteristic frequencies consistent with the idea that variability time scales scale with mass (e.g., Edelson & Nandra 1999, Czerny et al. 2001, Uttley et al. 2002, Markowitz et al. 2003, McHardy et al. 2004). The comparison of XRB with AGN is of particular interest as the physics is likely similar but different observational regimes apply. We typically receive more X-ray photons per dynamical time scale from AGN than from XRB, making it easier, in principle, to study such fast variability in the time domain. X-ray binaries of course have much higher photon fluxes so that background is less of an issue and it is easy to cover very large numbers of dynamical time scales (a hundred million per day) and reliably determine the *parameters* of the stochastic process characterizing the variability rather than observing just one particular *realization* of it. The possibility to compare neutron-star and black-hole systems is unique to X-ray binaries as well.

2.5 **Source states**

Time variability and spectral properties are found to be correlated, presumably because of their common origin in physical processes in the inner, X-ray emitting part of the accretion flow. *Source states* are qualitatively different, recurring patterns of spectral and timing characteristics. They are thought to arise from qualitatively different, somewhat persistent, inner flow configurations. Both timing and spectroscopy are usually required to determine source state. Luminosity, and the way in which power spectrum and X-ray spectrum vary on time scales of minutes and longer (called source *behaviour*) can be used as additional state indicators, but note that luminosity does *not* determine source state (below).

The qualitative changes in phenomenology used to define state include the appearance of a spectral or variability component, a sudden step in luminosity, or a clear bend in a CD/HID track, events which often coincide, indicating a qualitative change in the flow. As observations improve, 'sudden' transitions become resolved, so eventually somewhat arbitrary boundaries need to be set to make state definitions precise. Depending on which criteria are chosen, authors may differ on what is the 'correct' subdivision of the phenomenology into states. Nevertheless, the concept is central in describing the behaviour of X-ray binaries, and in this chapter, the rapid X-ray variability is discussed as a function of state. How X-ray spectral fit parameters depend on source state and what in detail this might imply is beyond the scope of this chapter (see e.g., di Salvo & Stella 2002, Done & Gierlinsky 2003, Gilfanov et al. 2003 for neutron stars and §4 for black holes).

Table 2.1 lists the source states distinguished in this chapter ordered from spectrally hard, generally characterized by low variability frequencies and luminosities at the bottom, towards soft, with higher frequencies and often higher luminosities at the top. Typical band-limited noise (BLN, §2.2) frequencies ν_b corresponding to the state transitions are given (see §§2.6.2 and 2.7). These frequencies are indicative, and in practice depend somewhat on source, and on the precise definition of each state. The most striking variability (strong sharp kHz QPOs (§2.6.1), black-hole high-frequency QPOs (§2.6.1), sharp low-frequency QPOs (§2.6.2) tends to occur in the intermediate states (HB, LLB, IS, IMS, VHS, see Table 2.1) both in neutron stars and in black holes. Note that Z sources so far appear to lack true low-frequency

Table 2.1. *Source states of low magnetic-field compact objects.*

HIGH frequencies		disk-dominated; thermal; SOFT spectra	
$Q, L_{x,short}$ generally increase upward	Z	Atoll	weak LMXB
	FB	UB	
	—	—	
	NB	LB	HS
	50		
	20	LLB	
	HB	10	10
		IS	
	2	2	IMS/VHS
		EIS	
LOW frequencies		corona-dominated; non-thermal; HARD spectra	
<i>rms, L_{radio}</i> generally increase downward			

Q : variability coherences; $L_{x,short}$: X-ray luminosity with long term variations filtered out, i.e., $L_x/\langle L_x \rangle$ where $\langle L_x \rangle$ is L_x averaged over a day, cf. §2.9.1.1; rms : variability amplitudes and L_{radio} : radio flux. FB: flaring branch; NB: normal branch; HB: horizontal branch; UB: upper banana; LB: lower banana; LLB: lower left banana; IS: island state; EIS: extreme island state; HS: high state; IMS: intermediate state; VHS: very high state; LS: low state. Numbers indicate typical BLN frequencies ν_b (in Hz) delineating the states (§2.6.2); ‘—’ indicates the BLN is usually undetected. Reversals in ν_b occur beyond the highest frequencies in Z and atoll sources (§2.6.2).

states. That a rough ordering of states such as in Table 2.1 is possible suggests, of course, that there are physical similarities between the states in the different source types (e.g., van der Klis 1994a,b), but a considerable amount of uncertainty still surrounds this issue, as well as the exact nature of the states themselves.

In neutron stars, X-ray luminosity L_x tends to correlate with state only within a source, not across sources, and, in a given source, much better on short (hours to days), than on longer time scales (§§2.5.2, 2.9.1.1 and, e.g., van der Klis 2000 and references therein); in black holes, the predictive value L_x has with respect to state is even more tenuous (§2.5.1 and, e.g., Miyamoto et al. 1995, Nowak et al. 2002, Maccarone & Coppi 2003). Note, however, that a really low L_x , $<0.01L_{Edd}$ or so, will reliably produce a hard state in most sources. In general, X-ray spectral shape (position in the colour diagram) predicts timing characteristics much better than L_x (e.g., van der Klis et al. 1990, Hasinger et al. 1990, Kuulkers et al. 1994, 1996, van der Klis 1994a,b, 1995a, Ford et al. 1997b, Kaaret et al. 1998, Méndez & van der Klis 1999; Homan et al. 2001, Wijnands & Miller 2002, Rossi et al. 2004, Belloni 2004). The range of correlations in neutron stars between state as defined in Table 2.1 and L_x is schematically illustrated in Fig. 2.2; a full systematic population study has so far only been performed for states with kHz QPOs (Ford et al. 2000). Clearly, the overall correlation of state to L_x is not good. What causes neutron stars to exhibit

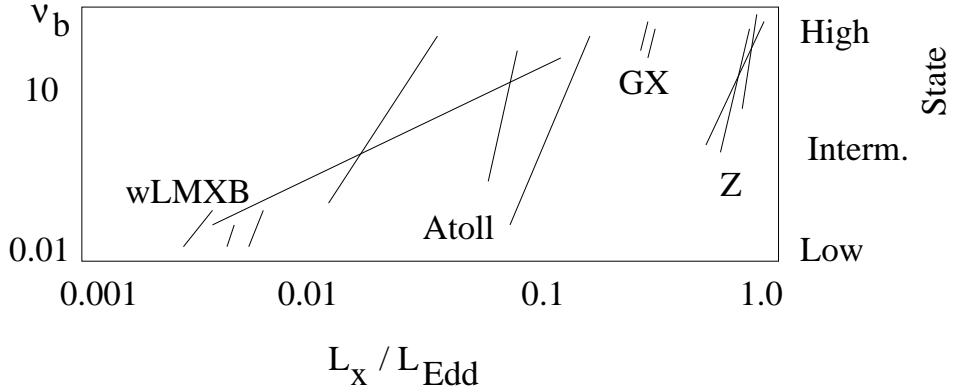


Fig. 2.2. States and luminosities attained by Z sources, GX atoll sources, ordinary atoll sources and weak LMXBs, respectively. Similar states occur at very different luminosities; not all states are seen in all object types. The issue of L_x overlaps between these source types is undecided.

similar states at very different L_x levels, while short-term state changes *correlate* to changes in L_x , and why some sources cover a wider range of states than others, is uncertain. Note that not only the differences between Z and atoll sources need explanation, but also those *among* atoll sources. Differences in magnetic field (e.g., Miller et al. 1998a) have been considered. Clearly, this would allow for intermediate cases, but these are rare (§2.9.5).

If, as often assumed, accretion rate \dot{M} , varying due to processes outside the strong-field region (e.g., instabilities further out in the disk), and increasing from bottom to top in Table 2.1 would underly the state differences, then \dot{M} would have to govern both timing and spectral properties, but *not* the long-term changes in measured X-ray flux nor the L_x differences between sources (e.g., van der Klis 1995a). This could arise if mass outflows or (in black holes) radiatively inefficient (advection) inflows (§4) destroy the expected \dot{M} - L_x correlation by providing sinks of mass and (kinetic) energy (e.g., Ford et al. 2000), or if the flux we measure is not representative for the true luminosity because there are large and variable anisotropies or bolometric corrections in the emission (e.g., van der Klis 1995a). However, in neutron stars differences in X-ray burst properties as a function of observed L_x (§3), suggest that the \dot{M} - L_x correlation is at least fair, and hence that the \dot{M} -state correlation is not so good. Possibly, the \dot{M} that sets source state is not total \dot{M} , but only one component of it, e.g., that through the X-ray emitting part of the disk, \dot{M}_d , while there is also a radial inflow \dot{M}_r (e.g., Fortner et al. 1989, Kuulkers & van der Klis 1995, Kaaret et al. 1998, van der Klis 2000, 2001, Smith et al. 2002). A more radical solution is that L_x does track \dot{M} but that source state is governed by a physical parameter not correlating well to *any* \dot{M} (perhaps, inner disk radius r_{in} , van der Klis 2000). The question then becomes what, if not a varying accretion rate, *does* cause the changes. A clue is the hysteresis observed in the state transitions of various sources (§§2.5.1, 2.5.2), which suggests that the history of a source's behaviour affects its

current state. S-curve disk-flow solutions (§13) have this property, but a smoothed response of \dot{M}_r to variations in \dot{M}_d where r_{in} is set by \dot{M}_d/\dot{M}_r may cause hysteresis as well (see §2.9.1.1). So, while it seems out of the question that the states *as well as* the differences between sources are all just caused by differences in (instantaneous) \dot{M} , differences in \dot{M} *and* in some time average over \dot{M} might still in principle be sufficient. However, the influence of other parameters seems likely. More than one mechanism may be at work. In this chapter, when referring to source states I use the terms *high* and *soft* vs. *low* and *hard* in the general sense implied by Table 2.1, with the understanding that the relation to L_x is complex.

2.5.1 *Black-hole states*

In black holes the 1–20 keV X-ray spectrum can be decomposed into a *hard*, non-thermal, power-law component with photon index typically 1.5–2 and a *soft* (also: 'ultralow'), thermal, black-body like component with $kT < 1$ keV (§1.3.4, §4). The latter is usually attributed to thermal emission from the accretion disk, the former to a *corona* containing energetic electrons. There is no agreement about the nature or energetics of this corona (see e.g., Maccarone & Coppi 2003): it could be located within the inner disk edge or cover part of the disk, it could be quasi-spherical, a thin layer on, or magnetic loops anchored in, the disk, or be the base of the radio jets. It could be quasi-static or part of the accretion flow (azimuthally and/or radially). Its electrons' energy could be thermal or due to bulk motion, and the radiation mechanism could be either Compton or synchrotron.

In the classic black-hole *low state* (LS) in the 2–20 keV band, the hard component dominates (hence it is also called 'low hard state'), and strong (up to typically $\sim 50\%$ rms) flat-topped BLN (§2.2) is present which has a low characteristic frequency (down to typically $\nu_b \sim 0.01$ Hz), in the *high state* (HS) the soft component dominates (hence 'high soft state') and weak ($\lesssim 3\%$) power-law noise occurs, and in the *very high state* (VHS) L_x is high in the range of both spectral components, and strong 3–12 Hz QPOs and BLN that is weaker and higher-frequency (up to ~ 10 Hz) than in the LS as well as power-law noise stronger than in the HS occur, with rapid transitions between these two noise types (Miyamoto et al. 1991). Both LS and HS have turned out to occur over a wide and largely overlapping L_x range in the spectrally hard and soft parts of the HID, respectively (Figs. 2.3, 2.5), and an *intermediate state* (IMS) with timing properties similar to the VHS and at intermediate spectral hardness, but likewise covering a wide L_x range (e.g., Homan et al. 2001; see Fig. 2.3) was identified. To maintain continuity with existing literature (cf., Table 2.7), I continue to refer to these states as LS for the hard low-frequency states and HS for the soft states with weak power-law noise, respectively. I take the IMS to include the VHS as the highest- L_x intermediate state in a source (usually attained early in a transient outburst). Somewhat fortuitously, 'low', 'high' and 'intermediate' can also be taken to refer to BLN frequency (although in a full-blown HS the BLN is not detected). Note that in §4 McClintock and Remillard take another approach: they call HS 'thermal dominant state', and depending on the results of X-ray spectral continuum fits classify some instances of the IMS together with the LS as 'low hard state' and others as 'steep power law state'. Timing in the low- L_x quiescent or 'off' state, down to levels where this can be checked, is consistent with the LS but with ν_b down to

perhaps 0.0001 Hz (§2.10.2). QPOs in both the 1–30 Hz and 100–450 Hz ranges are most prominent in the VHS/IMS, but occasional \sim 0.01–20 Hz QPOs are also seen in LS and HS.

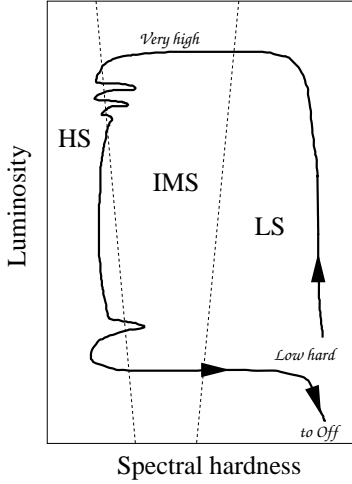


Fig. 2.3. Black-hole states plane. Main states are LS, IMS and HS (low, intermediate and high state) as indicated; locations of classic low/hard, very high and off states are shown as well. Thick curve shows path of typical black-hole transient outburst, inspired by observations of XTE J1550–564 (Homan et al. 2001) and GX 339–4 (Belloni 2004). Contours of ν_b might be a way to delineate the three states in this plane; as these lines are not accurately known, the dashed lines shown are only indicative. See Fig. 2.8 for typical power spectra observed in these states.

In a 'standard' black-hole transient outburst (Figs. 2.3, 2.5) sources tend to follow a harder trajectory from low to high luminosity than vice versa, and make the main hard-soft (LS \rightarrow HS) transition at much higher luminosity than the soft-hard (HS \rightarrow LS) one, behaviour that is often called *hysteresis* (Miyamoto et al. 1995, Nowak 1995, van der Klis 2001, Nowak et al. 2002, Smith et al. 2002, Maccarone & Coppi 2003), expressing the idea of a driving force and a memory effect in the response to that force (§2.5); whether this is truly what is going on requires further investigation. Transitions to and from the IMS can be rapid, suggesting an obvious delineation between states, but slower transitions occur as well, and in these cases the exact transition point becomes a matter of definition (§2.10.2). It might be possible to base such definitions on values of ν_b (cf., Table 2.1), perhaps defining ν_b contours in CD/HIDs as in Fig. 2.3), but it should be noted that the issue is currently in flux and that in particular the best way to deal with the IMS/VHS is surrounded by some controversy (see also §4). Further subdivisions probably exist in the IMS (e.g., Miyamoto et al. 1994), but different boundaries are drawn depending on whether spectral fit parameters (as in §4) or rapid variability (Belloni et al. 2004, Klein-Wolt et al. 2004b) are given precedence in defining the sub-states.

Various spectral characteristics can serve to define the black hole states plane. Flux, intensity or soft color can track the 'luminosity' parameter, which physically might be dominated by the accretion rate through the inner disk \dot{M}_d . The 'state' parameter, which could be a measure for the strength or size of the corona can be defined as, e.g., hard colour or a spectral-component luminosity ratio ('thermal fraction'; L_{soft}/L_{total} , 'power-law ratio'; L_{hard}/L_{total} , etc.; e.g., Miyamoto et al. 1994, Nowak 1995, Rutledge et al. 1999, Remillard et al. 2002c).

On physical grounds one might expect spectral and timing properties to be affected not only by state, but also by the large ($>$ factor 10) differences in L_x within each

state, but certainly in HS (e.g., Homan et al. 2001) and LS (e.g., Belloni 2004) the L_x effect appears to be modest. Historically, after LS and HS (Tananbaum et al. 1972), the VHS was identified first (Miyamoto et al. 1991); the intermediate state was initially noticed as a HS \rightarrow LS transitional state with 10-Hz BLN similar to that in the VHS in the decay of the transient GS 1124–68 (Belloni et al. 1997), and as a 10-Hz BLN state at much lower L_x than the VHS in GX 339–4 (Méndez & van der Klis 1997). Intermediate states with 10-Hz BLN and/or strong power-law noise were then also seen in Cyg X-1 (Belloni et al. 1996) and a number of other sources (e.g., Kuulkers et al. 1997b), and in XTE J1550–564 during excursions at various L_x levels from the HS to a somewhat harder state characterized by 10-Hz BLN, LF QPOs and occasional rather strong power-law noise (§2.10.3, Homan et al. 2001). This led to the two-dimensional paradigm of Fig. 2.3. Weak QPOs >100 Hz occur in the VHS (§2.6.1) but were also found at least once in the IMS at lower L_x (Homan et al. 2001).

That the variability frequencies decrease (§2.6) when the spectrum gets harder suggests a relation with inner disk radius r_{in} (stronger corona for larger r_{in}) and some spectroscopic work points into the same direction (§4), but this entire picture is firmly within the realm of the working hypotheses. Nevertheless, most modeling of black-hole states approximately conforms to this generic framework. The strength of the corona has a relation to that of the radio jets, and as both rely on energetic electrons for their emission, it is natural to suspect a physical relation between these structures (§9). Even at a purely empirical level, there is still considerable uncertainty associated with the motion of the sources through Fig. 2.3, e.g., why do many sources approximately take the depicted 'canonical' path while some deviate from this, are all areas in this plane accessible or are some forbidden, what kind of state transitions are possible at each luminosity level? Yet the diagram and its segmentation into three areas representing three main source states provides a useful template embodying the broad correlation between variability frequencies and spectrum occurring largely irrespectively of L_x level, against which black-hole behaviour can be matched.

2.5.2 *Low magnetic-field neutron-star states*

In low magnetic-field neutron stars spectral decomposition is much less obvious than in black holes, perhaps because of the presence of two thermal emission sites (disk and star) and cooling of the hot electrons in the corona by the stellar flux. The spectra become neither as hard nor as soft as in black holes, but weak hard components are sometimes seen and similarly explained by Comptonization (e.g., Barret & Vedrenne 1994, di Salvo & Stella 2002). Contrary to the case in black holes, CD/HIDs show rather reproducible tracks that embody a one-dimensional states sequence (except at the lowest luminosity levels, see §2.5.2.2).

2.5.2.1 *Z sources*

Z sources on time scales of hours to a day or so trace out roughly Z shaped tracks (Fig. 2.4c) in CD/HIDs consisting of three branches connected end-to-end and called *horizontal branch*, *normal branch* and *flaring branch* (HB, NB, FB). Curve length S_z (§2.3), defined to increase from HB via NB to FB (Fig. 2.4c) performs a

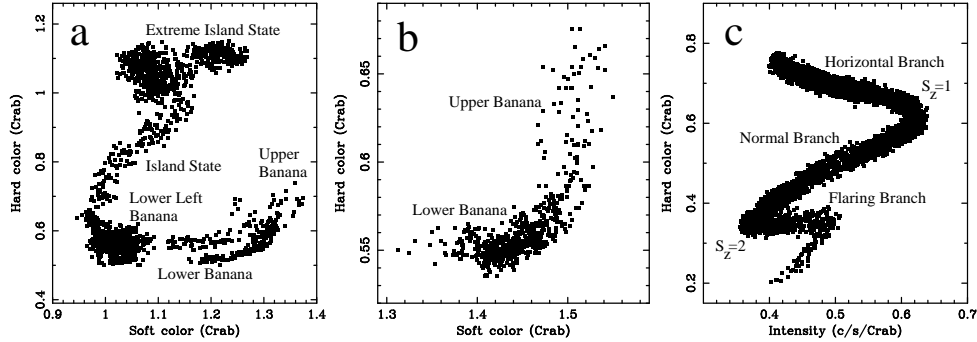


Fig. 2.4. Spectral branches of neutron stars. (a) CD of the atoll source 4U 1608–52, (b) CD of the ‘GX’ atoll source GX 9+1, and (c) HID of the Z source GX 340+0. RXTE/PCA data; soft colour 3.5–6/2–3.5 keV, hard colour 9.7–16/6–9.7 keV, intensity: 2–16 keV, all normalized to Crab. Conventional branch names and S_z values are indicated; for S_a the choice of values differs between authors (though not in sense, see text). Compare van Straaten et al. (2003), Reerink et al. (2004), Jonker et al. (2000a).

random walk; it varies stochastically but shows no jumps. kHz QPOs and a 15–60 Hz QPO called HBO occur on the HB and upper NB, an \sim 6 Hz QPO called NBO on the lower NB, and mostly power-law noise <1 Hz on the FB; see §2.6. With increasing S_z the band-limited noise (LFN, see §2.6.2) becomes weaker and flux and frequencies generally increase, although at high S_z reversals occur (§2.6.2). Z tracks differ somewhat between sources (e.g., Hasinger & van der Klis 1989, Kuulkers 1995, Muno et al. 2002), and also show slow drifts (‘secular motion’) that do not much affect the variability and its strong correlation with S_z (e.g., Hasinger et al. 1990, Kuulkers et al. 1994, Jonker et al. 2002a); some occasionally show shape changes which *do* affect the variability (Kuulkers et al. 1996). There is no evidence for hysteresis in either the Z tracks or the rapid variability.

2.5.2.2 Atoll sources and weak LMXBs

At high L_x atoll sources trace out a well-defined, curved *banana branch* in the CD/HIDs (Fig. 2.4a,b; Hasinger & van der Klis 1989, Reerink et al. 2004) along which, like in Z sources, sources move back and forth with no hysteresis on time scales of hours to a day or so, and which sometimes shows secular motion not affecting the variability (e.g., van der Klis et al. 1990, di Salvo et al. 2003, Schnerr et al. 2003). The banana branch is further subdivided into the *upper banana* (UB) where the <1 Hz power law noise (VLFN, §2.9.4) dominates, the *lower banana* (LB) where dominant several 10-Hz BLN occurs (§§2.6.2, 2.9.3), and the *lower left banana* (LLB) where twin kHz QPOs (§§2.6.1, 2.9.1) are observed.

The spectrally harder parts of the CD/HID patterns are traced out at lower L_x . CD motion is often much slower here (days to weeks), and observational windowing can cause isolated patches to form, which is why this state is called *island state* (IS; Hasinger & van der Klis 1989); it is characterized by dominant BLN (§2.6.2), becoming stronger and lower-frequency as flux decreases and the >6 keV spectrum

gets harder. The hardest, lowest luminosity island states (the *extreme island state*; EIS; e.g., Prins & van der Klis 1997, Reig et al. 2000a; van Straaten et al. 2003 and references therein) are similar to the black-hole LS, with strong, low-frequency flat-topped noise (§2.6.2) and a hard power-law X-ray spectrum. Curve length S_a (§2.3) increases from EIS to UB, generally anti-clockwise (Fig. 2.4a). With increasing S_a the BLN tends to become weaker; frequencies generally increase up to the LB, from where in bright sources ν_b decreases again (§2.6.2). Most atoll sources show a banana branch as well as island states but the four GX atoll sources (§§2.4.2, 2.5; Reerink et al. 2004) are (nearly) always in the banana branch (LB and UB, Fig. 2.4b), and the weak LMXBs (nearly) always in the EIS (e.g., Barret et al. 2000, Belloni et al. 2002a).

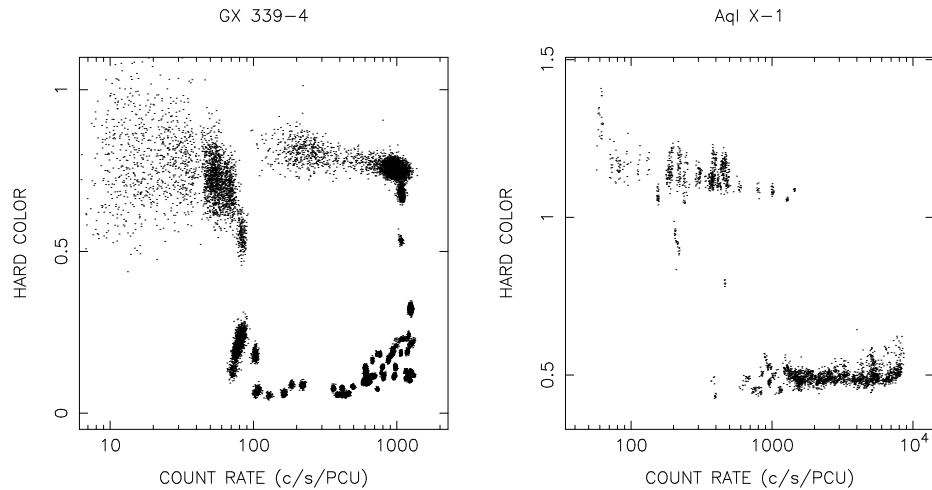


Fig. 2.5. Hardness-intensity diagrams of the black hole GX 339-4 and the neutron-star LMXB transient Aql X-1. Note the orientation of these diagrams, which is similar to that of Fig. 2.4 and transposed compared to Fig. 2.3. Compare Belloni (2004), Reig et al. (2004).

In the island states two-dimensional motion (i.e., not following one well-defined track) is often observed, perhaps because secular motion and motion along the branch happen on similar time scales. In transient atoll sources this takes the form of hysteresis (§2.5.1) during relatively rapid (~ 1 day) transitional IS episodes between EIS and banana state (Fig. 2.5): similarly to black-hole transients, hard to soft transitions occur at higher luminosity than the reverse, but neutron stars lack the hard, high- L_x states (e.g., Barret et al. 1996, Olive et al. 2003, Maccarone & Coppi 2003). Persistent sources can transit to and from the EIS tracing out a one-dimensional IS branch (Fig. 2.4a), suggesting hysteresis is related to the abruptness or speed of the transition. The full picture concerning the EIS, of which only glimpses were seen before (e.g., Mitsuda et al. 1989, Langmeier et al. 1989, Yoshida et al. 1993), is only now becoming clear. In some cases several parallel horizontal EIS branches form, where >6 keV spectral hardness, not luminosity or the <6 keV spectrum, determines

the source state (van Straaten et al. 2003). Similarities between this CD behaviour in the EIS and the Z-source HB were pointed out by a number of authors (Muno et al. 2002, Gierliński & Done 2002b, see also Langmeier et al. 1989), but do not extend to the way in which the branches connect, nor to the timing behaviour (Barret & Olive 2002, van Straaten et al. 2003, Olive et al. 2003, Reig et al. 2004, §2.6.2), where the HB is more like the IS/LLB than like the EIS (Table 2.1).

Similarities of atoll CD/HID behaviour with that of Z sources are mostly confined to the banana branch. Similar one-dimensional motion on similar (hrs-day) time scales and, in the persistent sources, covering similar L_x ranges takes place there through similarly slowly drifting tracks (which, however, are shaped differently and also intrinsically wider in atoll sources). In island states the CD behaviour is quite different from that of Z sources: it shows hysteresis and other forms of two-dimensional motion, and often takes place on longer (days to weeks) time scales over much larger L_x ranges (factors of 5–10, up to 10^3 for transients). This behaviour is more similar to that of black holes than that in other neutron-star states, possibly because in low states the inner-disk radius is larger, further away from the compact object.

2.6 Variability components

Table 2.2 summarizes the rapid X-ray variability components seen in low magnetic-field neutron stars and black holes that we will discuss, grouped into high-frequency phenomena ($\gtrsim 100$ Hz), the low-frequency complex (a group of correlated 10^{-2} – 10^2 Hz phenomena), power-law components (usually dominating mainly the low frequencies), and other phenomena. Typical characteristic frequency ranges are also given, as well as names used for phenomena in particular source types. Here we introduce the high-frequency and low-frequency-complex components, emphasizing relations across source types. Further details, and discussion of the power-law and other components are provided in §§2.9–2.10.

2.6.1 High-frequency phenomena

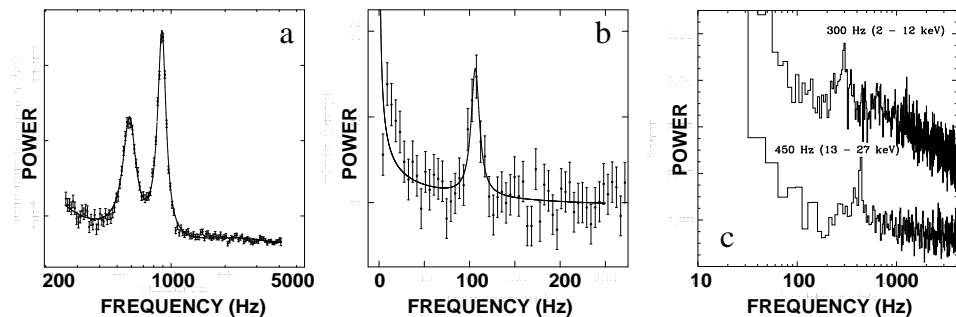


Fig. 2.6. (a) Twin kHz QPOs in Sco X-1 (van der Klis et al. 1997), (b) hectohertz QPO in 4U 0614+09, (c) HF QPOs in GRO J1655–40 (Strohmayer 2001a).

Table 2.2. Variability components

	Name	Low magnetic-field neutron stars			Black holes	Typical frequency range ^a (Hz)
		Z sources	Atoll sources	Weak LMXBs		
High-frequency	kHz QPOs	•	•	—		300–1200
	HF QPO				•	100–500
	hHz QPO	○	•	—		100–200
Low-frequency complex	BLN	• ¹	• ^b	•	• ²	0.01–50
	LF hump/QPO	• ³	•	•	•	0.1–50
	3d Lor.	—	• ⁴	• ⁴	•	1–100
	4th Lor.	—	• ⁵	• ⁵	○	10–500 ^c
Power law	VLFN	• ^d	• ^d	—	• ^{6,e}	— ^f
Other	N/FBO	•	○	—	—	4–20
	1 Hz QPOs	—	—	• ^g	—	0.5–2
	mHz QPOs	—	•	—	•	0.001–0.01

•: observed; ○: some doubt (uncertain, ambiguous, atypical, rare and not clearly seen, etc.); —: variability of similar type as in the other source types not reported. HF: high frequency; LF: low-frequency; BLN: band limited noise; Lor.: Lorentzian; VLFN: very-low frequency noise; N/FBO: normal/flaring branch oscillation. Alternative names: ¹ LFN (low frequency noise), ² LS (low state) noise, ³ HBO (horizontal branch oscillation), ⁴ $L_{\ell_{\text{low}}}$, ⁵ L_u , ⁶ HS (high state) noise. Notes: ^a ν_{max} , cf., §2.2, ^b Sub-components, see §2.6.2, ^c See note to Table 2.3, ^d Sub-components, see §2.9.4, ^e Stronger power law noise in IMS, see §2.10.3, ^f Often only detected < a few Hz, ^g e.g., dipper QPOs; 1 Hz flaring in SAX J1808.4–3658 §2.9.4.

Neutron-star kilohertz QPOs The fastest variability components in X-ray binaries are the *kilohertz quasi-periodic oscillations* (kHz QPOs; van der Klis et al. 1996, Strohmayer et al. 1996; van der Klis 1998 for a historical account) seen in nearly all Z sources (in HB and upper NB) and atoll sources (in IS and LLB) as well as a few weak LMXBs, including msec pulsars (Wijnands et al. 2003). Two QPO peaks (the *twin peaks*) occur in the power spectrum (Fig. 2.6a) and move up and down in frequency together in the 200–1200 Hz range in correlation with source state (cf., Fig. 2.9). The higher-frequency of these two peaks is called the *upper kHz QPO*, frequency ν_u , the other the *lower kHz QPO* at ν_ℓ ; towards the edges of their observed frequency range peaks also occur alone. The several 100-Hz *peak separation* $\Delta\nu \equiv \nu_u - \nu_\ell$ is typically within 20% of the neutron-star spin frequency, or half that, depending on source, and usually decreases by a few tens of Hz when both peaks move up by hundreds of Hz. Most models involve orbital motion in the disk at one of the kHz QPO frequencies (§2.8). Weak sidebands in the kHz domain have been reported in some kHz QPO sources (§2.9.1).

Black-hole high-frequency QPOs The fastest black-hole phenomenon are the *high-frequency* (HF) QPOs (Remillard et al. 1999c) seen in the IMS (usually VHS). Frequencies ν_{HF} range from 100 to 450 Hz (their relation to QPOs in the 27–67 Hz range, Morgan et al. 1997, is unclear), and are reported to usually occur at fixed values different in each source, perhaps inversely proportional to black-hole mass. In a few cases harmonically related (2:3; §2.10.1) frequencies have been seen (Fig. 2.6c). The phenomenon is weak and transient so that observations are difficult, and discrepant frequencies occur as well. The constant frequencies might indicate a link with neutron-star hectohertz QPOs (below), but it is not excluded that black-hole HF and neutron-star kHz QPOs can be reconciled within a single explanation (§2.10.1).

Neutron-star hectohertz QPO The *hectohertz* (hHz) QPO (Ford & van der Klis 1998) is a peaked noise phenomenon (sometimes coherent enough to be called a QPO, §2.2) with a frequency ν_{hHz} in the 100–200 Hz range that is seen in atoll sources in most states (Fig. 2.6b). It stands out from all other neutron-star components by its approximately constant frequency (Fig. 2.9) which is quite similar across sources, perhaps because ν_{hHz} derives from compact-object properties and the neutron stars in these systems are all similar (§2.8). In addition to a possible link with black-hole HF QPOs, a link with the features between 10 and 100 Hz reported by Nowak (2000) in Cyg X-1 and GX 339–4 has been suggested (van Straaten et al. 2002) which may allow a $1/M$ scaling of frequency .

This concludes the summary of the >100 Hz phenomena. Neutron stars have much more broad-band power in the kHz range than black holes (Sunyaev & Revnivtsev 2000, Klein-Wolt et al. 2004b), but there is no indication that this is due to other components than those already mentioned here. The 'high-frequency noise' reported from neutron stars in earlier work (e.g., Dieters & van der Klis 2000) may variously be due to the (low Q) upper kHz QPO at low frequency, hHz QPO, an HBO harmonic (below) and/or instrumental effects (cf., Berger & van der Klis 1994). Sporadic strong millisecond time-scale bursts were reported from Cyg X-1 (Rothschild et al. 1974, 1977, Meekins et al. 1984, Gierliński & Zdziarski 2003) but detecting such phenomena in a strongly variable source is fraught with statistical difficulties (e.g., Press & Schechter 1974, Weisskopf & Sutherland 1978, Giles 1981); instrumental problems caused some of the reported detections (Chaput et al. 2000).

2.6.2 *The low-frequency complex*

In the 0.01–100 Hz range a set of usually two to five band-limited noise, peaked-noise and QPO components is observed whose frequencies all correlate. This *low-frequency complex* is often dominated by strong (up to 60% rms), *flat-topped BLN* with a break at frequency ν_b in the ∼0.01–50 Hz range and peaked noise (the *LF hump*) at frequency ν_h roughly a factor 5 above ν_b (Wijnands & van der Klis 1999a). Both components sometimes feature QPOs located around ν_b and/or around (or instead of) the hump near ν_h . The QPO near ν_h may show several harmonics and is often called the LF QPO (at ν_{LF}). The BLN at ν_b goes under various names (LFN; §2.9.3, LS noise; §2.10.2, broken power law, flat-topped noise) and is often

just called 'the' BLN, or L_b (L for 'Lorentzian', Belloni et al. 2002a). By analogy, other components go by names such as L_h , L_{LF} , L_ℓ , L_u for the LF hump/QPO, lower/upper kHz QPO, etc; see Table 2.3.

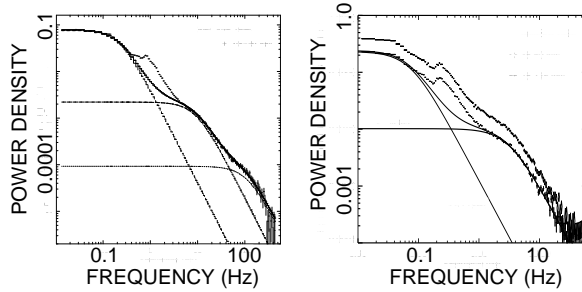


Fig. 2.7. The power spectra of neutron stars (left: 1E 1724-3045) and black holes (right: GRO J0422+32) in the low state can be strikingly similar. Note, however, the subtle *differences* in characteristic frequencies, power levels and number of detectable components, which may in fact be part of a systematic neutron-star black-hole distinction; cf., Fig. 2.8 LS and EIS. After Olive et al. (1998).

Low states When L_b and L_h are at low frequency ($\nu_b \lesssim 1$ Hz; black-hole LS and atoll EIS, cf., Table 2.1), a third BLN component is often present above the frequency of the LF hump/QPO. The combination of these three noise components leads to the characteristic power-spectral shapes displayed in Fig. 2.7 that can be remarkably similar between neutron stars and black holes (van der Klis 1994a and references therein, Olive et al. 1998, Wijnands & van der Klis 1999a, Belloni et al. 2002a), and also show similar time lags (Ford et al. 1999). This third component has been suggested to be the lower kHz QPO, L_ℓ , but at frequencies as low as ~ 10 Hz (§2.7), and is designated L_{low} here. In neutron stars a fourth, > 100 Hz, BLN component occurs above L_{low} whose frequency connects smoothly with that of the upper kHz QPO and, like it, is designated L_u .

Low to intermediate states When atoll sources and black holes move out of these low states ($\nu_b \gtrsim 1$ Hz) towards the IMS/VHS or via the island state (IS) to the lower-left end of the banana (LLB), respectively, all components increase in frequency and become weaker and, often, more coherent. By the time that $\nu_b \sim 10$ Hz, L_b and L_h are much weaker and L_{low} is below detection. Black holes in this state often show narrow 1–30 Hz LF QPO peaks with sometimes several harmonics that differ in strength, phase lags and coherence between odd and even ones, as well as energy dependencies in L_b (and hence, ν_b , §2.10.2); sometimes no BLN is detected but only power-law noise (§2.5.1, §2.10.3). In the atoll sources L_b attains substructure and often needs to be described by two components, a peaked noise/QPO plus a BLN a factor 2–3 below it which is sometimes called L_{b2} .

Z sources, where ν_b is always > 1 Hz, are similar to this in the HB and upper NB. L_b is sometimes called 'low-frequency noise' (LFN) and has ν_b varying between 2 and 20

Table 2.3. *High frequency and low frequency complex component names & symbols*

	Name	Symbol	Frequency (Hz)
High-frequency	Upper kHz	L_u	500–1200
	Lower kHz	L_ℓ	300–1000
	High frequency	L_{HF}	100–500
	hectoHz	L_{hHz}	100–200
Low-frequency complex	BLN	L_b, L_{b2}	0.01–50
	LF hump, LF QPO	L_h, L_{LF}	0.1–50
	3d Lorentzian	L_{low}	1–100
	4th Lorentzian	L_u	10–500 ^a

^a In neutron stars 140–500 Hz, probably the upper kHz QPO at low Q; in black holes 10–100 Hz.

Hz. A 15–60 Hz LF QPO superimposed on this called 'horizontal-branch oscillation' (HBO) sometimes has several observable harmonics, with alternating high- and low-Q harmonics somewhat reminiscent of those in black-hole LF QPOs; warped disk geometries have been suggested as a cause of this (e.g., Jonker et al. 2000a, 2002a).

Intermediate to high states When atoll sources move further onto the banana, the frequencies of the L_b subcomponents rise (the QPO to 30–80 Hz and the BLN to 20 Hz) and then, in the LB, decrease again (e.g., di Salvo et al. 2003, Reerink et al. 2004). The low-frequency complex components weaken until in the UB they become undetectable. A similar evolution (including sometimes frequency reversals, e.g., Wijnands et al. 1996) is observed in Z sources on the NB, and for black holes moving into the HS, where dominant $\alpha=0.7$ –1.4 power-law noise is also regularly observed at this point (§2.10.3), but no clear evidence for frequency reversals has been reported (photon energy dependencies in ν_b in the IMS further complicate the issue). Several more components may occur in the range of the low-frequency complex (§2.9.3, §2.10.2) and disentangling them is sometimes difficult.

The <100 Hz variability of black-hole LS and neutron-star EIS are very similar and there is little doubt that they are physically related. There also obviously are close relations with, and between, variability in black-hole IMS/VHS, atoll source IS/(L)LB, and Z source HB/upper NB, but even empirically the exact nature of these relations is not yet fully established (but see Klein-Wolt et al. 2004b for recent progress). An important clue is provided by the correlations between the component frequencies (and strengths) which helps to identify components across sources. These are discussed next.

2.7 Frequency correlations

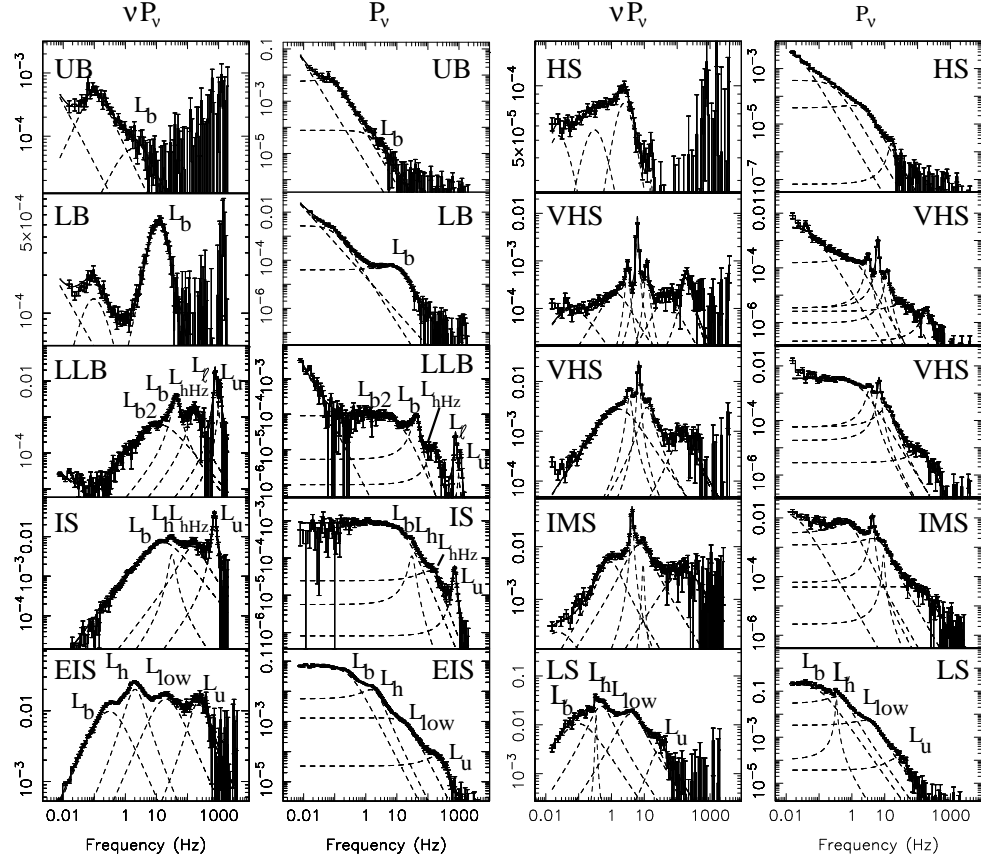


Fig. 2.8. Power spectra in *left*: atoll sources and *right*: black holes in their various states (§2.5) in P_v and νP_v representations. Two examples of VHS power spectra are shown, with and without strong BLN. Atoll source variability component names are indicated (except the lowest-frequency, VLFN, components in UB, LB and LLB; cf., Reerink et al. 2004). The analogous broad-band components in the black hole LS are also identified; the narrow component is L_{LF} .

2.7.1 Frequency correlations in neutron stars

Fig. 2.9a displays the frequency correlations of four well-studied atoll sources and four weak LMXBs (faint burst sources, §2.4.2). The frequencies of all components described in §2.6 are plotted vs. ν_u . Source state designations corresponding to the colour-colour diagrams in Fig. 2.4 are also indicated. As L_u becomes undetectable $\gtrsim 1200$ Hz, the frequency evolution beyond that point is not covered in Fig. 2.9a. The figure includes data from sources covering an order of magnitude in luminosity when in the same state, yet they display very similar power spectra and essentially the same frequency correlations. The tracks of ν_b (and subcomponent ν_{b2}), ν_h , ν_{low} , ν_{hHz} and ν_ℓ vs. ν_u are clearly recognizable. This plot can usefully serve as a template against which to match the rapid X-ray variability of other objects.

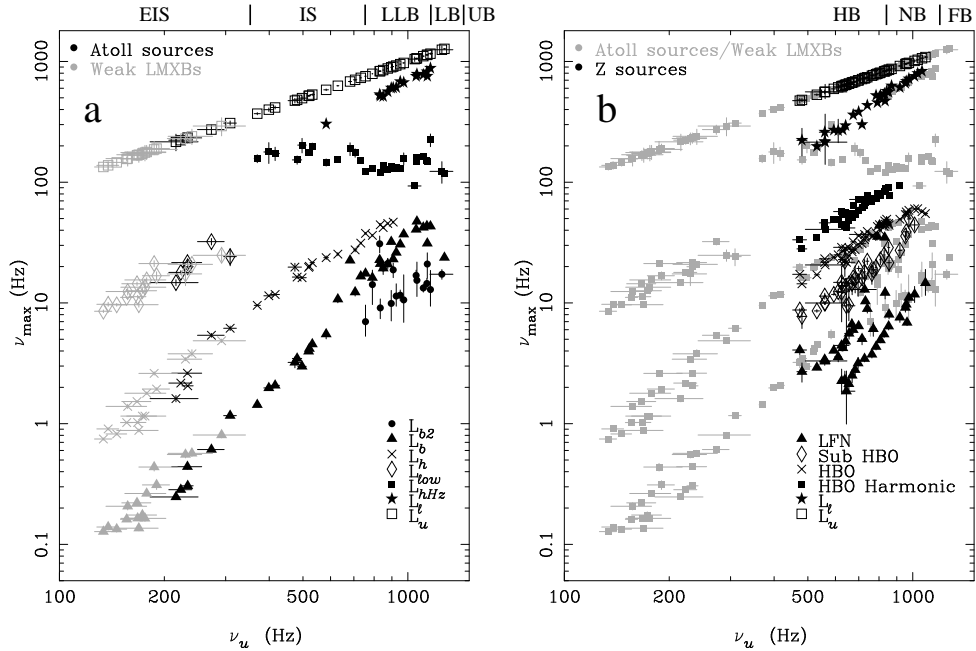


Fig. 2.9. Frequency correlations. (a) Atoll sources and weak LMXBs, (b) Z sources compared with these objects. The characteristic frequencies (ν_{max} , §2.2) of the components are plotted as indicated; approximate source state ranges are indicated at the top.

Fig. 2.9b compares measurements for the Z sources with the atoll source data. The kHz QPOs match, as well as do the HBO and L_h . Differences are that in Z sources no hectohertz QPO has been reported so far, and that an additional HBO harmonic and 'sub-harmonic' occur. How precisely these, and the LFN (the Z source variant of L_b) which varies even among the Z sources themselves, relate to atoll source components is undecided. The dependence of ν_h and related QPOs on ν_u is approximately quadratic in both Z and atoll sources (Stella & Vietri 1998 and, e.g., Psaltis et al. 1999b, Jonker et al. 1998, Homan et al. 2002, van Straaten et al. 2003; Fig. 2.10) suggesting that Lense-Thirring precession of an orbit with frequency ν_u might be causing the LF QPO (§2.8.2), but in GX 17+1 at high frequency the HBO frequency (and X-ray flux) start decreasing while ν_u continues increasing (Homan et al. 2002).

An interesting discrepancy occurs in the frequencies of some millisecond pulsars: in SAX J1808.4–3658 a pattern of correlated frequencies occurs very similar to Fig. 2.9a, but with relations that are offset. At low frequencies, the match can be restored by multiplying the ν_u values and the single measured ν_ℓ with ~ 1.45 , which suggests a link with the 2:3 frequency ratios in black holes (§2.6.1); at higher frequencies the identification of the L_b subcomponents is uncertain (van Straaten et al. 2004). Of the other millisecond pulsars, XTE J0929–314 and XTE J1807–294 behave in the same way, but XTE J1751–305 and XTE J1814–338 are like ordinary atoll sources in this

respect. This suggests ν_u and ν_ℓ form one group of correlated frequencies and the LF complex another, independent one; the case of GX 17+2 above supports this.

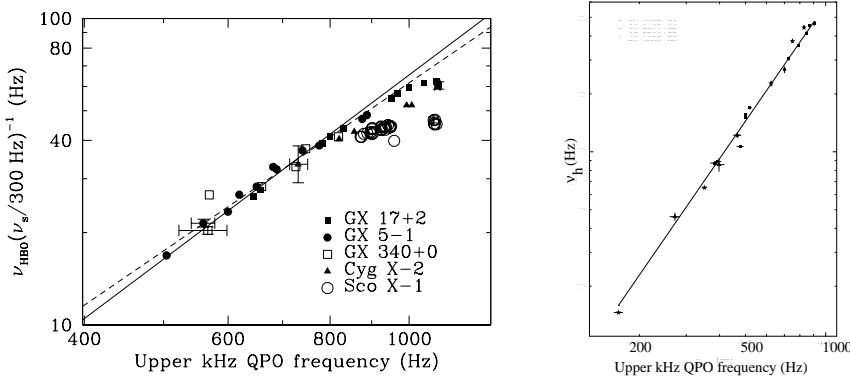


Fig. 2.10. The relation between upper kHz QPO frequency and, *left*: HBO frequency in Z sources (scaled between sources by an inferred spin frequency), drawn line is for a quadratic relationship, dashed line is best power-law fit, *right*: ν_h in atoll sources, line is power law with index 2.01. In a Lense-Thirring interpretation (§2.8.1) a value of I_{45}/m of ~ 4 would be implied in both cases (see also §2.8.2). From Psaltis et al. (1999b) and van Straaten et al. (2003).

2.7.2 Frequency correlations of black holes compared to neutron stars

Black holes can not be directly compared to Fig. 2.9 as L_u is not reliably detected. However, correlations between other frequencies in Fig. 2.9, and one between frequency and power, provide intriguing links between neutron stars and black holes.

BH relation Belloni & Hasinger (1990a) noticed that in Cyg X-1 ν_b and the power-density level $P_{\nu flat}$ of the BLN flat top anti-correlate (Fig. 2.11a), an effect later also seen in other black holes in the LS and neutron stars in the (E)IS (e.g., Méndez & van der Klis 1997, van Straaten et al. 2000, Belloni et al. 2002a). For $\nu_b < 1$ Hz the relation is consistent with a BLN rms amplitude that remains constant while ν_b varies; this constant amplitude is less for neutron stars than for black holes and might even depend on mass (Belloni et al. 2002a), but note that photon-energy dependencies can affect $P_{\nu flat}$ as well. Above 1 Hz the BLN clearly weakens, but the relation appears to extend to the black-hole I/VHS (van der Klis 1994b) at ν_b up to ~ 10 Hz, and to $\nu_b > 10$ Hz in neutron stars (van Straaten et al. 2000).

WK relation Wijnands & van der Klis (1999a; WK) noted that in atoll sources (including weak LMXBs) and black holes ν_b and ν_h are correlated over 3 orders of magnitude (Fig. 2.11b, with the hump at ν_h a factor 8 to 2 above the break, decreasing with ν_b). This relation is that between the two lower traces in Fig. 2.9. Z sources are slightly above the main relation (cf., §2.7.1), with ν_h an also decreasing factor 10 to 3 above ν_b . Of course, the QPOs on the break of band-limited noise components mentioned in §2.6.2 hug the line $\nu_{BLN} = \nu_{QPO}$; these may

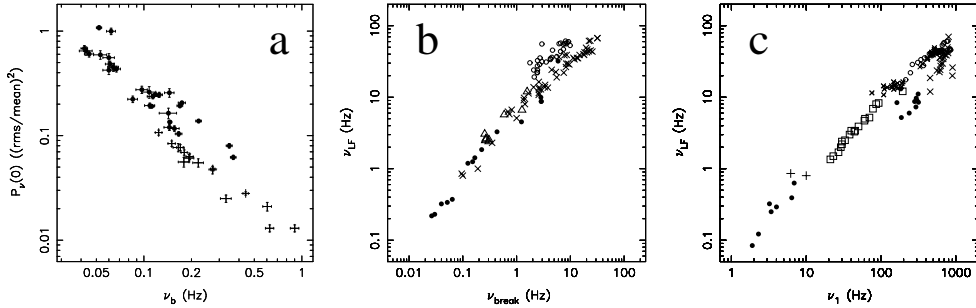


Fig. 2.11. Frequency and power correlations across neutron stars and black holes. (a) BLN flat-top power level vs. break frequency (after Belloni et al. 2002a), (b) low-frequency hump/QPO vs. noise break frequency (after Wijnands & van der Klis 1999a), (c) low-frequency hump/QPO vs. ν_ℓ or $\nu_{\ell\text{low}}$ (after Psaltis et al. 1999a). Filled circles represent black-hole candidates, open circles Z sources, crosses atoll sources, triangles the millisecond pulsar SAX J1808.4-3658, pluses faint burst sources and squares Cir X-1. .

be physically the same components and are not shown in Fig. 2.11. Cases of QPOs below the noise break have also been reported (e.g., Brocksopp et al. 2001), and while in some instances in the fits they could be reinterpreted as the reverse, this may indicate that the description of the low-frequency complex is not yet complete.

PBK relation Psaltis et al. (1999a; PBK) found a rather good correlation between the frequencies of L_ℓ and $L_{\ell\text{low}}$ on the one hand and L_h and L_{LF} on the other spanning nearly three decades in frequency, with the Z and atoll sources populating the ν_ℓ (> 100 Hz) range and the weak LMXBs and black holes in the LS the $\nu_{\ell\text{low}}$ (< 10 Hz) one, and Cir X-1 (§2.9.5) filling in the gap between L_ℓ and $L_{\ell\text{low}}$ (Figs. 2.11c, 2.14b). The correlation combines features from different sources with very different Q values with relatively little overlap, and, as Psaltis et al (1999a) note, although the data are suggestive, they are not conclusive. Whether the black-hole HF QPOs contributing to the small branch below the main relation in Fig. 2.11c are part of these correlations is questionable in view of their presumed constant frequencies (§2.6.1) — on the other hand, in XTE J1550-564 a correlation does occur between *observed* HF and LF QPO frequencies (and spectral hardness; see §2.10.1).

Further work (e.g., van der Klis 1994b, Crary et al. 1996, van der Hooft et al. 1996, Belloni et al. 1996, 2002a,b, Méndez and van der Klis 1997, Ford & van der Klis 1998, Méndez et al. 1998d, van der Hooft et al. 1999a, Wijnands & van der Klis 1999b, Nowak 2000, Remillard et al. 2002c, Revnivtsev et al. 2000c, van Straaten et al. 2000, 2002, 2003, 2004, di Salvo et al. 2001a, Kalemci et al. 2001, 2003 Wijnands & Miller 2002, Yu et al. 2003, Olive et al. 2003, Reig et al. 2004, Klein-Wolt et al. 2004b) produced many examples of power spectra confirming these correlations, with in particular the weak LMXBs and some ordinary atoll sources, as well as some transient black holes in their decay bridging the gap between neutron stars and black holes in the PBK relation. In black holes a feature perhaps similar to L_u

in neutron stars in the 10–100 Hz range was reported (Nowak 2000, Belloni et al. 2002a). However, some possible discrepancies also turned up in some of these same works (e.g., Belloni et al. 2002a, van Straaten et al. 2002, 2004, Pottschmidt et al. 2003) and as there is no direct observation of a gradual transition, the identification of the high-Q lower kHz QPO in Z and atoll sources with the low-Q L_{low} component in the neutron-star and black-hole low states remains conjectural.

Consequences of the correlations The relations of Fig. 2.11 suggest that physically similar phenomena cause the frequencies plotted there. If so, then these phenomena are extremely tunable, in some cases over nearly three orders of magnitude in frequency, and occur in neutron stars as well as black holes, which probably means they arise in the disk. In §2.8 we look at some of the models for this.

Warner & Woudt (2002) and Mauche (2002), noted that the 'PBK' relation may even extend to white dwarf systems (§10) down to frequencies a factor 10^2 below those in X-ray binaries, which would mean that strong field gravity *per se* is not a requirement for the accretion disk to produce the correlated frequencies ν_ℓ and ν_b . Note that even then orbital motion in the strong-field region of neutron stars and black holes is implicated by the high frequencies observed, and that producing the second kHz QPO may require strong-field gravity. As remarked above, the identification of the variability phenomena across source types is difficult, so these results should be interpreted with caution.

2.8 Orbital and epicyclic frequency models

Because of their direct link with physical time scales, interpretation of observed characteristic frequencies dominates the discussion about the nature of rapid X-ray variability. What modulates the X-ray flux (§2.8.7) and why the phenomenon is quasi-periodic rather than periodic (§2.8.6) often gets less attention. Many QPO models are essentially models for a periodic phenomenon (e.g., orbital motion) supplemented with a decohering mechanism (e.g., damping). Some broad-band noise models also work in this way, but many (and some QPO models as well) are instead intrinsically aperiodic (e.g., shots), with characteristic frequencies arising through, e.g., correlations in the signal (cf., §2.12.3). Another important distinction is that between constant variability frequencies, which may be expressible in parameters of the compact object (M, R, J) alone, and variable ones, which involve flow, or radiation-field parameters.

Phenomena that occur in both neutron stars and black holes can not rely on physical properties unique to either object, such as either a material surface or a horizon, a magnetic field not aligned with the spin or extreme values of J/M . Hence, these essentially require an origin in the accretion flow. Instead, in phenomena unique to either neutron stars or black holes a role for unique compact-object properties is likely.

For accretion-flow phenomena, the most obvious source of variability is the disk, which with Keplerian orbital motion at each radius and various oscillation modes provides a multitude of variability frequencies. Other structures, e.g., the 'corona' from X-ray spectral models (§2.5.1), a magnetosphere, a neutron-star/disk boundary layer, or a jet (§9) can contribute as well. Nevertheless, orbital motion (including

general-relativistic epicyclic motions, §2.8.1) and disk oscillations (§2.12.1) are the mechanisms most often considered for QPO phenomena.

In the current section we look at the interpretations of variability frequencies that involve orbital and epicyclic motions in the accretion disk. Some interpretations recur in various models and can be considered model 'building blocks'. Models based on flow instabilities, and interpretations of other aspects of the variability (amplitude, coherence, phase and their photon-energy dependencies) are discussed in §2.12. Some specific models proposed for specific variability components are mentioned in §§ 2.9–2.10.

2.8.1 General-relativistic orbital motion

In classical physics, free-particle orbits around a spherically symmetric mass M are closed, and occur with Keplerian frequency

$$\nu_K = \sqrt{GM/r^3}/2\pi \approx 1184 \text{ Hz} \left(\frac{r}{15 \text{ km}} \right)^{-3/2} m_{1.4}^{1/2} \approx 184 \text{ Hz} \left(\frac{r}{100 \text{ km}} \right)^{-3/2} m_{10}^{1/2},$$

where $m_{1.4}$ and m_{10} are the compact object's mass in units of 1.4 and 10 M_\odot , respectively, and r is the orbital radius. In general relativity, orbits are not closed, as the frequencies of azimuthal, radial and vertical motion differ (Fig. 2.15, e.g., Merloni et al. 1999): in addition to the azimuthal motion at the *general-relativistic orbital frequency* ν_ϕ , there are the *radial* and *vertical epicyclic* frequencies ν_r and ν_θ .⁴ Due to this, eccentric orbits waltz at the *periastron precession frequency* $\nu_{peri} = \nu_\phi - \nu_r$ and orbits tilted relative to the equatorial plane of a spinning central mass wobble at the *nodal precession frequency* $\nu_{nodal} = \nu_\phi - \nu_\theta$.

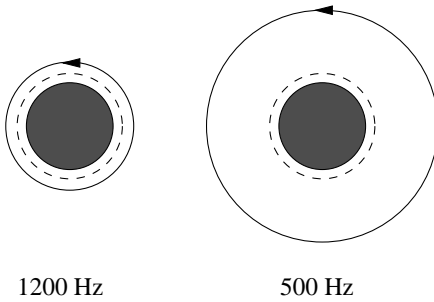


Fig. 2.12. A 10-km radius, $1.4M_\odot$ neutron star with the corresponding innermost stable circular orbit (ISCO; dashed circles) and orbits (drawn circles) corresponding to orbital frequencies of 1200 and 500 Hz, drawn to scale.

For equatorial circular orbits in Kerr spacetime (i.e., around a spinning point mass M with angular momentum J) the orbital frequency is given by

$$\nu_\phi = \frac{\sqrt{GM/r^3}/2\pi}{1 + j(r_g/r)^{3/2}} = \nu_K (1 + j(r_g/r)^{3/2})^{-1},$$

where $j \equiv Jc/GM^2$ is the Kerr angular-momentum parameter⁵; $0 < j < 1$ for prograde orbits, $-1 < j < 0$ for retrograde ones, and $r_g \equiv GM/c^2$. For the

⁴ Various other terms are used for these motions: e.g., 'longitudinal' for ν_ϕ ; 'latitudinal' or 'meridional' for ν_θ .

⁵ The quantity j is also sometimes called a_* or, exceptionally, a . Most authors let a denote Jc/GM , some use $a = J/M$, e.g., Stella & Vietri (1998). r_g sometimes denotes $2GM/c^2$.

Schwarzschild geometry, $j = 0$, we have $\nu_\phi = \nu_K$. Infinitesimally tilted and eccentric orbits will have radial and vertical epicyclic frequencies of

$$\nu_r = \nu_\phi \left(1 - 6(r_g/r) + 8j(r_g/r)^{3/2} - 3j^2(r_g/r)^2 \right)^{1/2}, \text{ and}$$

$$\nu_\theta = \nu_\phi \left(1 - 4j(r_g/r)^{3/2} + 3j^2(r_g/r)^2 \right)^{1/2}$$

(Fig. 2.15). For arbitrary-inclination orbits, see Sibgatullin (2002). All these frequencies are as observed by a static observer in asymptotically flat spacetime, i.e., at infinity. In a Schwarzschild geometry a local observer, due to gravitational time dilation, sees a frequency higher by $(1 - 2(r_g/r))^{-1/2}$; in the general case, the locally observed frequency also depends on the observer's angular motion.

General relativity predicts (e.g., Bardeen et al. 1972) that in a region close to a compact object no stable orbital motion is possible; hence the above expressions are directly useful only outside that region. In a Schwarzschild geometry the *innermost stable circular orbit* (ISCO) or *marginally stable orbit* has a radius

$$r_{ms} = 6r_g = 6GM/c^2 \approx 12.5m_{1.4} \text{ km} \approx 89m_{10} \text{ km},$$

and the corresponding orbital frequency, the highest stable orbital frequency, is

$$\nu_{ms} = c^3/2\pi 6^{3/2} GM \approx (1566/m_{1.4}) \text{ Hz} \approx (219/m_{10}) \text{ Hz}.$$

For prograde orbital motion in the equatorial plane of a Kerr geometry the ISCO is smaller; as $j \rightarrow 1$, $r_{ms} \rightarrow r_g$ and

$$\nu_{ms} = c^3/4\pi GM \approx (1611/m_{10}) \text{ Hz}.$$

This is still outside the hole, because the horizon radius

$$r_{horizon} = r_g(1 + (1 - j^2)^{1/2})$$

shrinks from $2r_g$ at $j = 0$ to r_g as $j \rightarrow 1$ as well. The corresponding frequency increases with j , and hence for a black hole of known mass a high (test-particle) orbital frequency can be used to argue for its spin (Sunyaev 1973; see also §2.8.5). The full expression for the ISCO radius (Bardeen et al. 1972) follows from the condition $r^2 - 6r_g r + 8r_g^{3/2} r^{1/2} j - 3r_g^2 j^2 \geq 0$ for stable orbits and is somewhat tedious; substitution into the expression for ν_ϕ yields the Kerr geometry ISCO frequency in closed form. To first order in j (Kluśniak et al. 1990, Miller et al. 1998a,b)

$$r_{ms} \approx (6GM/c^2)(1 - 0.54j) \quad \text{and} \quad \nu_{ms} \approx (c^3/2\pi 6^{3/2} GM)(1 + 0.75j).$$

Some disk flows can penetrate down to inside the ISCO before the matter plunges in (e.g., Abramowicz et al. 2004, cf., §2.8.5), but not beyond the marginally bound orbit at $r_{mb} = r_g(2 - j) + 2r_g(1 - j)^{1/2}$, which is inside the ISCO (at $4r_g$ in the Schwarzschild geometry).

Spacetime outside a spherically symmetric non-rotating star is Schwarzschild. For *spinning* stars the exterior spacetime is Kerr to first order in j ; to higher order the metric, and hence the precise frequencies, depend on the mass distribution (Hartle & Thorne 1968; see Miller et al. 1998a, Shibata & Sasaki 1998, Morsink & Stella 1999, Marković 2000, Sibgatullin 2002, Abramowicz et al. 2003a). Depending on mass

and EOS (§2.1), spinning neutron stars could have appreciable angular momentum (e.g., $j \sim 0.2$ and ~ 0.5 for 500 and 1000 Hz spins, respectively, Miller et al. 1998a). For small- j holes and slowly spinning neutron stars the first-order expressions above apply. In all cases ν_{ms} scales as $1/M$.

As ν_r and ν_θ are both $< \nu_\phi$, periastron and nodal precession are both prograde. Periastron precession is a consequence of the non- $1/r^2$ nature of gravity in general relativity; the classic example is Mercury's general-relativistic perihelion precession. Nodal or 'Lense-Thirring' precession (Lense & Thirring 1918) is due to the 'frame dragging' caused by the central object's spin and does not occur if $j = 0$; this 'gravito-magnetic'⁶ effect has not yet been detected with certainty in any system. In the weak-field ($r_g/r \ll 1$) slow-rotation ($j \ll 1$) limit the prediction is that $\nu_{nodal} = (GM)^2 j / \pi c^3 r^3 = 8\pi^2 \nu_\phi^2 I \nu_{spin} / Mc^2$, where I is the neutron-star moment of inertia and ν_{spin} its spin frequency: by measuring ν_{nodal} , ν_ϕ and ν_{spin} the neutron-star structure-dependent quantity I/M is constrained. In terms of I_{45}/m , where I_{45} and m are I and M in units of 10^{45} g cm^2 and M_\odot , respectively,

$$\nu_{nodal} = 13.2 \text{ Hz} \left(\frac{I_{45}}{m} \right) \left(\frac{\nu_\phi}{1000 \text{ Hz}} \right)^2 \left(\frac{\nu_{spin}}{300 \text{ Hz}} \right);$$

values of I_{45}/m between 0.5 and 2 are expected (Stella & Vietri 1998).

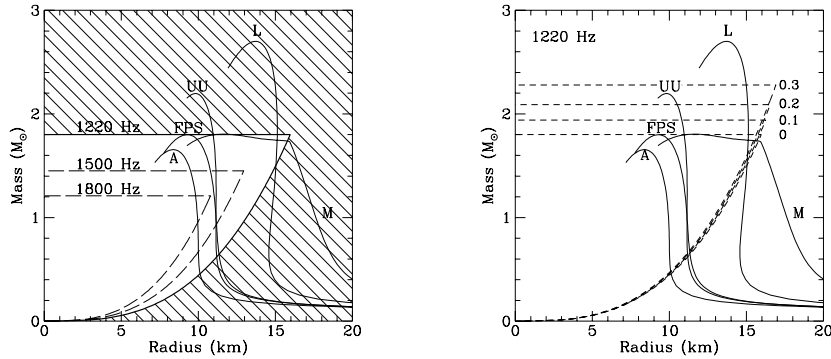


Fig. 2.13. Constraints on neutron-star M and R from orbital motion. *Left:* for $j = 0$, orbital frequencies as indicated; the hatched area is excluded if $\nu_\phi = 1220 \text{ Hz}$. *Right:* with first order corrections for frame dragging for the values of j indicated. Mass-radius relations for representative EOS are shown. (from Miller et al. 1998a)

The detection of stable orbital motion at frequency ν around a neutron star constrains both its mass M and radius R (Miller et al. 1998a): (i) R must be smaller than the orbital radius r , and (ii) the ISCO must *also* be smaller than r (assuming the orbit is circular). Condition (i) through the expression for ν_ϕ translates into a mass-dependent upper limit on R , and condition (ii) is an upper limit on

⁶ This term does not refer to any magnetic field, but to an analogy with electromagnetism.

M , in Schwarzschild geometry: $6GM/c^2 < (GM/4\pi^2\nu^2)^{1/3} \Rightarrow M < c^3/(2\pi 6^{3/2}G\nu)$. Fig. 2.13 shows these limits in the neutron-star mass-radius diagram.

Detection of the ISCO would constitute direct proof of a qualitative strong-field general-relativistic effect and at the same time demonstrate that the neutron star is smaller than the ISCO. This possibility was discussed since early on (e.g., Kluźniak & Wagoner 1985, Paczyński 1987, Biehle & Blandford 1993). Miller et al. (1998a) pointed out that when the inner edge of the accretion disk reaches the ISCO, the associated kHz QPO frequency might reach a ceiling while \dot{M} continues rising (see also §2.9.1.3).

2.8.2 Relativistic precession models

The term *relativistic precession model* (Stella & Vietri 1998) is used for a class of models in which observed frequencies are directly identified with orbital, epicyclic, and precession frequencies. These models need additional physics to pick out one or more particular radii in the disk whose frequencies correspond to those observed (§2.8.5). Stella & Vietri (1998, 1999) identify the upper kHz QPO frequency ν_u (§2.6.1) with the orbital frequency ν_ϕ at the inner edge of the disk (§2.8.5), and relate ν_ℓ and ν_h (or related QPOs, §2.6.2) with, respectively, periastron precession (ν_{peri}) and nodal precession (ν_{nodal}) of this orbit.

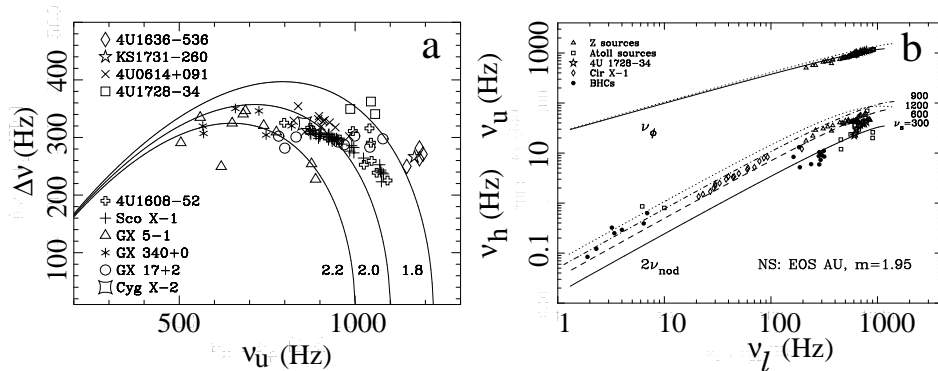


Fig. 2.14. Predicted relations between (a) ν_u and $\Delta\nu$ and (b) ν_ℓ and ν_h as well as ν_u for different values of the spin frequency (300 Hz, 600 Hz, etc.) in the relativistic precession model, compared with observed values. (Stella & Vietri 1999, Stella et al. 1999). See §2.7.2 for a discussion of the data in the right-hand frame.

So, ν_h is predicted to be proportional to ν_u^2 (§2.8.1), which is indeed as observed (§2.7.1), and kHz QPO peak separation $\Delta\nu \equiv \nu_r$. Stellar oblateness affects the precession rates and must be corrected for (Morsink & Stella 1999, Stella et al. 1999). This model does not explain why $\Delta\nu$ is commensurate with the spin frequency, nor how neutron stars with different spins can have the same $\nu_u - \nu_h$ relation (van Straaten et al. 2004). A clear prediction is that $\Delta\nu$ should decrease not only when ν_u increases (as observed) but also when it sufficiently decreases (Fig. 2.14, see also §2.9.1.2). For acceptable neutron-star parameters (I/M , see §2.8.1), ν_h is several times larger than

the ν_{nodal} predicted. In a warped disk geometry ν_h could be $2\nu_{nodal}$ or $4\nu_{nodal}$ (Morsink & Stella 1999). Cui et al. (1998b) propose identifications of some black-hole frequencies with ν_{nodal} (see also Merloni et al. 1999).

A precise match between model and observations requires additional free parameters. Stella & Vietri (1999) propose that orbital eccentricity systematically varies with orbital frequency. Stella et al. (1999), identifying ν_ℓ and ν_{low} with ν_{peri} , and ν_h and ν_{LF} with $2\nu_{nodal}$ (cf., §2.6), produce an approximate match to the PBK relation (§2.7) across neutron stars and black holes (Fig. 2.14b) for reasonable black-hole masses and $j=0.1\text{--}0.3$, but requiring neutron-star spin rates higher than measured and masses of $\sim 2M_\odot$. For critical discussions of these models see Psaltis et al. (1999b) and Marković & Lamb (1998, 2000). Vietri & Stella (1998) and Armitage & Natarajan (1999) have performed calculations relevant to the problem of sustaining the tilted orbits required for Lense-Thirring precession in a viscous disk. Miller (1999) calculated the effects of radiation forces on Lense-Thirring precession.

Relativistic precession models are very predictive, as the frequency relations are set by little more than compact-object parameters and general relativity, and in unmodified form most are contradicted by observations (e.g., Homan et al. 2002, van Straaten et al. 2004). Yet the observed quadratic dependencies between ν_u and ν_h (§2.7.2) which suggest Lense-Thirring precession (§2.8.1), are striking. Calculations of the theoretically expected QPO sideband patterns produced by luminous clumps in orbits with epicyclic motions (Karas 1999a, Schnittman & Bertschinger 2004), and observations of such patterns, can help to further test models in this class. Certain disk oscillation models are predicted to produce frequencies close to the orbital and epicyclic ones and may be considered one way to implement the models described here; hydrodynamic effects are expected to somewhat modify the frequencies and to produce combinations between them, which may allow to better fit the data. These models are discussed in §2.12.1. The general idea that an observed frequency is the orbital frequency ν_ϕ at the appropriate radius in the disk is applied very often, and papers identifying observed frequencies with orbital frequencies of clumps, vortices, etc., are too numerous to cite (see e.g., Chagelishvili et al. 1989, Abramowicz et al. 1992, Bao & Østgaard 1994, 1995, Karas 1999b, Wang et al. 2003 and §2.9.1.3).

2.8.3 Relativistic resonance models

Relativistic resonance models (Kluźniak & Abramowicz 2001, Abramowicz & Kluźniak 2001) make use of the fact that at particular radii in the disk the orbital and epicyclic frequencies have simple integer ratios or other commensurabilities with each other or with the spin frequency. At these radii resonances may occur which show up in the observations: general relativity itself picks out the frequencies from the disk. Various different physical effects can produce resonance. A type of resonance invoked in some of these models is 'parametric resonance': resonance in a system whose eigenfrequency ν_0 is itself perturbed at a frequency ν_1 commensurate with ν_0 ; resonances occur when $\nu_0/\nu_1 = 2/n$, $n = 1, 2, 3, \dots$.

Various resonant radii have been discussed (Fig. 2.15): the radii where ν_r/ν_ϕ equals 1/2 or 1/3 (Kluźniak & Abramowicz 2001), that where $\nu_r/\nu_\theta = 2/3$ (Kluźniak & Abramowicz 2002; parametric resonance with $n = 3$, the lowest value allowed as $\nu_r < \nu_\theta$), and those where $\nu_\theta = 2\nu_r$ or $\nu_\theta = 3\nu_r$ (Abramowicz & Kluźniak

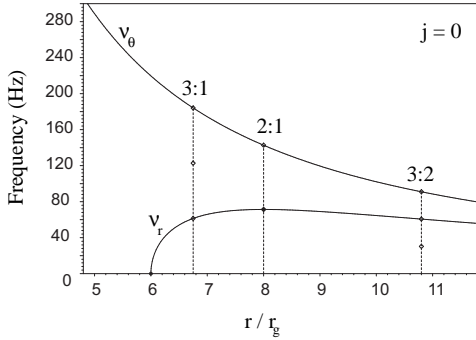


Fig. 2.15. Radial and vertical epicyclic frequencies vs. r/r_g in Schwarzschild geometry. Three resonant radii are indicated. After Abramowicz et al. (2004).

2004) can all be used to explain the observed 2:3 ratios for HF QPOs in black holes (§2.10.1), with other resonant frequencies (1:2:3:5) also being predicted (Klużniak & Abramowicz 2003). Like the ISCO frequencies, all these resonant frequencies are predicted to scale with $1/M$ (Abramowicz et al. 2004), and if the observed resonance is identified they can be used to constrain both M and J .

In the interaction between the neutron-star spin and the disk, resonances could arise as well (e.g., Psaltis 2001, van der Klis 2002). Klużniak et al. (2004) suggest several ways in which the epicyclic frequencies can resonate with spin (either ν_{spin} or $\nu_{\text{spin}}/2$; see also Wijnands et al. 2003 who suggest $\nu_\phi - \nu_r$ equals ν_{spin} or $\nu_{\text{spin}}/2$ and Lee et al. 2004, who consider $\nu_\theta - \nu_r = \nu_{\text{spin}}/2$), which is relevant to neutron-star kHz QPOs and their commensurabilities with the spin frequency (§2.9.1.2), and also point out that disk g-modes (§2.12.1) may resonate in a frequency ratio tending to $\sqrt{2}$, all of which may be relevant to the twin kHz QPOs observed in SAX J1808.4–3658 (§2.9.1.2). Lamb & Miller (2003) propose a resonance at the 'spin-resonance' radius where the spin-orbit beat frequency equals the vertical epicyclic one: $\nu_{\text{spin}} - \nu_\phi = \nu_\theta$; at this radius the pulsar beam stays pointed at particles in the same *phase* (e.g., an antinode) of their vertical epicyclic motion. This radius is sufficiently far out in the disk that $\nu_\phi \approx \nu_\theta$, i.e., $\nu_\phi \approx \nu_{\text{spin}}/2$, which may explain why the observed kHz QPO separation is sometimes the spin frequency, sometimes half that (§2.9.1.2).

The radii at which a resonance condition applies are fixed, so these models in principle produce constant frequencies, which is appropriate to black-hole HF QPOs, but analytic (Rebusco 2004) and numerical (Abramowicz et al. 2003b) work on 'tunable' versions which might be applicable to kHz QPOs has been done. Tunable frequencies can also be produced by beating constant resonant frequencies with a variable one (Lamb and Miller 2003; see §2.8.4). Observationally, the 2:3 ratios in black holes (§2.10.1), the half-spin separation of some kHz QPOs (§2.9.1.2) and the factor ~ 1.45 offsets of some of the frequency correlations in accreting millisecond pulsars (§2.7.1) all suggest that resonances play a role, but it is not yet entirely clear exactly which are the frequency ratios that can occur, when they occur, and what is the incidence

of each ratio. Clarifying this will allow to test the various proposals for frequency commensurabilities that have been put forward.

2.8.4 Beat-frequency models

By 'beating' orbital frequencies with the spin frequency of a central neutron star more frequencies can be produced (e.g., Alpar & Shaham 1985, Lamb et al. 1985, Miller et al. 1998a). This requires that some azimuthally non-uniform structure co-rotating with the spin, e.g., a non-aligned magnetic field or radiation pattern, reaches out to the relevant orbital radius. These models do not work for black holes, for which in view of the no-hair theorem no such structures are expected. Additionally there must be some azimuthal structure in orbit to interact with the spin; the mechanism will not work if the flow is completely axi-symmetric.

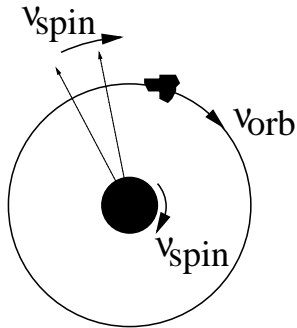


Fig. 2.16. Example of a beat-frequency interaction. The clump orbiting with ν_{orb} periodically overtakes the magnetic-field lines or the pulsar beam that is sweeping around with ν_{spin} . This happens ν_{beat} times per unit of time, where $\nu_{beat} = \nu_{orb} - \nu_{spin}$ is the beat frequency.

Spin-orbit interaction then takes place at the difference frequency between the orbital and spin frequencies: the *beat frequency* $\nu_{beat} = \nu_{orb} - \nu_{spin}$. This is the natural disk/star interaction frequency: the frequency at which a particle orbiting in the disk periodically overtakes a given point on the spinning star. An example of an interaction making ν_{beat} observable would be the periodic illumination of an orbiting blob by a pulsar beam sweeping around at ν_{spin} (Fig. 2.16). Only *one* beat frequency (a 'single sideband') is produced: for prograde orbital motion no signal occurs at $\nu_{orb} + \nu_{spin}$ while for retrograde motion *only* this sum frequency is generated. If the beat interaction occurs at the magnetospheric radius (see §1) of an accreting magnetic star one expects $\nu_{spin} < \nu_{orb}$, but in other settings, if the relevant orbit is sufficiently far out, $\nu_{spin} > \nu_{orb}$ is possible, and for a variable orbital radius ν_{beat} could go through zero.

If there is an n -fold symmetric azimuthal pattern associated with spin and/or orbit, frequency multiples occur (e.g., for 2 pulsar beams $\nu_{beat} = 2(\nu_{orb} - \nu_{spin})$). If spin and orbit have an n_{spin} and n_{orb} -fold symmetry, respectively, then a degeneracy occurs and $\nu_{beat} = \mu(n_{spin}, n_{orb})(\nu_{orb} - \nu_{spin})$, where $\mu(x, y)$ denotes the least common multiple (Wijnands et al. 2003; additionally non-sinusoidal signals include harmonics to the fundamental frequency, and if these also interact a complex spectrum results, Miller et al. 1998a). Usually ν_{orb} is the orbital frequency ν_{ϕ} , but other azimuthal motions, e.g., periastron and nodal precession, could beat with the spin as well.

In the magnetospheric beat-frequency model, the spin interacts with clumps orbiting just outside the magnetosphere (§2.8.5; Alpar & Shaham 1985, see also Alpar & Yilmaz 1997). The model was originally applied to CVs (Patterson 1979) and to the HBO (§2.9.3); similar models have been proposed for kHz QPOs (§2.9.1) by Cui (2000) and Campana (2000). In the sonic-point beat-frequency model for kHz QPOs (Miller et al. 1998a) ν_u and ν_ℓ are identified with respectively ν_ϕ and ν_{beat} at the sonic radius r_{sonic} (§2.8.5). The beat occurs as an X-ray pulsar beam irradiates clumps orbiting at r_{sonic} once per beat period, modulating the rate at which the clumps' material accretes. In its pure form the model predicts $\Delta\nu$ to be constant at ν_{spin} , contrary to observations (§2.9.1.2). However, if the clumps spiral down while their material accretes, $\Delta\nu$ can be less than this (Lamb & Miller 2001). The observation of twin kHz QPOs separated by half the neutron-star spin frequency is inconsistent with this model (see §2.9.1.2). Lamb & Miller (2003) have proposed that a beat-frequency interaction between orbital motion at r_{sonic} and an azimuthal structure at the spin-resonance radius (§2.8.3) explains ν_ℓ (and maintain that $\nu_u = \nu_\phi(r_{sonic})$). So, in this scenario the beat is between two different radii in the disk. With the spin frequencies of an increasing number of low magnetic-field neutron stars in LMXBs becoming known (§2.9.1.2), further testing of the predictions of beat-frequency models for the QPO frequencies in these systems can be expected to put further rigorous constraints on the theoretical possibilities.

This completes the summary of the 'orbital motion' QPO models. How can observations discriminate between these various models? As it turns out, every physical frequency model predicts its own 'fingerprint' set of parasitic, weaker frequencies in addition to the strong ones it set out to explain in the first place (e.g., Miller et al. 1998a). These predicted patterns of weaker frequencies provide a strong test of each model. Searches for such weaker power-spectral features are very difficult because this is really work at (or beyond) the limit of the sensitivity of current instrumentation, and the distinct impression of the observers is that there is still much hiding below the formal detection levels. However, a small number of weak sidebands have been detected in neutron stars (Jonker et al. 2000b, Wijnands et al. 2003; §2.9.1) and the 2:3 ratio HF QPOs in black holes (Strohmayer 2001a, Miller et al. 2001, Remillard et al. 2003; §2.10.1) provide similar constraints on possible models. These detections have led to only a very limited number of proposed precise theoretical explanations in each case (e.g., Psaltis 2000, Klužniak and Abramowicz 2001), an unusual situation that testifies to the discriminating power of such additional frequencies. However, too few of these frequencies have been detected yet for the full power of this method to be applied; more sensitivity to weak timing features is required for this. To some extent these fingerprint patterns depend on the way in which the frequencies physically modulate the X-ray flux; models for this are discussed next.

2.8.5 Preferred radii

In models involving frequencies depending strongly on radius (e.g., of orbital and epicyclic motion), *preferred radii* in the disk are required to produce specific frequencies. Constant and variable radii produce corresponding frequencies. Variable radii usually depend on \dot{M} through disk physics (e.g., r_{mag} , below), whereas constant

radii follow from just the compact object's parameters, perhaps through strong-field gravity effects (e.g., the ISCO radius r_{ms} , §2.8.1 or resonant radii, §2.8.3).

The 'inner edge of the disk' at radius r_{in} , where the near-Keplerian flow ends and the radial velocity becomes appreciable compared to the azimuthal one, provides a natural preferred radius. The density contrast at r_{in} can be sharp, as the radial velocity of the flow can change suddenly (e.g., Miller et al. 1998a); this is a strong-field gravity effect related to the small difference in orbital angular momentum between different radii (see Paczyński 1987). In the absence of magnetic stresses, r_{ms} (for standard thin disks) or r_{mb} (for low radiative efficiency disks such as ADAFs, slim disks and super-Eddington flows; §2.8.1) set a lower limit to the flow, but for magnetized flows predictions are uncertain; e.g., Abramowicz et al. 1978, Liang & Thompson 1980, Lai 1998, Krolik & Hawley 2002, Watarai & Mineshige 2003a). In neutron stars the surface provides a fixed radius R limiting r_{in} ; depending on the EOS may be smaller or larger than r_{ms} , but note that some modulation models (§2.8.7) do not work if the disk actually extends down to the star.

Radiation drag by photons emitted from within r_{in} removing angular momentum from the disk flow through the Poynting-Robertson effect can truncate the flow at radius r_{rad} (Miller et al. 1998a). As the radiation providing the drag is produced by the same accretion flow that it interacts with on the way out, to first order this radius is fixed, but details of flow and scattering geometries can make it variable. According to Miller et al. (1998a) r_{rad} can not be larger than $\sim 15GM/c^2$, and shrinks when \dot{M} increases. For a sufficiently magnetic neutron star, electromagnetic stresses truncate the disk well outside the ISCO and r_{rad} , at the magnetospheric radius (§1) r_{mag} which shrinks when \dot{M} increases; note that according to some authors orbital motion of part of the accreting matter down to r_{rad} still occurs within r_{mag} (e.g., Miller et al. 1998a). Both these disk truncation mechanisms may only work for neutron stars: black holes are not expected to have a sufficiently strong magnetic field (§1), and may also have difficulty to produce a sufficiently strong, and low specific angular-momentum, radiation field from within r_{in} .

Some authors treat the radius of maximum flux from the disk (e.g., Gruzinov 1999) or the radius of maximum pressure in a toroidal flow (Kluźniak et al. 2004) as preferred; in such cases one needs to investigate if the function whose extremum is used to define the radius is sufficiently narrow to produce the observed QPO. Laurent & Titarchuk (2001) proposed an interesting model where just the presence of a Comptonizing converging flow makes one particular disk orbital frequency stand out.

2.8.6 Decoherence

The lack of coherence (aperiodicity) of particular observed frequencies attributed to orbital and epicyclic phenomena is usually taken to more or less naturally follow from the sheared and turbulent nature of the flow, where any feature such as a density enhancement ('clump') or a vortex will have a finite lifetime (see §2.12.3). Although suggested by the Lorentzians used to describe QPO peaks (§2.2), and sometimes implicitly assumed in calculations (e.g., Titarchuk 2002), there is not much evidence that observed signals are produced by a (superposition of) exponentially damped harmonic oscillators. Rapid frequency fluctuations, for example

related to a varying preferred radius (e.g., a clump spiralling in, Stoeger 1980), or superposition of multiple frequencies, e.g., generated from a finite-width disk annulus are alternatives (e.g., Abramowicz et al. 1992, Nowak 1994, Bao & Østgaard 1994). As noted by Belloni et al. (2002a), the distinction (§2.2) between a QPO (with two frequencies, ν_0 and λ) and a BLN (with just one break frequency) becomes much less fundamental when interpreted in terms of the width of a disk annulus than when described in terms of damped harmonic oscillators. This may be why the use of ν_{max} (§2.2) to summarize both cases seems to work empirically.

2.8.7 Modulation

Orbital and epicyclic motions must modulate the X-ray flux for them to be observable. A classic mechanism (Cunningham & Bardeen 1972, Sunyaev 1973; see the end of §2.8.2 for further references) is that of a self-luminous blob orbiting a black hole in general-relativistic spacetime. Doppler boosting and gravitational light bending produce the modulation. Related models that are considered are centrally-illuminated scattering blobs (e.g., Lamb & Miller 2003) and self-luminous turbulent disk flows (e.g., Armitage & Reynolds 2003). Variable obscuration of central emitting regions by matter orbiting further out is often invoked, but is attractive only if the predicted inclination dependencies occur. This is for example the case for the ~ 1 Hz dipper QPOs (§2.9.4), where a similar modulation of all emission (persistent and bursts, different photon energies) further strengthens the case for this mechanism (Jonker et al. 1999).

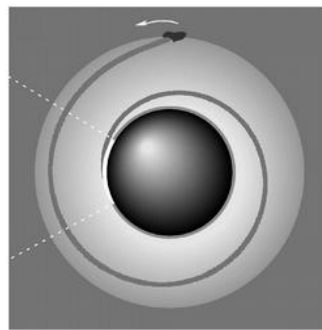


Fig. 2.17. Example of a modulation mechanism (see §2.8.7). The clump with its spiral flow and the emission from the flow's footpoint (dashed lines) in the Miller et al. (1998a) model all rotate at the same angular velocity (that of the clump's orbit), irrespective of the stellar spin, and produce a beaming modulation at that frequency. From Miller et al. (1998a).

A fundamentally different mechanism is modulation of the accretion rate into the inner regions, either taking the form of an actual modulation of total \dot{M} (e.g., Lamb et al. 1985) or affecting only the pattern by which the matter accretes (e.g., Miller et al. 1998a). Likewise, either the total emitted flux can be modulated (*luminosity modulation*), or only its angular distribution (*beaming modulation*). 'Beaming' here is any anisotropy in the emission. Scattering material around the source suppresses a beamed modulation much more effectively than a luminosity modulation (Wang & Schlickeiser 1987, Brainerd & Lamb 1987, Kylafis & Klimis 1987, Bussard et al. 1988, Asaoka & Hoshi 1989, Miller 2000). In magnetospheric beat-frequency models the accretion of matter from orbiting clumps (and hence the luminosity) is modulated at ν_{beat} as accretion is easier near the magnetic poles (Lamb et al. 1985), leading to oscillating shots (§2.2) in which the luminosity oscillates at the

beat frequency and whose lifetime is that of a clump. In the sonic point model of Miller et al. (1998a), material from clumps orbiting at r_{in} gradually accretes following a fixed spiral-shaped trajectory in the frame co-rotating with the clumps (Fig. 2.17) at whose “footpoint” accretion, and hence emission, is enhanced. The resulting hot spot moves around the surface at $\nu_\phi(r_{in})$ irrespective of the star’s spin, and produces a beaming modulation. Both of these models predict surface hot spots (revolving at ν_{spin} or $\nu_\phi(r_{in})$, respectively) whose emission is itself modulated at ν_{beat} , leading to the potential for sideband formation.

Fully specified orbital and epicyclic flux-modulation models make specific predictions for fractional amplitude, harmonic content and sideband pattern, and energy dependencies (see also §2.12.2) of the variability, so there is no lack of stringent tests to distinguish between such models, and hence, the frequency models to which they are appropriate. As the modulation models shape up from the currently still common simple qualitative ideas to quantitatively described mechanisms, it can be expected that many simple models will turn out to need revision.

2.9 Low magnetic-field neutron stars

The main variability components and the correlations between their frequencies have already been summarized in §§2.6 and 2.7. Here (§§2.9–2.10) a more detailed overview of the observed timing properties of neutron stars and black holes, respectively, is provided. Tables 2.5 and 2.6 summarize the literature on neutron stars and reference codes in the current section are linked to those tables; likewise the codes in §2.10 refer to Table 2.7.

2.9.1 Kilohertz quasi-periodic oscillations

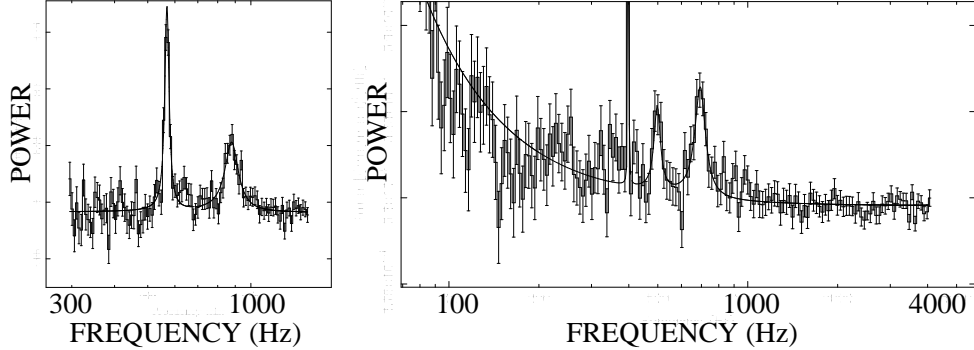


Fig. 2.18. Twin kHz QPOs in *left*: 4U 1608–52 (Méndez et al. 1998b) and *right*: the 401 Hz accreting pulsar SAX J1808.4–3658 (Wijnands et al. 2003; the 401 Hz pulsar spike is seen as well).

kHz QPOs (§2.6.1) are seen in a wide range of low magnetic-field neutron-star sources, including all Z sources, most atoll sources, several transients and two millisecond pulsars (14c,13b), but not the GX atoll sources (§2.4.2), which do not usually

reach the relevant states (§2.5.2.2). Table 2.5 lists all sources with kHz QPOs, as well as those with burst oscillations (§3) or millisecond pulsations (§2.9.1.2).

kHz QPO frequencies increase with source state (S_a , S_z) in all cases. Table 2.4 summarizes the typical frequencies seen in well-covered sources; see §2.7 for the corresponding states. Below ~ 500 Hz L_u turns into a BLN component (§2.6.2) which is seen (also in weak LMXBs) down to frequencies as low as 120 Hz (14e). A 10–20 Hz BLN (L_{low} , §2.6.2) seen in the EIS is sometimes interpreted as a low-frequency version of L_ℓ (4z, but see 14e).

kHz QPO amplitudes increase with photon energy by typically a factor 4 between 3 and > 10 keV (8a,b,g,j,9b,d,11a,19a,g,21a,27a). In similar bands, the QPOs are weaker in the more luminous sources, with 2–60 keV rms amplitudes ranging from nearly 20% in the weakest atoll sources to typically 2–5% in the Z sources (Jonker et al. 2001). They also weaken towards the extremes of their observable range (Fig. 2.19), where often only one peak is detected. At high energy, amplitudes are much higher (e.g., 40% rms > 16 keV in 4U 0614+09; 9d). This has been interpreted in different ways, e.g., as an effect of Comptonization in a central corona (Miller et al. 1998a) and as due to the combination of variable hard flux from a boundary layer with a constant, softer, disk flux (Gilfanov et al. 2003).

Table 2.4. kHz QPO frequencies (Hz)

Atoll & weak LMXBs		Z	
ν_ℓ	ν_u	ν_ℓ	ν_u
	(120)		
	(500)	(200)	(500)
300	600	(300)	600
500	800	500	800
800	1000	800	1000
1000	1200		

Typical observed kHz QPO frequency ranges. Exceptions include narrower ranges in GX 5–1 and GX 340+0 (maximum frequencies are 150–200 Hz less; 7b,16b). Parenthesized values refer to ranges in which usually $Q < 2$.

Peak widths are affected by variations in centroid frequency during the integration. Typical values are several 10–100 Hz, somewhat broader in Z sources than in atoll sources and usually higher-Q at higher frequency. L_ℓ in atoll sources can be very sharp ($Q \sim 100$), then attains excellent signal-to-noise and exhibits soft lags of 10–60 μ s (9c,19c). These lags are opposite to those expected from inverse Compton scattering, so they may originate in the QPO production mechanism rather than in propagation delays.

Weak sidebands 50–64 Hz above ν_ℓ with powers ~ 0.1 that of L_ℓ have been detected in three objects (Jonker et al. 2000b), as well as an additional high-frequency QPO peak 8–12 Hz above the 401 Hz pulse frequency in SAX J1808.4–3658 (Wijnands et al. 2003). In both cases the separation between main peak and sideband increased with QPO frequency, but was different from simultaneous LF QPO frequencies, complicating interpretation. These sidebands are the first examples of the “fingerprints” of weaker parasitic frequencies expected to accompany the kHz QPOs in all models (§2.8). Lense-Thirring precession, orbital motion within the inner disk edge (Jonker

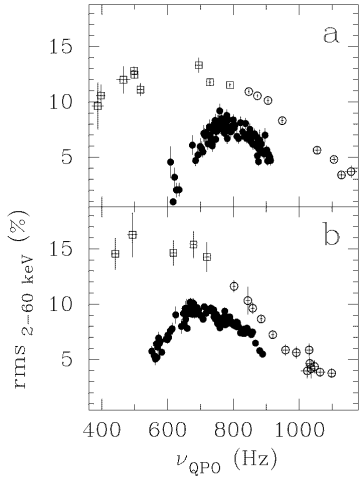


Fig. 2.19. Lower (filled symbols) and upper (open symbols) kHz QPO amplitudes as a function of their frequency for (a) 4U 1728-34 and (b) 4U 1608-52 (Méndez et al. 2001).

et al. 2000b) and relativistic disk-oscillation modes (Psaltis 2000) have been considered as explanations.

2.9.1.1 Relation with luminosity

On time scales of hours and in a given source kHz QPO frequency ν typically correlates well with L_x , but, remarkably, on longer time scales, and across sources, this ν - L_x correlation is lost, with the result that similar QPO frequencies are observed over two orders of magnitude in L_x (e.g., van der Klis 1997, 8b,9a; §2.5). Due to this, parallel tracks form in ν - L_x diagrams covering either (i) several sources (Fig. 2.20a), or (ii) several observations of a single source separated by $\gtrsim 1$ day (Fig. 2.20b). In a given source, QPO amplitude is affected much less by the L_x shifts between tracks than predicted if the shifts were caused by an extra source of X-rays unrelated to the QPOs (8g). This is also true across sources.

That different sources have different ν - L_x tracks might be because ν depends not only on L_x , but also (inversely) on a parameter related to average L_x (e.g., van der Klis 1997, 1998, Zhang et al. 1997b), such as magnetic-field strength B (White & Zhang 1997) which previously, on other grounds, was hypothesized to correlate to average L_x (e.g., Hasinger & van der Klis 1989). Alternatively, the two parallel-track phenomena might be explained *together* by noting that kHz QPO frequency seems to be governed not by L_x , but by how much L_x deviates from its time average $\langle L_x \rangle$ over a day or so (van der Klis 1999). This could arise if there is an L_x component (e.g., due to nuclear burning or the accretion of a radial inflow) that is proportional to some *time average* over the inner-disk accretion rate \dot{M}_d , whose effect is to make the frequency lower (e.g., via the Miller et al. 1998a radiative disk-truncation mechanism; §2.8.5). Frequency would then scale with \dot{M}_d/L_x where $L_x = \dot{M}_d + \alpha \langle \dot{M}_d \rangle$, with α the relative efficiency of the additional energy release (cf., §2.5). Simulations of this toy model (van der Klis 2001) reproduce the salient features of the observed

Table 2.5. Kilohertz QPOs and neutron-star spin

Source	kHz QPOs	$\Delta\nu$ (Hz)	ν_{burst} (Hz)	ν_{pulse} (Hz)	$\frac{\Delta\nu}{\nu_{spin}}$	Rem.	References
Millisecond pulsars							
XTE J0929-314	—	—	—	185	—	T	10a;14e
XTE J1751-305	—	—	—	435	—	T	12a;14e
XTE J1807-294	2	~190	—	191	~0.99	T	13a,b
SAX J1808.4-3658	3 ^a	195	401	401	0.49	T	14a-e
XTE J1814-338	—	—	314	314	—	T	15a,b;14e
Z sources							
Sco X-1 (1617-155)	2	245-310	—	—	—		4a-f,z,9g,h
GX 340+0 (1642-455)	2	280-410	—	—	—		16a,b;4f,z;8j;9g,h
GX 349+2 (1702-363)	2	265	—	—	—		17a-c
GX 5-1 (1758-250)	2	240-350	—	—	—		7a,b;4f,z;9g,h
GX 17+2 (1813-140)	2	240-300	—	—	—		11a-d;4f;9g,h
Cyg X-2 (2142+380)	2	345	—	—	—		3a,b;4f,z;9g,h
Atoll sources							
4U 0614+09	2	240-360	—	—	—		9a-h;4f;22h
2S 0918-549	1	—	—	—	—		18a
4U 1608-52	3 ^b	225-325	619	—	0.36-0.53	T	8a-j,t;4f;9c,e,g,h
4U 1636-53	3 ^b	240-330	582	—	0.41-0.57		19a-g;4f;8f,t;9c,g,h
4U 1702-43	2	320-340	330	—	0.97-1.03		20a;9h
4U 1705-44	1	—	—	—	—	T	21a,b;9h
4U 1728-34	3 ^b	275-350	363	—	0.76-0.96		22a-h;4f;8f,g,t;9g,h
KS 1731-260	2	260	524	—	0.50	T	23a;4f;9g,h
4U 1735-44	2	295-340	—	—	—		24a,b;4f;9h
SAX J1750.8-2900	2 ^c	317 ^c	601	—	—	T	32a
4U 1820-30	2	220-350	—	—	—	G	25a-e;4f;9g,h
Aql X-1 (1908+005)	1	—	549	—	—	T	26a-e;8g,t;9g,h
4U 1915-05	2	290,350 ^g	272	—	1.07,1.29 ^g	D	33a,d
XTE J2123-058	2	255-275	—	—	—	T	34a,b
Other sources^d							
EXO 0748-676	1	—	—	—	—	T,D	27a
MXB 1659-298	—	—	567	—	—	T,D	28a
XTE J1723-376	1 ^e	—	—	—	—	T	29a
MXB 1743-29	—	—	589	—	—	f	30a;9g
SAX J1748.9-2021	—	—	410	—	—	T,G	31a

References see Table 2.6. kHz QPOs: number of kHz QPO peaks and sidebands with $Q \geq 2$; ν_{burst} : see also §3.4. Remarks: T: transient; D: dipper; G: in globular cluster. Notes: ^a Sideband to pulsation, ^b Sideband to lower kHz QPO, ^c Second QPO tentative, ^d Faint, transient, unidentified, etc., and not unambiguously classified, ^e QPO not confirmed, ^f Source identification uncertain, ^g Two incompatible values of $\Delta\nu$ reported, 33a.

parallel tracks seen in Fig. 2.20; testing this requires sustained monitoring of the $\nu-L_x$ correlation.

kHz QPOs are sensitive to very short-term L_x variations as well. In Sco X-1 amplitudes and frequencies systematically vary on sub-second time scales, in phase with the 6-Hz flux variations of the NBO (§2.9.4; 4d). In 4U 1608-52, kHz QPO frequency ν has been observed to increase, as usual, with \dot{M} -induced L_x increases, but to decrease in response to probable nuclear-burning ('mHz' QPO, §2.9.4) induced L_x increases (8h), confirming a prediction of the Miller et al. (1998a) model, where the QPO occurs at ν_ϕ of the inner disk radius r_{in} (§2.8.5) which increases in response to the extra, nuclear-burning generated luminosity component.

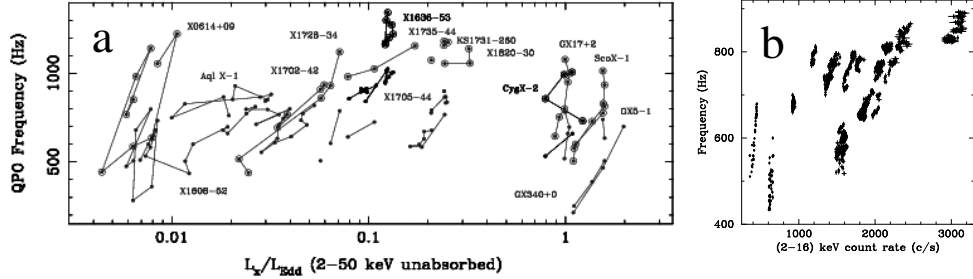


Fig. 2.20. The two parallel tracks phenomena. (a) Across sources (Ford et al. 2000; upper and lower kHz peaks are indicated with different symbols). (b) In time, in the source 4U 1608–52 (Méndez et al. 1999), frequency plotted is ν_ℓ .

2.9.1.2 Relation with neutron-star spin

Peak separation $\Delta\nu$ usually decreases with increasing kHz QPO frequency ν (Fig. 2.21a; 4b,c,7b,8d,19f,22c). In the two cases where a probable positive $\nu-\Delta\nu$ correlation occurred, this was at the lowest detectable frequencies (11b,22f).

$\Delta\nu$ is approximately commensurate with ν_{spin} (Table 2.5), and this is the main motivation for beat-frequency models (§2.8.4). Of course, $\Delta\nu$ varies so any commensurability can not be exact. Spin is measured directly in millisecond pulsars; also, burst oscillations (as verified in two msec pulsars; 14b,d,15b) likely occur very near ν_{spin} (§3). In the eight sources where both $\Delta\nu$ and spin were measured by one of these two methods (Table 2.5), $\Delta\nu$ was between 0.7 and 1.3 times ν_{spin} for $\nu_{\text{spin}} < 400$ Hz, and 0.36–0.57 times ν_{spin} for $\nu_{\text{spin}} > 400$ Hz (Fig. 2.21b); the largest offsets of the ratios from 1.0 and 0.5, respectively, are $\sim 8\sigma$ but usually the discrepancies are much less. In the two pulsars the ratios are 0.49 and 0.99. So, a commensurability with spin does indeed seem to exist where $\Delta\nu \approx \nu_{\text{spin}}$ for low, and $\Delta\nu \approx \nu_{\text{spin}}/2$ for high ν_{spin} .

That the spin frequency can be twice $\Delta\nu$ was initially suspected based on measurements of burst oscillations, where an alternative explanation, namely that $\nu_{\text{burst}} = 2\nu_{\text{spin}}$ could not be excluded (see §3). However, the case of the 401 Hz pulsar SAX J1808.4–3658 now leaves little doubt that $\Delta\nu$ can indeed be half the spin frequency (Wijnands et al. 2003). This falsifies the direct spin-orbit beat-frequency interpretation (§2.8.4) even when allowing for multiple neutron-star hot spots or orbiting clumps, but may be explained by models involving resonances, perhaps combined with a beat (§2.8.3; 14c). Sixteen low magnetic-field neutron-star spins have now been measured (thirteen burst oscillations and five msec pulsars, with an overlap of two sources), and ten more spins are known up to a factor of two. Table 2.5 lists these 26 objects. The spin frequencies are between ~ 200 and ~ 700 Hz, suggesting a cut off well below the limit set by observational constraints and indicating that a braking mechanism limits ν_{spin} (see Chakrabarty et al. 2003). If the stars spin at the magnetospheric equilibrium spin rates (§1) corresponding to their current L_x , this predicts a tight correlation between L_x and magnetic-field strength B (White &

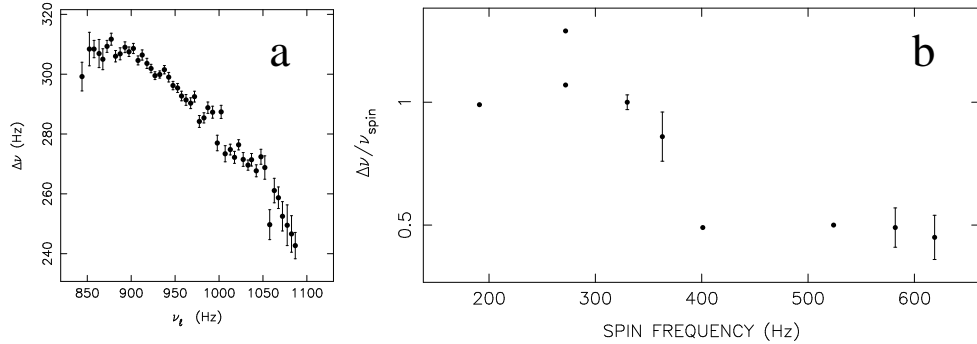


Fig. 2.21. (a) The variation in kHz QPO peak separation as a function of the lower kHz QPO frequency in Sco X-1, after Méndez & van der Klis (1999); (b) $\Delta\nu/\nu_{\text{spin}}$ vs. ν_{spin} , after Table 2.5. Vertical bars indicate the range of variation in $\Delta\nu$.

Zhang 1997; a similar possibility came up to explain the similar kHz QPO frequencies at very different L_x , §2.9.1.1). Another possibility is that gravitational radiation limits ν_{spin} by transporting angular momentum out as fast as accretion is transporting it in; this predicts these sources to be the brightest gravitational-wave sources, with a known ν_{spin} facilitating their detection (Bildsten 1998, Andersson et al. 1999, 2000, also Levin 1999, and e.g., Rezzolla et al. 2000, Bildsten & Ushomirsky 2000, Brown & Ushomirsky 2000, Ushomirsky et al. 2000, Yoshida & Lee 2001, Wagoner 2002).

Some caution is advised in interpreting the SAX J1808.4–3658 kHz QPO result, as the twin peaks were observed only once in this pulsar, its $\Delta\nu$ (195 Hz) is lower than in non-pulsars, and other commensurabilities also exist between the observed frequencies (14c). kHz QPOs in XTE J1807–294 have a $\Delta\nu$ close to its 191 Hz spin frequency (13b). The frequency correlations of some pulsars are a factor ~ 1.45 off the usual ones (§2.7). Clearly, further detections of twin kHz QPOs in millisecond pulsars would help to clarify the systematics in this phenomenology. While the kHz QPO frequency ratio ν_l/ν_u is certainly not constant, Abramowicz et al. (2003c) propose that ratios near 2:3 may occur more often than others, which might provide a link with black-hole high-frequency QPOs.

2.9.1.3 Interpretations

kHz QPO models include beat-frequency, relativistic precession and relativistic resonance models (§2.8) as well as disk-oscillations and other flow instabilities (§2.12). All proposals involve plasma motion in the strong-field region, and with one exception (photon bubbles, §2.12.4) in all models the QPOs originate in the disk. Most identify ν_u with orbital motion at a preferred radius in the disk (in models of Titarchuk and co-workers ν_l has this role), Fig. 2.13 illustrates the constraints the orbital-motion hypothesis provides on neutron-star parameters. The highest measured ν_u of 1329 ± 4 Hz in 4U 0614+09, when interpreted as ν_ϕ for $j = 0$, implies

$M_{NS} < 1.65M_{\odot}$ and $R_{NS} < 12.4$ km, imperiling the hardest equations of state; for a 300 Hz spin these numbers become $1.9M_{\odot}$ and 15.2 km (van Straaten et al. 2000).

The maximum kHz QPO frequencies in well-studied sources are constrained to a relatively narrow range of $\nu_u = 850$ –1330 Hz. If this is the ISCO frequency ν_{ms} (§2.8.1), the neutron-star masses are near $2M_{\odot}$ (Zhang et al. 1997b, see also Kaaret et al. 1997). An apparent leveling off of ν_u as a function of count rate, flux and S_a at ~ 1060 Hz was found in 4U 1820–30 (25b-d), but further observations cast doubt on this (25e). A tendency to level off (but without a true 'ceiling') may be a general feature of the parallel-tracks phenomenon (cf., Fig. 2.20); indeed, the toy model described in §2.9.1.1 predicts such a pattern as a consequence of ν_u depending on $M_d/\langle \dot{M}_d \rangle$.

Calculations exploring to what extent kHz QPOs constrain the EOS, usually assuming $\nu_u = \nu_{\phi}$, have further been performed by e.g., Miller et al. (1998b), Datta et al. (1998, 2000), Akmal et al. (1998), Klužniak (1998), Bulik et al. (1999, 2000), Thampan et al. (1999), Li et al. (1999), Schaab & Weigel (1999), Kalogera & Psaltis (2000), Stergioulas et al. (1999), Heiselberg & Hjorth-Jensen (1999), Zdunik et al. (2000), Glendenning & Weber (2001), Gondek-Rosinska et al. (2001), Ouyed (2002) and Mukhopadhyay et al. (2003).

The evidence for orbital motion as the cause of kHz QPOs is not yet iron-clad. Orbital motion could be empirically demonstrated by a number of different possible measurements, such as independent measurements of frequency and orbital radius, where radius could be measured from continuum or line spectroscopy, demonstrating the predicted frequency - radius relation, measurements of orbital and epicyclic frequencies varying together in the way predicted by general relativity, measurements of the Doppler effect in an orbiting hot spot or measurements of the orbital frequency ceiling predicted at the ISCO. Indications for some of these possibilities have already been obtained.

2.9.2 Hectohertz QPOs

Figs. 2.6 and 2.8 show examples of hHz QPOs, and Fig. 2.9 illustrates their approximately constant frequencies (§2.6.1) in the 100–200 Hz range. hHz QPOs occur in atoll sources (including the millisecond pulsar SAX J1808.4–3658) when $\nu_b \gtrsim 1$ Hz (8i,9f,14a, e,21b,22b,e,f,g,h,26e, see also Fragile et al. 2001), but have not been seen in most weak LMXBs (which may not reach the relevant states) nor in black holes. It may also occur in Z sources (e.g., 11g). At low ν_b (~ 0.2 Hz) confusion occurs with L_u . The phenomenon is usually rather low-Q, but occasionally peaks up to $Q > 2$, has an amplitude between 2 and 20% (rms) and becomes weaker and more coherent as ν_b rises. The near-constant frequency allows diskoseismic modes as a model (§2.12.1) and suggests a link with black-hole HF QPOs (see §2.6.1). Fragile et al. (2001) suggest ν_{hHz} could be the orbital frequency at the radius where a warped disk is forced to the equatorial plane by the (strong-field gravity) Bardeen & Petterson (1975) effect. Titarchuk (2003) proposed Rayleigh-Taylor gravity waves at the disk-star boundary layer as the origin of hHz QPOs (cf. Brugmans 1983).

2.9.3 The low-frequency complex

Components of the low-frequency complex have been studied in Z and atoll sources since the 1980's (e.g., 7c,3B; van der Klis 1995a for a review). The 15–60 Hz LF QPO in the Z-source HB and upper NB (the 'horizontal branch oscillation' or HBO) and the 0.1–30 Hz BLN component (formerly called 'low-frequency noise' or LFN in Z sources and confusingly, sometimes 'high-frequency noise' in atoll sources, 3B,8l) were first detected in GX 5–1 (7c); HBO harmonics were sometimes seen (e.g., 11g). Frequencies were found to correlate with spectral state (4i-l,n,7e,i,j,38a,b,3h,q,y,B, 11f-i,19h). The variations were spectrally hard (e.g., 16d,7i,k), and the HBO showed hard lags of a few ms (e.g., 7f,k). Similarities with black-hole LS and VHS variability were pointed out (e.g., van der Klis 1994a,b, 8l,m). The BLN was sometimes peaked (in atoll sources, e.g., 38a,b,25f,g, and in Z sources, e.g., 11b,17d,4k,n), but in atoll sources QPOs were only rarely seen (25g,8l). The classic Z and atoll tracks in CDs and HIDs (§2.5.2) were known (3B and e.g., 19h,7i,j), but the fainter EIS was hardly explored (e.g., 8k,21c,19i).

In recent work, with the exploration of the fainter sources and states, similarities in the phenomenology across source types were clarified (§2.6), with the frequency correlations between, and among, kHz and LF phenomena (§2.7) particularly revealing (e.g., 4a,b,e,24b,3a,20a,33a,16b,7b,11b,3b,s,22g,21b,26e), and the EIS–LS match confirmed (§2.5). This led to the synthesis summarized in §§2.6.2 and 2.7 (4f,y,z,9c,f,11c,22g,h,8i,14e). Clear examples of LF QPOs were found in atoll sources (23a,39a,24a,20a,9f,33a,22g,h,21b,26e,11c,8i) and millisecond pulsars (14e) and these were incorporated into the general picture, although the phenomenology of these QPOs is not yet entirely clear, with apparently both L_b and L_h often producing a narrow ($Q > 2$) peak when they move to high (> 30 Hz) frequency, and indications for two harmonically related QPOs in the 0.2–2 Hz range (and once near 80 Hz) very roughly a factor 2 below ν_h (8i,l,11c,14e).

Models for LF QPO (particularly, the Z-source HBO) include the magnetospheric beat-frequency model (§2.8.4), Lense-Thirring precession (§2.8.2) and various disk oscillations (§2.12.1), e.g., the magnetically warped precessing-disk model (Lai 1999, Shirakawa & Lai 2002a). The frequency correlations among low-frequency complex phenomena and with kHz QPOs, and in particular the factor ~ 1.5 shifts observed in those relations in some millisecond pulsars (§2.7.1) are among the main observational features to be accounted for in model scenarios, but presently are too fresh to have affected the models reported here.

2.9.4 Other phenomena

A 1–3% rms $Q \sim 2$ QPO near 6 Hz occurs in Z sources in the NB (e.g., 4h,i,j,n,11b,g,i,3h,r,7b,i,j,l,3o,16b). $\sim 180^\circ$ energy-dependent phase lags occur in some of these QPOs which can be interpreted in terms of a quasi-periodically pivoting X-ray spectrum with a pivot point between 3 and 7 keV (3g,r,4o,7m). In some sources, this 'normal branch oscillation' or NBO seems to jump to 10–20 Hz when the source moves into the FB (e.g., 4j,l,n,11g,i) while in others it disappears. The 6–14 Hz QPOs rarely seen at the tip of the UB in some atoll sources may be related to this N/FBO (25h,45a,47a,26e). In Z sources the phenomenon has been modeled as a radiation-force feedback instability in spherical near-Eddington accretion (Fortner et al. 1989),

Table 2.6. *Neutron-star variability and states (a.)*

Source	HB/NB/FB	LF noise	HB/N-FB/kHz QPOs	References
Z sources				
Sco X-1 (1617–155)	○/●/○	●	●/○/●	4a-A;3A,B;9g,h
GX 340+0 (1642–455)	●/○/●	●	●/○/●	16a-e;3A,B;4y,z;8j,r;9g,h
GX 349+2 ^a (1702–363)	○/●/○	●	○/-/●	17a-j;3A,B
GX 5–1 (1758–250)	●/○/●	●	●/○/●	7a-q;3A,B;4f,y,z;9g,h;8r
GX 17+2 (1813–140)	●/○/●	●	●/○/●	11a-l;3A,B;4f,x,y;9g,h;8r
Cyg X-2 (2142+380)	●/○/●	●	●/○/●	3a-B;4f,n,x-z;7d,f;8r;9g,h
Z source candidates^a				
RX J0042.6+4115	○/○/○	-	-/-/-	35a
LMC X-2 (0521–720)	○/○/○	-	-/-/-	36a-c
Cir X-1 (1516–569)	○/○/○	●	●/-/-	37a-j;4f,x;11c

HB: horizontal branch, NB: normal branch, FB: flaring branch. ●: variability of this type observed, ○: some doubt (uncertain,ambiguous, atypical, rare and not clearly seen, etc.), -: not reported. Note:

^a Z/atoll character somewhat ambiguous, or evidence incomplete.

but detections in atoll sources occur at luminosities well below Eddington. Disk oscillation models for NBO have also been proposed (e.g., Alpar et al. 1992, Wallinder 1995).

An $\alpha = 1.2\text{--}2$ power-law component called very-low frequency noise (VLFN) with an rms amplitude of usually a few percent often dominates the variability $\lesssim 1\text{ Hz}$. This component is detected in all Z (e.g., 7b,f,i,j,4j,l,n,11b,g,i,3h,o,17c,e,f) and atoll sources (e.g., 9f,19d,22g,25f,8i), including some faint and/or transient sources (31a,47a,b) as well as the Rapid Burster and Cir X-1 (§2.9.5). It is rarely detected in the EIS and usually becomes stronger (up to typically 6% rms but sometimes much stronger, 7b) and often also steeper (up to $\alpha=2$) towards higher states. It has been variously ascribed to accretion-rate variations and unsteady nuclear burning (§2.12.4). In recent work, breaks and broad $<1\text{ Hz}$ Lorenzians have sometimes been detected in the VLFN range (e.g., 39b,26e,38h), which provides some support for models that produce the VLFN from a superposition of finite events such as nuclear 'fires' (Bildsten 1995).

In X-ray dip sources (§1), a 0.6–2.4 Hz QPO occurs (41a,27b,40a) which, contrary to nearly all other variability has an amplitude (5–10% rms) that hardly depends on photon energy. Its occurrence in dippers suggests a link with high system inclination; the QPO persists at near-constant fractional amplitude right through X-ray bursts and dips, so quasi-periodic obscuration of central emitting regions by structure above the plane of the disk is an attractive model (cf. 3z). Titarchuk & Osherovich (2000) proposed a specific global normal disk mode that might accomplish this. The 401 Hz pulsar SAX J1808.4–3658 in the late decay of its outbursts sometimes exhibits violent $\sim 1\text{ Hz}$ highly non-sinusoidal flaring (14e,j,k) the nature of which is unclear.

Revnivtsev et al. (2001a) discovered 'mHz' (0.007–0.009 Hz) QPOs that only occurred in a very particular L_x range and at energies $<5\text{ keV}$ in 4U 1608–52 and 4U 1636–53 and interpreted them as possible variations in nuclear burning on the

Table 2.6. Neutron-star variability and states (b.)

EIS/IS/B	Strong BLN	LF/kHz/kHz QPOs	References
Millisecond pulsars			
XTE J0929-314	•/-/-	•	10a;14e
XTE J1751-305	○/-/-	•	12a;14e,j
XTE J1807-294	-/-/○	-	13a,b;14j
SAX J1808.4-3658	●/○/○	•	14a-k;4x,y;8q
XTE J1814-338	○/-/-	•	15a-c;14e,j
Atoll sources			
4U 0614+09	●/○/●	•	9a-k;4f,y;8q;22h
2S 0918-549	○/○/○	•	18a
4U 1608-52	●/○/●	•	8a-t;4x,y;3B;9c,e,g,h
4U 1636-53	○/○/○	•	19a-j;3B;8f,m,p,t;9c,g,h
4U 1702-43	-/-/○	○	20a,b;8p;9h
4U 1705-44	●/○/○	•	21a-e;3B;4x,y;8m,q-s;9h,l
4U 1728-34 (GX354-0)	●/○/●	•	22a-j;3B;4f,y;8f,g,p-r,t;9g,h
GX 9+9 (1758-169)	-/-/○	-	3A,B;38h
KS 1731-260	-/-/○	-	23a,b;4f;8p,q;9g,h
4U 1735-44	-/○/○	-	24a-e;3B;4f,y;9h
GX 3+1 (1744-265)	-/-/○	-	38a-h;3A,B
SAX J1750.8-2900	-/○/○	-	32a
GX 9+1 (1758-205)	-/-/○	-	3A,B;38h
GX 13+1 (1811-171) ^a	-/○/○	-	39a-d;3A,B;8r
4U 1820-30 (NGC6624)	-/○/○	-	25a-i;3B;4f;8r;9g,h
Ser X-1 (1837+049)	-/-/○	-	38c;8r;25i
Aql X-1 (1908+00)	●/○/●	•	26a-f;4x;8g,p,r,s;9g,h
4U 1915-05	○/○/○	○	33a-d
XTE J2123-058	○/○/●	-	34a,b
Weak LMXBs / atoll source candidates^b			
EXO 0748-676	-/○/○	-	27a,b
4U 1323-62	-/-/-	-	41a
MXB 1659-298	○/-/○	-	28a,b
XTE J1709-267	-/-/-	•	42a
XTE J1723-376	-/-/-	-	29a
1E 1724-3045 (Ter 2)	●/-/-	•	43a;4f,y;8q;11c;14e;23b
MXB 1730-335 (Lil 1; RB)	-/-/-	•	44a-m
SLX 1735-269	●/-/-	•	45a;8q;11c;14e;23b
4U 1746-37 (NGC6441)	-/○/●	-	40a
GRS 1747-312 (Ter 6)	-/○/-	-	46a
SAX J1748.9-2021 (NGC6440)	-/-/○	-	31a,b
XTE J1806-246	○/○/○	•	47a,b
4U 1812-12	-/-/-	•	48a
GS 1826-238	●/-/-	•	49a;4f;8q,r;11c;14e;23b
4U 1850-08 (NGC6712)	-/○/-	-	50a

EIS: extreme island state, IS: island state, B: banana state. •: variability of this type observed, ○: some doubt (uncertain, ambiguous, atypical, rare and not clearly seen, etc.), -: not reported. Strong BLN: > 15% rms. RB: rapid burster. Notes: ^a Z/atoll character somewhat ambiguous, ^b Evidence incomplete, ^c ~1 Hz 'dipper' QPO, §2.9.4.

neutron-star surface (cf., §3). These QPOs have been found to affect the kHz QPOs (8h, §2.9.1.1).

2.9.5 Peculiar low magnetic field neutron stars

Cir X-1, apart from behaviour attributed to periodic surges of mass transfer at periastron in its 17-d highly eccentric orbit and ill-understood long-term changes (Murdin et al. 1980 and references therein), is also peculiar in that it sometimes seems

-
- References in Table 2.6a and b: 3a Wijnands et al. 1998a, 3b Kuznetsov 2002a, 3c Branduardi et al. 1980, 3d Hasinger et al. 1986, 3e Norris & Wood 1987, 3f Hasinger 1987, 3g Mitsuda & Dotani 1989, 3h Hasinger et al. 1990, 3i Vrtilek et al. 1990, 3j Chiapetti et al. 1990, 3k Hjellming et al. 1990a, 3l Hirano et al. 1995, 3m Kuulkers et al. 1995, 3n Focke 1996, 3o Wijnands et al. 1997c, 3p Smale 1998, 3q Kuulkers et al. 1999, 3r Wijnands & van der Klis 2001, 3s Kuznetsov 2001, 3t Piraino et al. 2002, 3u O'Brien et al. 2004, 3v di Salvo et al. 2002, 3w Done et al. 2002, 3x Vrtilek et al. 2003, 3y Kuulkers et al. 1996, 3z Kuulkers & van der Klis 1995, 3A Schulz et al. 1989, 3B Hasinger & van der Klis 1989, 3C Dubus et al. 2003; 4a van der Klis et al. 1996, 4b van der Klis et al. 1997, 4c Méndez & van der Klis 2000, 4d Yu et al. 2001, 4e Kuznetsov 2002b, 4f Psaltis et al. 1999a, 4g Illovaisky et al. 1980, 4h Middleditch & Priedhorsky 1986, 4i Priedhorsky et al. 1986, 4j van der Klis et al. 1987b, 4k Hasinger et al. 1989, 4l Hertz et al. 1992, 4m Kallman et al. 1998, 4n Dieters & van der Klis 2000, 4o Dieters et al. 2000a, 4p White et al. 1985, 4q Hjellming et al. 1990b, 4r Vrtilek et al. 1991, 4s Augusteijn et al. 1992, 4t Barnard et al. 2003a, 4u McNamara et al. 2003, 4v Santolamazza et al. 2003, 4w Bradshaw et al. 2003, 4x Done & Gierliński 2003, 4y Wijnands & van der Klis 1999a, 4z Psaltis et al. 1999b, 4A Canizares et al. 1975, 4B Robinson & Warner 1972; 7a Wijnands et al. 1998c, 7b Jonker et al. 2002a, 7c van der Klis et al. 1985, 7d Elsner et al. 1986, 7f van der Klis et al. 1987a, 7f van der Klis et al. 1987c, 7g Norris et al. 1990, 7h Mitsuda et al. 1991, 7i Lewin et al. 1992, 7j Kuulkers et al. 1994, 7k Vaughan et al. 1994, 7l Kamado et al. 1997, 7m Vaughan et al. 1999, 7n van der Klis et al. 1991, 7o Tan et al. 1992, 7p Blom et al. 1993, 7q Asai et al. 1994; 8a Berger et al. 1996, 8b Yu et al. 1997, 8c Méndez et al. 1998a, 8d Méndez et al. 1998b, 8e Méndez et al. 1999, 8f Jonker et al. 2000b, 8g Méndez et al. 2001, 8h Yu & van der Klis 2002, 8i van Straaten et al. 2003, 8j Gilfanov et al. 2003, 8k Mitsuda et al. 1989, 8l Yoshida et al. 1993, 8m Berger & van der Klis 1998, 8n Revnivtsev et al. 2001a, 8o Gierliński & Done 2002a, 8p Muno et al. 2004, 8q Sunyaev & Revnivtsev 2000, 8r Muno et al. 2002, 8s Gierliński & Done 2002b, 8t Méndez 1999; 9a Ford et al. 1997a, 9b Ford et al. 1997b, 9c Vaughan et al. 1997, 1998, 9d Méndez et al. 1997, 9e Kaaret et al. 1998, 9f van Straaten et al. 2000, 9g Psaltis et al. 1998, 9h Ford et al. 2000, 9i Ford et al. 1999, 9j Méndez et al. 2002, 9k Singh & Apparao 1994; 10a Galloway et al. 2002; 11a Wijnands et al. 1997b, 11b Homan et al. 2002, 11c Belloni et al. 2002a, 11d Kuulkers et al. 2002, 11e Stella et al. 1987b, 11f Langmeier et al. 1990, 11g Penninx et al. 1990, 11h Wijnands et al. 1996, 11i Kuulkers et al. 1997a, 11j Penninx et al. 1988, 11k di Salvo et al. 2000; 12a Markwardt et al. 2002; 13a Markwardt et al. 2003, 13b Markwardt 2004 priv. comm; 14a Wijnands & van der Klis 1998b, 14b in 't Zand et al. 2001, 14c Wijnands et al. 2003, 14d Chakrabarty et al. 2003, 14e van Straaten et al. 2004, 14f Uttley 2004, 14g Wijnands & van der Klis 1998a, 14i Menna et al. 2003, 14j Gierliński et al. 2002, 14j Wijnands 2004, 14k van der Klis et al. 2000; 15a Markwardt & Swank 2003, 15b Strohmayer et al. 2003, 15c Wijnands & Homan 2003; 16a Jonker et al. 1998, 16b Jonker et al. 2000a, 16c van Paradijs et al. 1988a, 16d Penninx et al. 1991, 16e Oosterbroek et al. 1994; 17a Zhang et al. 1998a, 17b Kuulkers & van der Klis 1998, 17c O'Neill et al. 2002, 17d Ponman et al. 1988, 17e O'Neill et al. 2001, 17f Agrawal & Bhattacharyya 2003, 17g di Salvo et al. 2001b, 17h Agrawal & Sreekumar 2003, 17i Iaria et al. 2004; 18a Jonker et al. 2001; 19a Zhang et al. 1996a,b; 19b Méndez et al. 1998c, 19c Kaaret et al. 1999a, 19d di Salvo et al. 2003, 19e Méndez 2002a, 19f Jonker et al. 2002b, 19g Wijnands et al. 1997a, 19h Prins & van der Klis 1997, 19i van der Klis et al. 1990, 19j Damen et al. 1990; 20a Markwardt et al. 1999a, 20b Oosterbroek et al. 1991; 21a Ford et al. 1998a, 21b Olive et al. 2003, 21c Langmeier et al. 1989, 21d Langmeier et al. 1987, 21e Barret & Olive 2002; 22a Strohmayer et al. 1996, 22b Ford & van der Klis 1998, 22c Méndez & van der Klis 1999, 22d Piraino et al. 2000, 22e Migliari et al. 2003a, 22f Migliari et al. 2003b, 22g di Salvo et al. 2001a, 22h van Straaten et al. 2002, 22i van Straaten et al. 2001, 22j Franco 2001; 23a Wijnands & van der Klis 1997, 23b Barret et al. 2000; 24a Wijnands et al. 1998b, 24b Ford et al. 1998b, 24c Penninx et al. 1989, 24d van Paradijs et al. 1988b; 24e Corbet et al. 1989; 25a Smale et al. 1997, 25b Zhang et al. 1998b, 25c Kaaret et al. 1999b, 25d Bloser et al. 2000a, 25e Méndez 2002b, 25f Dotani et al. 1989, 25g Stella et al. 1987a, 25h Wijnands et al. 1999a, 25i Migliari et al. 2004; 26a Zhang et al. 1998c, 26b Cui et al. 1998a, 26c Yu et al. 1999, 26d Reig et al. 2000a, 26e Reig et al. 2004, 26f Yu et al. 2003; 27a Homan & van der Klis 2000, 27b Homan et al. 1999b; 28a Wijnands et al. 2001b, 28b Wijnands et al. 2002b; 29a Marshall & Markwardt 1999; 30a Strohmayer et al. 1997; 31a Kaaret et al. 2003, 31b in 't Zand et al. 1999a; 32a Kaaret et al. 2002; 33a Boirin et al. 2000, 33b Bloser et al. 2000b, 33c Narita et al. 2003, 33d Galloway et al. 2001; 34a Homan et al. 1999a, 34b Tomsick et al. 1999; 35a Barnard et al. 2003b; 36a Smale & Kuulkers 2000, 36b Smale et al. 2003, 36c McGowan et al. 2003; 37a Tennant 1987, 37b Tennant 1988, 37c Ikegami 1986, 37d, Makino 1993, 37e Oosterbroek et al. 1995, 37f Shirey et al. 1996, 37g Shirey et al. 1998, 37h Shirey et al. 1999, 37i Qu 2001, 37j Ding et al. 2003; 38a Lewin et al. 1987, 38b Makishima et al. 1989, 38c Oosterbroek et al. 2001, 38d Makishima et al. 1983, 38e dal Fiume et al. 1990, 38f Asai et al. 1993, 38g den Hartog et al. 2003, 38h Reerink et al. 2004; 39a Homan et al. 1998, 39b Schnerr et al. 2003, 39c Matsuba et al. 1995, 39d Homan et al. 2003c; 40a Jonker et al. 2000c; 41a Jonker et al. 1999; 42a Jonker et al. 2003; 43a Olive et al. 1998; 44a Tawara et al. 1982, 44b Stella et al. 1988a, 44c Stella et al. 1988b, 44d Dotani et al. 1990, 44e Kawai et al. 1990, 44f Lubin et al. 1991, 44g Tan et al. 1991, 44h Lubin et al. 1992a, 44i Lubin et al. 1992b, 44j Lubin et al. 1993, 44k Rutledge et al. 1995, 44l Kommers et al. 1997, 44m Fox et al. 2001; 45a Wijnands & van der Klis 1999b; 46a in 't Zand et al. 2000; 47a Wijnands & van der Klis 1999c, 47b Revnivtsev et al. 1999a; 48a Barret et al. 2003; 49a in 't Zand et al. 1999b; 50a Kitamoto et al. 1992.
-

to exhibit the correlated spectral and <100 Hz timing behaviour of an ordinary atoll source (37e) and at other times, at higher L_x , that of a (somewhat atypical) Z source

(37h). However, no kHz QPOs have been reported, which sets it apart from both classes. BLN is seen and LF QPOs with frequencies from 30 down to ~ 1 Hz, as well as broad noise out to several 100 Hz (37a,b,f-h). Both the timing properties and the hard X-ray spectrum actually make the source resemble a black hole, but the detection of X-ray bursts from the field, nearly certainly from the source itself (Tennant et al. 1986), strongly argues in favour of a neutron star.

The *Rapid Burster* (MXB 1730–335) is a transient source with thermonuclear bursts (§3) as well as repetitive 'type II' bursts attributed to a recurrent accretion instability (e.g., Lewin et al. 1993) possibly related to similarly-interpreted phenomena seen in the high magnetic-field neutron star GRO J1744–28 (§2.11, cf., Lewin et al. 1996) and the black hole GRS 1915+105 (§2.10.4). In addition to ~ 0.05 Hz wave trains with gradually increasing frequency apparently excited by the type II bursts (44i,l), complex 0.5–7 Hz QPOs are observed both in- and outside the type II bursts (references see Table 2.6) which can be quite strong (up to 35% rms, 44b) with sometimes (usually weak) harmonics. Apart from the similar frequencies and the fact that correlations exist with flux and spectral parameters, no obvious similarities exist between the correlated spectral and timing behaviour of the Rapid Burster and other LMXBs. A link with Z-source NBOs was suggested (44d), but the properties of the source do not fit in well with those of either Z or atoll sources, or Cir X-1 (44k). No significant kHz variability has been detected (44m). Models for type II bursts in which the neutron-star magnetic field temporarily interrupts accretion (e.g., Hanawa et al. 1989) provide a setting where QPOs can be produced through magnetic interactions with the accretion flow (e.g., Hanami 1988); non-magnetic disk oscillations are a possibility as well (e.g., Cannizzo 1997).

Other sources which do not fit seamlessly within the framework sketched here are GX 13+1 and GX 349+2 which show somewhat ambiguous Z/atoll behaviour (cf., 3B and other references in Table 2.6), and the millisecond pulsar XTE J1751–305 (14e). The other millisecond pulsars have properties similar to those of other weak LMXBs (14e,j).

2.10 Black holes

The reference codes in this section refer to those listed with Table 2.7.

2.10.1 High-frequency QPOs

The 7 black holes from which HF QPOs (§2.6.1) > 100 Hz have been reported (2x,z,A,C,6b,f,h,i,m,59c,g,60b,61c,e,68a,74a,b) are listed in Table 2.7 (some possibly related < 100 Hz oscillations are discussed at the end of this section). HF QPOs are weak, transient, and energy dependent, and are detected only at high count rate. In many cases they hover around formal detection levels, so there is considerable uncertainty about their exact properties, but typically Q ranges between less than 2 and 10, and amplitudes are between 0.5 and 2% rms (2–60 keV). HF QPOs usually occur in the VHS, but in XTE J1550–564 a 250-Hz QPO was seen in an IMS at a count rate 70–85% below the VHS (6f).

In two objects two peaks at an approximate 2:3 frequency ratio were detected together (GRO J1655–40: ~ 300 and ~ 450 Hz, 61e, see also 6m,61c; XTE J1550–564: 188 ± 3 and 268 ± 3 Hz, 6h; see also 6m and 6b,f,i,). A similar case (but not

simultaneous) has been mentioned but not yet fully reported for GRS 1915+105 (113 \pm 3 Hz and 165 \pm 3 Hz, 2C; §4.4.3). The frequencies of the 2:3 pairs may scale with inverse black-hole mass (6m), but there is some choice in frequencies and the systematic uncertainties in the masses are considerable. Marginal cases involving 1:2 frequency ratios have also been discussed (92 Hz in XTE J1550–564, 6m; 328 Hz in GRS 1915+105, 2z). Usually HF QPO peaks are seen alone, but with a tendency to occur near fixed frequencies, in addition to sources mentioned above: 184 \pm 5 Hz in 4U 1630–47 (59c,g), 250 \pm 5 Hz in XTE J1650–500 (60b), 240 Hz in H1743–322 (68a) and, marginally, at 150 $^{+17}_{-28}$ and 187 $^{+14}_{-11}$ Hz in XTE J1859+226 (74a,b). However, values well off the nominal values 184 and 276 Hz occur in XTE J1550–564 (e.g., 123 \pm 2 Hz, 6f, but see 6m; 141 \pm 3 Hz, 6i).

Below 6 keV the HF QPOs are usually not detected, while at higher energies amplitudes up to 5% rms have been measured. The higher-frequency peak is more evident at energies >13 keV in GRO J1655–40 (61e) but not in XTE J1550–564 (6h). In XTE J1550–564 and GRO J1655–40 the higher harmonic becomes stronger when the spectrum becomes softer (6f,m), i.e, while all other variability frequencies increase (§2.10.2). In XTE J1550–564 this, together with the QPOs off the fixed frequencies, produces a correlation between the frequencies of actually observed HF and LF QPOs (6f). An observed correlation with LF QPO type and coherence (6i,m) is related to this.

In GRS 1915+105 a 67-Hz QPO occurs (2b,x) whose frequency varies by only a few percent in no apparent correlation to factor-several X-ray flux changes. Q is usually around 20 (but sometimes drops to 6; 2A), the amplitude is \sim 1% (rms), and hard lags up to 2.3 rad occur (2y). The spectral characteristics of this QPO depend strongly on the peculiar rapid state changes of this source (§2.10.4, 2p). QPOs at 40 and possibly 56 Hz sometimes occur with the 67-Hz one (2q), and a 27-Hz QPO, again strongly dependent on the rapid state changes, occurs on other occasions (2p). Note that 27:40:56:67 is close to 2:3:4:5. The relation of these QPOs to the \gtrsim 100 Hz HF QPOs is unclear, but of course the reported 113/165 Hz pair in GRS 1915+105 (above) complicates their interpretation. In XTE J1550–564, a possibly related Q \sim 4.4 QPO near 65 Hz has been reported (6g).

The high frequencies of the QPOs discussed in this section, similar to ISCO frequencies in stellar mass black holes, strongly suggest an origin in the strong-field region. In view of the reported constant frequencies, diskoseismic modes (§2.12.1) are a candidate explanation, but these models do not predict harmonic sets of frequencies such as seen in HF QPOs (Nowak et al. 1997, Pérez et al. 1997, Ortega-Rodriguez & Wagoner 2000, Silbergleit et al. 2001). Rezzolla et al. (2003) calculated p-modes in a toroidal accretion geometry which can explain some of the key HF QPO properties such as the integer frequency ratios. Cui et al. (1998b) proposed that HF QPOs occur at ν_{nodal} (§2.8.2). Relativistic resonance models (§2.8.3) predicted constant frequencies in small integer ratios which were then found in GRO J1655–40 (Strohmayer 2001a, Abramowicz & Kluźniak 2001). The previously mentioned models of Schnittman & Bertschinger (2004, see §2.8.1) and Laurent & Titarchuk (2001, see §2.8.5) both aim at explaining HF QPOs.

HF QPO properties, to the extent that it has been possible to establish them for this somewhat elusive phenomenon, seem quite different from those of neutron-star

kHz QPOs: the neutron-star QPOs come in pairs with a separation related to the star's spin, have strongly tunable frequencies and low harmonic content, while the black-hole ones are single, but with high harmonic content, and have a much more stable frequency. Yet, the two phenomena might still be reconciled within a single theoretical description. For example, the variable frequencies in neutron stars might occur because the phenomenon occurs at a variable (e.g., inner disk) radius, set by interaction of the disk flow with either a magnetic field or radiation from the stellar surface, while in black holes, in the absence of these influences, the same phenomenon occurs at a more constant radius (perhaps close to the ISCO); the second QPO may occur only in neutron stars because it is due to an interaction with the spin; the high harmonic content in black-hole QPOs may be due to relativistic effects (e.g., as a simple example, extreme Doppler boosting near the ISCO of a spinning black hole) on the flow and its emission that become important only near the ISCO. Future observations at higher sensitivity will help much in understanding this phenomenon and elucidating the relation with kHz QPOs.

2.10.2 The low-frequency complex

The strong BLN in the LS was first noticed in Cyg X-1 (Oda et al. 1971) and initially interpreted in terms of a 73 msec periodicity. Later shot-noise models (§2.2) were applied to this noise (see also §2.12.3). Nolan et al. (1981) presented the first power spectrum unambiguously showing the characteristic $\nu_b=0.01-1$ Hz flat-topped noise shape (Fig. 2.8, LS). The energy dependence of the noise amplitude is generally small in the 2–40 keV range, above that the rms may decrease (e.g., 1m,I,5n,v,51a,b,c,57a,), although background subtraction issues may have affected some of these results. While the noise is well correlated between energy bands (0.1–10 Hz cross-coherence, §2.2, is ~ 1), hard ~ 0.1 rad lags are seen between < 6 and > 15 keV, increasing logarithmically with energy. Contrary to predictions from basic Comptonization light travel-time models (§2.12.2), time lag is not constant but decreases with Fourier frequency as $\nu^{-0.7}$, with some structure possibly related to the characteristic noise frequencies (ν_b, ν_h , §2.6.2; 1d,l,m,u,z,5n,w,64b,67a,71a). While in some scattering geometries this could be understood (Kazanas et al. 1997, Hua et al. 1997), lack of the expected smearing of the variability towards higher photon energies by light travel time effects makes models of this type unlikely (1J,K) and favours propagation models for the lags instead (§2.12.2).

In the IMS/VHS, ν_b is higher, from 0.1–1 Hz to > 10 Hz (2–60 keV). Energy dependencies in noise amplitude, time lags and coherencies tend to be larger and more complex and variable here than in the LS (1s,t,5h,6a,c,d,52d,56c,e,60a,72b,79c), possibly due to competition between the contribution of hard and soft spectral components to these quantities, and characteristic frequencies depend on energy as well (e.g., 1i,j,t,6a,f,55d,56b,60a,61c). GRS 1915+105 in its hard state (C state; 2B) has noise similar to this (i.e., this state probably corresponds to a VHS/IMS, 2f, see also, e.g., 2n,o,t).

Noise amplitude is less in the 6–7-keV (Fe-line) region (1k,o,L,72b,79a,). This effect is seen in the IMS, but is more pronounced in the LS, particularly > 5 Hz. Perhaps this is due to a larger line forming ('reflection') region in that state (1k,o, see also 79a).

Table 2.7. *Black-hole rapid X-ray variability*

Source	LS/IMS/HS	Strong BLN	LF QPO	HF QPO	References
GRO J0422+32	•/-/-	•	○	—	51a-d;1v;5s;64d
LMC X-1 (0538-641)	-/-/•	—	•	—	52a-d
LMC X-3 (0540-679)	•/-/•	•	•	—	53a-e;52c,d
A0620-00	○/○/○	○	—	—	54a-b,56d,f
XTE J1118+480	•/-/-	•	•	—	55a-j;64d
GS 1124-68	•/-/•	•	•	—	56a-f;1t
GS 1354-64	•/-/-	•	•	—	57a,b;1v;64d
4U 1543-47	•/-/•	•	•	—	58a
XTE J1550-564	•/-/•	•	•	•	6a-r;1A,H;5s,x;61g
4U 1630-47	•/-/-	•	•	•	59a-g;1y;5x,6l;61g
XTE J1650-500	•/-/•	•	•	•	60a-d;5u;61g
GRO J1655-40	•/-/•	•	•	•	61a-h;1v,y,A;5s,x;6e,i,l
GX 339-4 (1659-487)	•/-/•	•	•	—	5a-w;1l,p,t-v,y,z,A,H,K;56b,e
IGR J17091-3624	•/-/-	•	—	—	62a
SAX J1711.6-3808 ^a	•/-/-	•	•	—	63a,b
GRO J1719-24 (1716-249)	○/-/-	—	•	—	64a-c
GRS 1737-31	•/-/-	•	—	—	65a
GRS 1739-278	-/-/•	—	•	—	66a,b
1E 1740.7-2942	•/-/-	•	•	—	67a,b;1v,y,K;5v
H1743-322	-/-/○	—	•	•	68a
XTE J1748-288	•/-/•	•	•	—	69a;1v,y;5x;6l;61g
XTE J1755-324	•/-/○	•	—	—	70a;1v,y
GRS 1758-258	•/-/•	•	•	—	71a,b;1v,A,K;5v;67a,b
XTE J1819-254	○/-/-	•	—	—	72a-d
EXO 1846-031	-/-/•	—	—	—	73a,b
IGR J18539+0727	•/-/-	•	—	—	62a
XTE J1859+226	-/-/-	—	•	•	74a-c;1H
XTE J1908+094	•/-/-	—	○	—	75a
GRS 1915+105	○/○/○	•	•	•	2a-C;1y,A;5s
4U 1957+11	-/-/•	—	—	—	76a-c
Cyg X-1 (1956+35)	•/-/○	•	•	—	1a-L;5p,t,v
GS 2000+25	•/-/•	•	○	—	77a-t
XTE J2012+381	-/-/•	—	—	—	78a-c
GS 2023+338	•/○/○	•	—	—	79a-c;1u

This is not a list of certified black holes; relevant low magnetic-field compact-object timing behaviour plus an absence of bursts and pulsations suffice for inclusion. LS: low state, IMS: intermediate state (includes VHS), HS: high state. •: variability of this type observed; ○: some doubt (uncertain, ambiguous, atypical, rare and not clearly seen, etc.); —: not reported. Strong BLN: >15% rms. Note: ^a Contamination by SAX J1712.6-3739, 63b.

QPOs ($Q > 2$) with amplitudes of a few to more than 10% rms are sometimes observed superimposed on the noise at frequencies (§2.7) a factor 2–8 above, or around, ν_b . This is seen in the LS (0.01–2 Hz, sometimes including a harmonic: 1s,5c,g,m,o,q,s, 6i,53b,55a,61b,67a,71a) where frequency often gradually increases through the initial LS rise of a transient outburst (in the 0.015–0.3 Hz range: 55b,d,57b,64a,d). It is also often observed in the IMS (1–33 Hz, often with rich harmonic structure: 1t,5h,r,6c,d,f,56a-c,58a,59d-f,60a,b,d,61b,c,g,63a,b,66a,b,69a). Transitions in frequency occur in the 0.08–13 Hz range between LS and IMS both in the rise (0.08–13 Hz range; 6a,e,i,s) and in the decay (6–0.2 Hz range; 6g,s,59e) of some transient outbursts. Transitions that are smooth in frequency may nevertheless be rapid in time and, depending on coverage, seem abrupt. IMS/VHS LF-QPO harmonic structure is intricate, with subsets of 1:2:3:4:6:8 frequency ratios all observed (references above). Time lags of opposite sign and different Q values are

References in Table 2.7: 1a Oda et al. 1971, 1b Terrell 1972, 1c Nolan et al. 1981, 1d Miyamoto & Kitamoto 1989, 1e Belloni & Hasinger 1990a, 1f Negoro et al. 1994, 1g Vikhlinin et al. 1994, 1h Crary et al. 1996, 1i Belloni et al. 1996, 1j Cui et al. 1997a,b, 1k Revnivtsev et al. 1999b, 1l Ford et al. 1999, 1m Nowak et al. 1999a,b, 1n Gilfanov et al. 1999, 1o Gilfanov et al. 2000, 1p Nowak 2000, 1q Uttley & McHardy 2001, 1r Churazov et al. 2001, 1s Pottschmidt et al. 2003, 1t Rutledge et al. 1999, 1u Miyamoto et al. 1992, 1v Wijnands & van der Klis 1999a, 1w Reig et al. 2002, 1x Berger & van der Klis 1998, 1y Sunyaev & Revnivtsev 2000, 1z Miyamoto et al. 1988, 1A Li & Muraki 2002, 1B Zdziarski et al. 2002, 1C Wen et al. 2001, 1D Frontera et al. 2001, 1E Gierliński et al. 1999, 1F Zhang et al. 1997a, 1G Ling et al. 1983, 1H Done & Gierliński 2003, 1I Kotov et al. 2001, 1J Maccarone et al. 2000, 1K Lin et al. 2000a, 1L Maccarone & Coppi 2002a; 2a Chen et al. 1997, 2b Morgan et al. 1997, 2c Paul et al. 1997, 2d Belloni 1998, 2e Swank et al. 1998, 2f Reig et al. 2003b, 2g Trudolyubov et al. 1999a,b, 2h Markwardt et al. 1999b, 2i Feroci et al. 1999, 2j Munro et al. 1999, 2k Naik et al. 2000, 2l Rao et al. 2000a,b, 2m Chakrabarti et al. 2000, 2n Reig et al. 2000b, 2o Lin et al. 2000c, 2p Belloni et al. 2001, 2q Strohmayer 2001b, 2r Nandi et al. 2001, 2s Tomsick & Kaaret 2001, 2t Munro et al. 2001, 2u Trudolyubov 2001, 2v Rodriguez et al. 2002a, 2w Ji et al. 2003, 2x Remillard & Morgan 1998, 2y Cui 1999, 2z Remillard et al. 2002b, 2A Remillard et al. 1999b, 2B Belloni et al. 2000, 2C Remillard et al. 2003; 5a Samimi et al. 1979, 5b Motch et al. 1982, 5c Motch et al. 1983, 5d Maejima et al. 1984, 5e Makishima et al. 1986, 5f Imamura et al. 1990, 5g Grebenev et al. 1991, 5h Miyamoto et al. 1991, 5i Méndez & van der Klis 1997, 5j Steiman-Cameron et al. 1997, 5k Kong et al. 2002, 5l Belloni et al. 1999a, 5m Smith & Liang 1999, 5n Nowak et al. 1999c, 5o Revnivtsev et al. 2001b, 5p van Straaten et al. 2003, 5q Nowak et al. 2002, 5r Nespoli et al. 2003, 5s Psaltis et al. 1999a, 5t Belloni & Hasinger 1990b, 5u Belloni 2004, 5v Lin et al. 2000a, 5w Vaughan & Nowak 1997; 6a Cui et al. 1999, 6b Remillard et al. 1999a, 6c Wijnands et al. 1999b, 6d Cui et al. 2000a, 6e Sobczak et al. 2000a, 6f Homan et al. 2001, 6g Kalemci et al. 2001, 6h Miller et al. 2001, 6i Remillard et al. 2002c, 6j Rodriguez et al. 2002b, 6k Belloni et al. 2002b, 6l Vignarca et al. 2003, 6m Remillard et al. 2002a, 6n Kubota & Done 2004, 6o Kubota & Makishima 2004, 6p Gierliński & Done 2003, 6q Rodriguez et al. 2003, 6r Sobczak et al. 2000b, 6s Reilly et al. 2001; 51a Denis et al. 1994, 51b Vikhlinin et al. 1995, 51c Grove et al. 1998, 51d van der Hooft et al. 1999a; 52a Ebisawa et al. 1989, 52b Schmidtko et al. 1999, 52c Haardt et al. 2001, 52d Nowak et al. 2001; 53a Treves et al. 1990, 53b Boyd et al. 2000, 53c Boyd et al. 2001, 53d Wilms et al. 2001, 53e Cowley et al. 1991; 54a Carpenter et al. 1976, 54b Kuulkers 1998; 55a Revnivtsev et al. 2000b, 55b Wood et al. 2000, 55c Malzac et al. 2003, 55d Frontera et al. 2003, 55e Hynes et al. 2003b, 55f Belloni et al. 2002a, 55g Kanbach et al. 2001, 55h Spruit & Kanbach 2002, 55i McClintock et al. 2001, 55j Esin et al. 2001; 56a Miyamoto et al. 1994, 56b Belloni et al. 1997, 56c Takizawa et al. 1997, 56d Hynes et al. 2003a, 56e Miyamoto et al. 1993, 56f Esin et al. 2000, 57e Esin et al. 1997, 58a Ebisawa et al. 1994; 57a Revnivtsev et al. 2000a, 57b Brocksopp et al. 2001; 58a Park et al. 2003; 59a Parmar et al. 1986, 59b Kuulkers et al. 1997b, 59c Remillard & Morgan 1999, 59d Dieters et al. 2000b, 59e Tomsick & Kaaret 2000, 59f Trudolyubov et al. 2001, 59g Klein-Wolt et al. 2004a; 60a Kalemci et al. 2003, 60b Homan et al. 2003b, 60c Tomsick et al. 2004, 60d Rossi et al. 2004; 61a Zhang et al. 1997c, 61b Méndez et al. 1998d, 61c Remillard et al. 1999c, 61d Yamaoka et al. 2001, 61e Strohmayer 2001a, 61f Sobczak et al. 1999, 61g Kalemci et al. 2004, 61h Hynes et al. 1998; 62a Lutovinov & Revnivtsev 2003; 63a Wijnands & Miller 2002, 63b in 't Zand et al. 2002; 64a van der Hooft et al. 1996, 64b van der Hooft et al. 1999b, 64c Revnivtsev et al. 1998a, 64d Brocksopp et al. 2004; 65a Cui et al. 1997c; 66a Borozdin & Trudolyubov 2000, 66b Wijnands et al. 2001a; 67a Smith et al. 1997, 67b Main et al. 1999; 68a Homan et al. 2003a; 69a Revnivtsev et al. 2000c; 70a Revnivtsev et al. 1998b; 71a Lin et al. 2000b, 71b Smith et al. 2001; 72a Wijnands & van der Klis 2000, 72b Revnivtsev et al. 2002, 72c Uemura et al. 2002, 72d Uemura et al. 2004; 73a Parmar et al. 1993, 73b Sellmeijer et al. 1999; 74a Cui et al. 2000b, 74b Markwardt 2001, 74c Brocksopp et al. 2002; 75a Woods et al. 2002; 76a Ricci et al. 1995, 76b Nowak & Wilms 1999, 76c Wijnands et al. 2002a; 77a Terada et al. 2002; 78a Vasiliev et al. 2000, 78b Naik et al. 2000, 78c Campana et al. 2002; 79a Oosterbroek et al. 1996, 79b Oosterbroek et al. 1997, 79c Zycki et al. 1999a,b.

sometimes seen between alternating harmonics (56b,c,6a,c,74a) reminiscent of what is observed in Z-source HBOs (§2.6.2). Source-state dependent QPO subtypes are distinguished based on differences in peak width, time lags and accompanying noise (6c,f,i,m, Ch. 4). In GX 339–4 a 6-Hz LF QPO fluctuated by about 1 Hz on time scales down to 5 sec in correlation with X-ray flux variations (5r). QPOs with similar harmonic structure and alternating time lags are also observed in the 0.5–12 Hz range in GRS 1915+105 in its hard state (e.g., 2a,b,g,h,j,l,n,o,s,v). In the HS, weak ($\lesssim 1\%$ rms) 0.02–0.08 and 14–27 Hz QPOs are occasionally seen whose relation to the other LF QPOs is unclear (6e,f,52a,61c,69a).

Correlations between the LF complex and X-ray spectral (usually, Comptonization and reflection) model parameters are mostly an expression of the source state dependencies already discussed above and in §2.6.2: as the spectrum hardens (power-law

fraction increases, blackbody flux decreases, coronal compactness increases, photon index decreases, etc.), amplitudes increase and frequencies decrease (e.g., 1n,s,5o,q,6g, 1,56a,59e,60c,61g,77a, also di Matteo and Psaltis 1999). Gilfanov et al. (2004) present a tentative correlation between QPO frequency and Fe line width (wider line for higher frequency) which is roughly in accordance with expectations if the QPO is an orbital frequency and the line width is determined by Doppler shifts due to motion in that orbit. Again, in the IMS correlations are more complex, perhaps due to competition between spectral components. In both XTE J1550–564 and GRO J1655–40 the QPO frequency increases with blackbody flux, but in XTE J1550–564 the photon index and total flux then both rise, whereas in GRO J1655–40 both fall (6e,i, who conclude that QPO frequency correlates with \dot{M}_d , §2.5, and that the power-law fraction should be >20% for QPOs to be observed).

In XTE J1650–500, in decay towards the off state at a luminosity a factor \sim 500 below that early in the outburst, a ν_b of 0.0035 Hz was measured (60c), so on the way to the off state ν_b apparently continues to decrease. Optical and UV power spectra in the low and off states are similar to those in X-rays, with ν_b as low as 0.0001–0.001 Hz in the off state (55e,56d). 0.02-Hz BLN and 0.1-Hz QPO were observed simultaneously in UV and X-rays in the LS in XTE J1118+480, with 1–2 sec UV lags possibly due to light travel time delays in reprocessing, but the detailed correlation is complex and not well understood (55c,e,g,h). In GRO J1655–40 in the VHS, 10–20 sec UV lags were observed (61h), while in XTE J1819–254 7-min *X-ray* lags were seen which were attributed to disk propagation effects (72c,d). In GX 339–4 optical BLN and QPOs occur in the 0.005–3 Hz range (e.g., 5b,c,f,j).

The BLN in black holes has been extensively modeled in terms of shot noise, often used as model for magnetic flares, and chaos-, and certain MHD-simulations of disk flows also produce power spectra reminiscent of LS noise (see §2.12.3). For the LF QPOs a variety of, nearly exclusively disk-based, models has been considered (orbiting hot spots, §2.8.1, Lense-Thirring precession, §2.8.2, disk oscillations, §2.12.1). Superposition of various oscillation frequencies can also produce BLN (Nowak 1994). Churazov et al. (2001) have proposed that ν_b is the orbital frequency of the inner edge of the optically thick disk, and explain the LS and IMS power spectra of Cyg X-1 by supposing that the variability is generated at the local orbital time scale in the hot optically thin regions of the flow located both within the inner edge, and sandwiching, the disk.

2.10.3 Power-law noise

Power-law noise (in this section defined as noise with no clear flat top in P_ν down to several 0.01 Hz) is not normally seen in the LS (strong BLN could mask it). The HS is characterized by weak (0.5–3%) power-law noise with index typically 0.7–1.2 (e.g., 51,6f,56c,59d,61b,d,69a) and sometimes a break to $\alpha = 1.5 – 2$ occurs around 3 Hz (Fig. 2.8, HS; 6f,61b). The most varied power-law noise is observed in the IMS.

Rapid (minutes to days) variations between \sim 1-Hz BLN-dominated and few-% rms $\alpha \sim 1$ power-law dominated power spectra in GS 1124–68 and GX 339–4 were an early defining characteristic of the VHS (5h,56c). In more recent work (2f,6f,52c,d,59b,61a-c), a 4–8% rms $\alpha = 0.8 – 1.5$ power-law component is commonly found, sometimes to-

gether with BLN, usually at the 'soft side' of the VHS/IMS, where the BLN weakens. While the noise in these various examples is clearly not flat-topped, it sometimes has a discernable curvature or break in the 1–10 Hz range, and steepens towards higher frequencies. When XTE J1550–564 moves from HS to gradually harder intermediate states, $\alpha=0.7$ –1.2 power-law noise, which can be as weak as 0.5% in the HS proper, becomes stronger, up to 5.6% in the VHS, 2.8% in lower-luminosity IMS and up to 8.9% on the way to the LS, with no BLN detected (6f). When the BLN appears, the power-law noise can still be detectable at low frequencies at levels of 1.5–4% rms, but as the BLN gets stronger and ν_b drops, it disappears below the detection level. In what may be a similar phenomenon, Cyg X-1 displays a strong (up to 33% rms, 1j,r) $\alpha=1$ power law, usually with a clear break to $\alpha=2$ around 10 Hz at the top of soft flares in what is usually called the 'high state' in this source, but is actually more similar to an IMS (1s,61g); when the spectrum gets slightly harder in this IMS, BLN with $\nu_b=1$ –3.5 Hz is seen together with a flat ($\alpha=0.3$ –0.8) power law at low frequency (1i,j). Because it dominates in the disk-dominated 'soft' state, Cui et al. (1997b) interpret this noise to originate in the disk, but Churazov et al. (2001) argue instead that it originates in the corona.

Like VLFN in neutron stars (§2.9.4), power-law noise in black holes may be due to \dot{M} variations, perhaps arising in the outer disk. Numerical simulations can produce power spectra that are red over several decades in frequency (Mineshige et al. 1994b, Kawaguchi et al. 2000, Hawley & Krolik 2001) but as noted in §2.10.2, flat tops are usually discernable in these cases. Clearly, models involving surface phenomena such as nuclear burning do not apply in the black-hole case, so such models for neutron-star power-law noise (§2.9.4) predict differences between neutron stars and black holes which should show up in comparative studies.

2.10.4 Other phenomena and peculiar objects

The number of black-hole X-ray binaries that is peculiar with respect to the timing characteristics and source states discussed here is small; mostly what makes systems peculiar is unusual variations on longer time scales, likely originating outside the strong-field region, or *lack* of variability (in possible black holes such as SS433, Cyg X-3 and C1 Cam; Grindlay et al. 1984, Berger & van der Klis 1994, Belloni et al. 1999b, but see van der Klis & Jansen 1985), usually plausibly attributable to external circumstances. This suggests that the innermost accretion flow, where the rapid variability arises, is dominated by the black-hole properties. XTE J1819–254 (V4641 Sgr) in its brief outburst showed unusually strong (46% rms) power-law noise with rapidly varying α (72a) and rapid optical fluctuations (72c,d). It may be an SS433-like super-Eddington accretor (72b). Objects showing properties not clearly characteristic for either low magnetic-field neutron stars or black holes include 4U 1957+11 (76a-c), possibly a black hole always in the HS, and 4U 1543–62 and 4U 1556–60, which might be atoll sources (Table 2.6; Farinelli et al. 2003).

A small number of rapid variability phenomena observed in black-hole systems do not fit the above categories. Transient oscillations in the 1–1000 mHz range are regularly observed in the very high state ('dips and flip-flops', 5h; e.g., 56c,59d,f) which may just be relatively rapid source-state transitions (e.g., Belloni et al. 2000) due to disk instabilities; the peculiar nature of GRS 1915+105 may be due to the source

showing such behaviour most of the time. Of course, faster and lower-luminosity phenomena could similarly be due to rapid state transitions (cf., Yu et al. 2001), but this is harder to check.

2.11 High-magnetic-field neutron stars

In the high magnetic-field neutron stars the typically 10^{12} G B field disrupts the disk flow at the magnetospheric radius $r_{mag} \sim 10^8$ cm and channels the plasma to the magnetic poles. The resulting strong periodic pulsations complicate the analysis of the stochastic variability. The dynamical time scale at r_{mag} is of order seconds, hence variability much faster than this is not *a priori* expected from the accretion disk (but see e.g., Orlandini & Morfill 1992, Orlandini and Boldt 1993, Klein et al. 1996a,b for possible rapid magnetospheric accretion-flow phenomena). Indeed, aperiodic variability tends to be dominated by strong (several 10% rms) flat-topped BLN with ν_b often (but not always) $\sim \nu_{spin}$ (e.g., Frontera et al. 1987, Belloni & Hasinger 1990b, Angelini et al. 1989, Takeshima et al. 1991, Takeshima 1992), suggesting that it arises in the disk outside r_{mag} . Possibly, such a BLN component is a characteristic of any disk flow truncated at 10^8 cm, and similar physics underlies this component in high magnetic-field neutron stars and in low magnetic-field compact objects in low states (e.g., Hoshino & Takeshima 1993, van der Klis et al. 1994b). However, as noted by Lazzati & Stella (1997), if the pulse amplitude is itself modulated, the strong periodic component can give rise to these noise components, complicating interpretation.

A broad QPO often seen at factors up to $\sim 10^2$ below ν_{spin} (see Table 1.1 in §1.2.1.2; references above and in Shirakawa & Lai 2002b, see also Li et al. 1980) is sometimes interpreted as a magnetospheric beat frequency (§2.8.4), implying that orbital motion at r_{mag} occurs at approximately the spin frequency. On occasion, when a QPO occurred above ν_{spin} (e.g., Angelini et al. 1989, Finger et al. 1996) its luminosity- or spin-up-rate related changes in frequency were consistent with either the beat frequency or the orbital frequency at r_{mag} , allowing to constrain neutron-star parameters. Upper and lower sidebands were seen separated from ν_{spin} by the QPO frequency (Kommers et al. 1998, Moon & Eikenberry 2001a,b), implying the pulse amplitude is modulated by the QPO; although this is what a beat-frequency model predicts, asymmetry between the two sidebands suggests that an orbital frequency in the disk contributes to the QPO signal. Disk oscillations (Titarchuk & Osherovich 2000) and warped disk modes (Shirakawa & Lai 2002b) have also been proposed for these QPOs. The peculiar 0.5-sec pulsar GRO J1744–28 which showed type II bursts (cf., §2.9.5) also produced 20, 40 and 60 Hz QPOs (Zhang et al. 1996c).

Jernigan et al. (2000) reported QPO features near 330 and 760 Hz in the 4.8 s accreting pulsar Cen X-3. They interpreted this in terms of the photon bubble model (§2.12.4). This is the only report of millisecond oscillations from a high-magnetic-field neutron star, but note that the QPO features are quite weak, and instrumental effects are a concern at these low power levels.

2.12 Flow-instability and non-flow models

In §2.8 we looked at models for observed variability frequencies based on orbital and epicyclic motions supplemented with decoherence and modulation mech-

anisms in order to fit the properties of observed QPO and noise components. In the current section, we discuss rapid X-ray variability models in which the variability arises in instabilities in the accretion flow. Models of this type often include the modulation mechanism as part of their physics, although the consequences of this have not always been fully explored yet in terms of predictions of observable phenomena. At the end of this section we look at neutron-star boundary-layer and surface phenomena.

2.12.1 Disk-oscillation models

The expressions in §2.8.1 are for free particle orbits. An accretion disk is a hydrodynamic flow, so the particles are not free but exert forces upon each other. This leads to the potential for oscillations in the flow. The resulting vibration modes of disk, corona, and disk/star and disk/magnetosphere boundary layers can lead to QPOs or noise. In a standard disk model several physical time scales are of the order of the local orbital time scale $1/\nu_\phi$ (Shakura & Sunyaev 1973, 1976, Thorne & Price 1975, Pringle 1981; §13.2.3). Many analytic as well as numerical explorations have been made of disk oscillation modes. Often the free-particle orbital and epicyclic frequencies can still be recognized (e.g., Wagoner 1999), but combination frequencies with (magneto-)hydrodynamic frequencies (e.g., of sound waves) occur as well (e.g., Psaltis 2000). In §§2.9–2.11 some examples of models in this class proposed for specific phenomena have already been mentioned. Here we emphasize models relevant to kHz QPOs and black-hole HF QPOs.

In the strong-field gravity region global oscillation modes with frequencies similar to the free-particle frequencies can occur which are 'trapped' in (can not propagate outside) particular disk annuli (Kato et al. 1998, Nowak and Lehr 1998, Wagoner 1999, Kato 2001, Lamb 2003, for useful summaries). This trapping is a predicted strong-field gravity effect; it does not occur in Newtonian gravity. Of these 'diskoseismic' modes, the g , c and p modes occur at approximately constant frequencies, which like the orbital frequency at the ISCO scale as $1/M$. The w modes depend on the inner disk radius and hence can vary in frequency. Diskoseismic modes were not found in simulations including MHD turbulent effects (Hawley & Krolik 2001).

If there is a sharp transition in the disk, according to Psaltis & Norman (2000) the transition radius can act as a filter with a response that has strong resonances near the epicyclic (and orbital) frequencies of that radius; predicted frequencies are similar to those of the relativistic precession model (§2.8.2), with hydrodynamic corrections and additional frequencies that might allow a better match to the LF QPO, kHz QPO and sideband data (but see also Marković & Lamb 2000). Oscillations associated with a viscous transition layer between Keplerian disk and neutron star, some involving the star's magnetic field but *not* requiring strong field gravity, and hence not involving the epicyclic frequencies, have been proposed to apply to high-frequency and other QPO and noise phenomena in neutron stars, black holes and white dwarfs, with at least 6 different observed frequencies and their correlations being predicted (Titarchuk et al. 1998, 1999, Osherovich & Titarchuk 1999, Titarchuk & Osherovich 1999, Titarchuk 2002; Titarchuk & Wood 2002, but see also Miller 2003 for a theoretical discussion of these ideas, and van Straaten et al. 2000, 2003 and Jonker et al. 2000a, 2002a for discrepancies with the observations). Oscillations associated with instabilities in

a disk-magnetosphere boundary have been explored as a model for high-frequency QPOs (Li & Narayan 2004, Kato et al. 2001). Hydrodynamic disk modes, some involving the effects of radiation and magnetic fields have further been explored by various authors (e.g., Hanami 1988, Fukue & Okada 1990, Spruit & Taam 1990, Okuda & Mineshige 1991, Alpar et al. 1992, Luo & Liang 1994, Chen & Taam 1994, 1995, Wallinder 1995, Abramowicz et al. 1995, Ipser 1996, Milsom & Taam 1996, 1997, Marković & Lamb 1998, Lai 1999, Kato et al. 2001, Gnedin & Kiikov 2001, Varniere et al. 2002, Shirakawa & Lai 2002a, Das et al. 2003, Mukhopadhyay et al. 2003, Watarai & Mineshige 2003b). Damping, or the superposition of many local frequencies (e.g., Nowak 1994) can turn intrinsically periodic disk oscillations into QPO or broad band noise.

Fluctuations in the density or temperature of a Comptonizing medium can produce a modulation in spectra formed by Comptonization (e.g., Boyle et al. 1986, Stollman et al. 1987, Alpar et al. 1992, Lee & Miller 1998), as can modulation of the rate at which photons are injected into the medium (e.g., Kazanas & Hua 1999, Laurent & Titarchuk 2001, Titarchuk & Shrader 2002). Various types of intrinsic flow instabilities can modulate the accretion rate onto the central object (e.g., hydrodynamic; Taam & Lin 1984, general-relativistic; Paczyński 1987, Kato 1990, and radiation-feedback instabilities; Fortner et al. 1989, Miller & Lamb 1992, Miller & Park 1995) and in this way produce relatively large-amplitude modulations in the X-ray flux. All disk oscillations to some extent directly affect the disk luminosity and the photon-energy dependence of the disk emissivity (references above and, e.g., Nowak & Wagoner 1993), yet many of the models that have been proposed essentially are variability-frequency models, predicting the frequency, or the power spectrum, of the fluctuations only in some physical flow parameter rather than in any observable quantity. Clearly, in order to allow further tests of disk oscillation models and to discriminate between them, such predictions of observables of the oscillations are essential.

2.12.2 Energy dependencies: amplitude, phase, cross-coherence

To the extent that the intrinsically periodic models discussed above and in §2.8 include explicit X-ray flux modulation mechanisms they are in principle severely constrained by the observed photon-energy dependencies of amplitude and phase (§2.2) of the modulation. To explain why the variability often has a harder spectrum than the average flux (i.e., larger fractional rms, §2.2, towards higher photon energies, see e.g., §§2.9.1 and 2.9.3, but see also §2.10.2) in models where the frequencies arise in the disk, which usually emits a *softer* than average flux, two main types of mechanism have been discussed: (i) modulation of the rate at which the disk is providing soft seed photons to the Comptonizing corona (references below), and (ii) modulation of the accretion rate into an inner region, such as a neutron-star boundary layer or black-hole inner corona whose X-ray spectrum is harder than that of the disk (e.g., Churazov et al. 2001, Gilfanov et al. 2003). Of course, another possible explanation for this is that the frequencies do not arise in the disk in the first place. QPOs and noise in black holes in the IMS tend to be more strongly energy dependent than in other states or in neutron stars; this may be related to

the large differences between the X-ray spectral components that are simultaneously prominent in black holes in this state.

Propagation of an X-ray signal through a hot cloud of Comptonizing electrons produces hard lags: on average, photons emerging later have undergone more scatterings and hence gained more energy; the time lag between bands E_1 and E_2 scales roughly as $\log(E_2/E_1)$ (Payne 1980, Miller 1995, Nowak & Vaughan 1996). This mechanism has been applied many times (see references in §§2.2, 2.8.7 and 2.12.1 and, e.g., Wijers et al. 1987, Miyamoto et al. 1988, Schulz & Wijers 1993, Nowak 1994, Nowak et al. 1999b, Hua & Titarchuk 1996, Hua et al. 1997, 1999, Böttcher & Liang 1998, Cullen 2000, Laurent & Titarchuk 2001, Titarchuk & Shrader 2002, Nobili et al. 2000), with detailed calculations of the effects of the cloud oscillating (e.g., Fortner et al. 1989, Stollman et al. 1987, Miller & Lamb 1992, Miller 1995, Lee & Miller 1998, Lee et al. 2001), and estimates of the effects of other Comptonizing geometries (e.g., Miller et al. 1998a, Shibasaki et al. 1988, Reig et al. 2003c, Nobili 2003). The applicability of these models to black-hole BLN lags has been addressed in §2.10.2; lags naturally arising from shot-noise models involving propagating clumps or waves (§2.12.3) may be more appropriate to explain these. Reprocessing by the disk of X-rays emitted above the disk plane ('reflection'; Poutanen 2002, see also Kaaret 2000), or by the companion star (Vikhlinin 1999) is another way to affect the energy dependencies in the variability. Körding & Falcke (2004) provide a detailed analysis of time lags produced by a pivoting power-law spectrum.

The observed energy dependencies in variability amplitude and phase are very constraining, and none of the models cited are able to explain everything observed. The unknown geometry of the emitting and scattering regions contributes to the considerable uncertainty with respect to the correct model. Clearly, this is an area where the observations are needed to guide the modeling, yet observational capabilities are not yet at the required level. If, for example, luminous blobs would be orbiting the compact object in the region of the disk where the relativistically broadened Fe line is generated, with sufficient sensitivity this would produce a very obvious signal due to Doppler-shifted features moving up and down through the line profile, but present instrumentation is not able to reliably detect signals of this kind. With the larger instruments currently under consideration, such work may become possible.

2.12.3 *Intrinsically aperiodic models*

The intrinsically aperiodic (§2.8) models most often used are in the class of shot-noise models (see also §2.2). Shots are sensible in various physical settings, e.g., magnetic flares (usually, storage of magnetic energy followed by release in a reconnection event, e.g., Wheeler 1977, Galeev et al. 1979, Pudritz & Fahlman 1982, Aly & Kuijpers 1990, Haardt et al. 1994, Mineshige et al. 1995, Poutanen & Fabian 1999, di Matteo et al. 1999, Merloni et al. 2000, Kato et al. 2001, Rodriguez et al. 2002c, Varniere et al. 2002, Krishan et al. 2003), infalling blobs or waves producing a flare ('propagation models', Nowak et al. 1999b: e.g., Miyamoto et al. 1988, Miyamoto & Kitamoto 1989, Kato 1989, Manmoto et al. 1996, Böttcher & Liang 1999, Misra 2000, Böttcher 2001) and finite-lifetime orbiting blobs (references see §2.2 and §2.8.2). In particular the propagation models may be able to produce the frequency-dependent

lags and relatively energy-independent high-frequency amplitudes (Lin et al. 2000a, Maccarone et al. 2000) appropriate to black-hole BLN (§2.10.2).

The observation that variability amplitude is linearly related to flux over a wide range of time scales, *including* those of the variability itself in SAX J1808.4-3658 and Cyg X-1 (Uttley & McHardy 2001, Uttley 2004, Gleissner et al. 2004, see also Bałucińska-Church et al. 1997) is incompatible with straightforward shot-noise models and instead suggests that slower variations are produced first, and are then operated on by faster processes to produce the higher frequency variability. In this context models seem appropriate where slow accretion rate variations originate far out in the disk (where correspondingly long dynamical time scales apply) and become observable after disturbances have propagated inward to the emitting regions, undergoing further modulation producing the faster variations on the way (Vikhlinin et al. 1994, Lyubarskii 1997, see also Źycki 2002, 2003, King et al. 2004).

Among chaos models (see also §2.2) for which some physical justification was put forward are the 'dripping handrail' model of Scargle et al. (1993), and models involving self-organized criticality of a disk as described in a cellular automaton model (Mineshige et al. 1994a,b, Abramowicz & Bao 1994, Takeuchi et al. 1995, Xiong et al. 2000). Autonomous flow instabilities are certainly suggested by direct and to some extent 'first principle' magnetohydrodynamic simulation of disks, which tend to produce broad noise spectra (Kawaguchi et al. 2000, Hawley & Krolik 2001, 2002, Armitage & Reynolds 2003).

2.12.4 Non-flow models: boundary layer, stellar surface

In addition to models associated with various aspects of the accretion flow, neutron-star oscillations or processes occurring on the neutron-star surface or in a boundary layer could produce variability. Clearly, such models exclude any possibility that the same phenomenon also occurs in a black hole. Processes like these are thought to cause the burst oscillations (§3.4), but they could also underlie some of the observed variability in the persistent emission. Radial (e.g., Shibasaki & Ebisuzaki 1989) and non-radial oscillations of various kinds (e.g., McDermott & Taam 1987, McDermott et al. 1988, Epstein 1988, Bildsten & Cutler 1995, Bildsten et al. 1996, Strohmayer & Lee 1996, Bildsten & Cumming 1998), can cause a variation in the surface emission properties; emission would be further modulated as the spin periodically modulates aspect and visibility of the 'spots' thus formed. Temporary surface features due to nuclear-burning processes, which were specifically proposed as a model for neutron-star VLFN (§2.9.4; Bildsten 1993, 1995, see §3) or magnetohydrodynamic effects (Hameury et al. 1985) have also been considered (see also Inogamov & Sunyaev 1999, Popham & Sunyaev 2001) and a ~ 0.01 Hz quasi-periodicity in nuclear burning rate has been suggested by Revnivtsev et al. (2001a; §2.9.4). Klein et al. (1996a,b) proposed a model where photon bubbles rise up by buoyancy through the accreted material and produce a flash of radiation when they burst at the top as a model for kHz QPOs and for QPOs in high-B neutron stars (§2.11).

2.13 Final remarks

Since the previous issue of this book (Lewin et al. 1995) rapid X-ray variability studies have come a long way towards strong-field gravity physics. For the first time we are seeing, and are able to study in some detail, variability at the dynamical time scale of the strong-field region in accreting low magnetic-field neutron stars as well as stellar-mass black holes. Strong-field gravity is an integral part of many of the models proposed. The aim of future timing work will be to turn the *diagnostics* of strong-field gravity and dense matter we now have into true *tests* of GR and *determinations* of the EOS. A theoretical framework for interpreting the observables of motion in the strong-field region in detail and for testing strong-field gravity theories is currently emerging (e.g., Weinberg et al. 2001, DeDeo & Psaltis 2004). What is needed on the observational side is a considerable increase in timing sensitivity coupled with good spectral capabilities. As timing sensitivity in the relevant regime is proportional to collecting area (not the square root of it; §2.2), this is an attainable goal. With future large-area timing instrumentation ($\sim 10 \text{ m}^2$, e.g., XEUS, see Barret 2004, or a dedicated timing array) the predicted patterns of weak sidebands and harmonics (“fingerprints”) of the variability phenomena would be mapped out as a spectrum of interrelated frequencies. This would make models that successfully predicted them unassailable, as of course they should be in order to be accepted as true tests of general relativity in the strong-field regime. Current observations are still clearly limited by the drop in QPO amplitude towards the extreme frequencies (Fig. 2.19). With more sensitivity the frequency range over which QPOs are detected would be considerably widened, likely making it possible to follow kHz QPOs up to the ISCO and check for the predicted frequency saturation there. A considerable synergy in terms of testing gravitation theories may occur with the results of gravitational wave instruments

Combining timing and spectroscopy is another way to clinch the models. For example, in an orbital motion model for a QPO phenomenon in the Fe line region, to zeroeth order the frequency provides the orbital period, and the line profile the orbital velocity, so that we can solve for orbital radius r and central mass M . So, combining spectral and timing measurements will provide strong tests of the models and allow to start using them to learn more about the curved spacetime near compact objects. By measuring the line-profile changes on short time scales, or equivalently the amplitude and phase differences between QPOs in several spectral bands within the line profile exciting tests are possible. The line widths are $\sim \text{keV}$, so moderate-resolution millisecond spectroscopy is sufficient to do this. Clearly, entirely different signals are expected from QPOs caused by luminous blobs orbiting in the strong-field region and from, e.g., spiral-flow modulated-accretion QPOs: hence, such measurements will decide the emission geometry and constrain the modulation model.

Finally, depending on the precise phenomenon, large area detectors will make it possible to detect the QPOs either within one cycle ν^{-1} , or one coherence time $(\pi\Delta\nu)^{-1}$, allowing to study them in the time domain. Wave-form studies will allow to quantitatively constrain compact object mass, radius and angular momentum, orbital velocity and gravitational ray bending by modeling approaches such as described by Weinberg et al. (2001) for neutron-star surface hot spots. The opportunities provided

by large-area detectors for doing strong-gravity and dense-matter physics by timing X-ray binaries are clearly excellent.

Acknowledgements: It is a pleasure to acknowledge the help of the many colleagues who either made data available before publication, provided, or produced new, figures, read versions of the manuscript or provided insightful discussion at various stages during the writing of this chapter: Marek Abramowicz, Didier Barret, Tomaso Belloni, Deepto Chakrabarty, Eric Ford, Jeroen Homan, Peter Jonker, Fred Lamb, Erik Kuulkers, Marc Klein-Wolt, Wlodek Klu{z}niak, Tom Maccarone, Craig Markwardt, Mariano M{e}ndez, Simone Migliari, Dimitrios Psaltis, Thomas Reerink, Pablo Reig, Roald Schnerr, Luigi Stella, Steve van Straaten, Phil Uttley, Rudy Wijndands, Wenfei Yu. I am particularly indebted to Cole Miller and Diego Altamirano. All errors are mine. This work was supported in part by the Netherlands Organization for Scientific Research (NWO) and the Netherlands Research School for Astronomy (NOVA).

References

- Abramowicz, M. & Bao, G. 1994, *PASJ*, 46, 523
 Abramowicz, M. A. & Klu{z}niak, W. 2001, *A&A*, 374, L19
 Abramowicz, M. A. & Klu{z}niak, W. 2004, in Rossi and beyond, AIP Conf. Proc. 714, 21; astro-ph/0312396
 Abramowicz, M., Jaroszynski, M., & Sikora, M. 1978, *A&A*, 63, 221
 Abramowicz, M. A., Lanza, A., Spiegel, E. A., & Szuszkiewicz, E. 1992, *Nature*, 356, 41
 Abramowicz, M. A., Chen, X., & Taam, R. E. 1995, *ApJ*, 452, 379
 Abramowicz, M.A., Almbergren, G.J.E., Klu{z}niak, W., & Thampam, A.V. 2003a, gr-gc/0312070
 Abramowicz, M. A., Karas, V., Klu{z}niak, W., Lee, W. H., & Rebusco, P. 2003b, *PASJ*, 55, 467
 Abramowicz, M. A., Bulik, T., Bursa, M., & Klu{z}niak, W. 2003c, *A&A*, 404, L21
 Abramowicz, M. A., Klu{z}niak, W., Stuchlik, Z., & Tork, G. 2004, astro-ph/0401464
 Agrawal, V. K. & Bhattacharyya, S. 2003, *A&A*, 398, 223
 Agrawal, V. K. & Sreekumar, P. 2003, *MNRAS*, 346, 933
 Akmal, A., Pandharipande, V.R., & Ravenhall, D.G. 1998, *Phys. Rev. C*, 58, 1804
 Alpar, M. A. 1986, *MNRAS*, 223, 469
 Alpar, M. A. & Shaham, J. 1985, *Nature*, 316, 239
 Alpar, M. A. & Yilmaz, A. 1997, *New Astronomy*, 2, 225
 Alpar, M. A., Hasinger, G., Shaham, J., & Yancopoulos, S. 1992, *A&A*, 257, 627
 Aly, J. J. & Kuijpers, J. 1990, *A&A*, 227, 473
 Andersson, N., Kokkotas, K.D., & Stergioulas, N. 1999, *ApJ*, 516, 307
 Andersson, N., Jones, D. I., Kokkotas, K. D., & Stergioulas, N. 2000, *ApJ*, 534, L75
 Angelini, L., Stella, L., & Parmar, A. N. 1989, *ApJ*, 346, 906
 Armitage, P. J. & Natarajan, P. 1999, *ApJ*, 525, 909
 Armitage, P. J. & Reynolds, C. S. 2003, *MNRAS*, 341, 1041
 Asai, K., Dotani, T., Nagase, F., Mitsuda, K., Kitamoto, S., et al. 1993, *PASJ*, 45, 801
 Asai, K., Dotani, T., Mitsuda, K., Nagase, F., Kamado, Y., et al. 1994, *PASJ*, 46, 479
 Asaoka, I. & Hoshi, R. 1989, *PASJ*, 41, 1049
 Augusteijn, T., Karatasos, K., Papadakis, M., Paterakis, G. et al. 1992, *A&A*, 265, 177
 Ba{u}ci{u}nska-Church, M., Takahashi, T., Ueda, Y., Church, M. J., et al. 1997, *ApJ*, 480, L115
 Bao, G. & {Ø}stgaard, E. 1994, *ApJ*, 422, L51
 Bao, G. & {Ø}stgaard, E. 1995, *ApJ*, 443, 54
 Bardeen, J. M. & Pettersson, J. A. 1975, *ApJ*, 195, L65
 Bardeen, J. M., Press, W. H., & Teukolsky, S. A. 1972, *ApJ*, 178, 347
 Barnard, R., Church, M. J., & Ba{u}ci{u}nska-Church, M. 2003a, *A&A*, 405, 237
 Barnard, R., Kolb, U., & Osborne, J. P. 2003b, *A&A*, 411, 553
 Barr, P., White, N. E., & Page, C. G. 1985, *MNRAS*, 216, 65P
 Barret, D., 2004, in Rossi and beyond, AIP Conf. Proc. 714, 405; astro-ph/0401099
 Barret, D. & Olive, J. 2002, *ApJ*, 576, 391
 Barret, D. & Vedrenne, G. 1994, *ApJS*, 92, 505
 Barret, D., McClintock, J. E., & Grindlay, J. E. 1996, *ApJ*, 473, 963
 Barret, D., Olive, J. F., Boirin, L., Done, C., Skinner, G. K., & Grindlay, J. E. 2000, *ApJ*, 533, 329
 Barret, D., Olive, J. F., & Oosterbroek, T. 2003, *A&A*, 400, 643
 Belloni, T. 1998, *New Astronomy Review*, 42, 585
 Belloni, T. 2004, in The restless high-energy universe, Nuclear Phys. B, 132, 337; astro-ph/0309028
 Belloni, T. & Hasinger, G. 1990a, *A&A*, 227, L33

- Belloni, T. & Hasinger, G. 1990b, *A&A*, 230, 103
- Belloni, T., Méndez, M., van der Klis, M., Hasinger, G., Lewin, W. H. G., et al. 1996, *ApJ*, 472, L107
- Belloni, T., van der Klis, M., Lewin, W. H. G., van Paradijs, J., Dotani, T., et al. 1997, *A&A*, 322, 857
- Belloni, T., Méndez, M., van der Klis, M., Lewin, W. H. G., & Dieters, S. 1999a, *ApJ*, 519, L159
- Belloni, T., Dieters, S., van den Ancker, M. E., Fender, R. P., et al. 1999b, *ApJ*, 527, 345
- Belloni, T., Klein-Wolt, M., Méndez, M., van der Klis, M., & van Paradijs, J. 2000, *A&A*, 355, 271
- Belloni, T., Méndez, M., & Sánchez-Fernández, C. 2001, *A&A*, 372, 551
- Belloni, T., Psaltis, D., & van der Klis, M. 2002a, *ApJ*, 572, 392
- Belloni, T., Colombo, A. P., Homan, J., Campana, S., & van der Klis, M. 2002b, *A&A*, 390, 199
- Belloni, T., Homan, J., Nespoli, E., Casella, P., et al. 2004, *A&A*, in prep.
- Benlloch, S., Wilms, J., Edelson, R., Yaqoob, T., & Staubert, R. 2001, *ApJ*, 562, L121
- Berger, M. & van der Klis, M. 1994, *A&A*, 292, 175
- Berger, M. & van der Klis, M. 1998, *A&A*, 340, 143
- Berger, M., van der Klis, M., van Paradijs, J., Lewin, W.H.G., Lamb, F., et al. 1996, *ApJ*, 469, L13
- Biehle, G. T. & Blandford, R. D. 1993, *ApJ*, 411, 302
- Bildsten, L. 1993, *ApJ*, 418, L21
- Bildsten, L. 1995, *ApJ*, 438, 852
- Bildsten, L. 1998, *ApJ*, 501, L89
- Bildsten, L. & Cumming, A. 1998, *ApJ*, 506, 842
- Bildsten, L. & Cutler, C. 1995, *ApJ*, 449, 800
- Bildsten, L. & Ushomirsky, G. 2000, *ApJ*, 529, L33
- Bildsten, L., Ushomirsky, G., & Cutler, C. 1996, *ApJ*, 460, 827
- Blom, J. J., in't Zand, J. J. M., Heise, J., Arefev, V., Borozdin, K., et al. 1993, *A&A*, 277, 77
- Bloser, P. F., Grindlay, J. E., Kaaret, P., Zhang, W., Smale, A. P., & Barret, D. 2000a, *ApJ*, 542, 1000
- Bloser, P. F., Grindlay, J. E., Barret, D., & Boirin, L. 2000b, *ApJ*, 542, 989
- Boirin, L., Barret, D., Olive, J. F., Blöser, P. F., & Grindlay, J. E. 2000, *A&A*, 361, 121
- Borozdin, K. N. & Trudolyubov, S. P. 2000, *ApJ*, 533, L131
- Böttcher, M. 2001, *ApJ*, 553, 960
- Böttcher, M. & Liang, E. P. 1998, *ApJ*, 506, 281
- Böttcher, M. & Liang, E. P. 1999, *ApJ*, 511, L37
- Boyd, P. T., Smale, A. P., Homan, J., Jonker, P. G., van der Klis, M., et al. 2000, *ApJ*, 542, L127
- Boyd, P. T., Smale, A. P., & Dolan, J. F. 2001, *ApJ*, 555, 822
- Boyle, C. B., Fabian, A. C., & Guilbert, P. W. 1986, *Nature*, 319, 648
- Bracewell, R.N. 1986, The Fourier Transform and its Applications, 2nd. ed., McGraw-Hill
- Bradshaw, C. F., Geldzahler, B. J., & Fomalont, E. B. 2003, *ApJ*, 592, 486
- Bradt, H. V., Rothschild, R. E., & Swank, J. H. 1993, *A&AS*, 97, 355
- Brainerd, J. & Lamb, F. K. 1987, *ApJ*, 317, L33
- Branduardi, G., Kylafis, N. D., Lamb, D. Q., & Mason, K. O. 1980, *ApJ*, 235, L153
- Brinkman, A. C., Parsignault, D. R., Schreier, E., Gursky, H., Kellogg, E. M., et al. 1974, *ApJ*, 188, 603
- Brocksopp, C., Jonker, P. G., Fender, R. P., Groot, P. J., et al. 2001, *MNRAS*, 323, 517
- Brocksopp, C., Fender, R. P., McCollough, M., Pooley, G. G., et al. 2002, *MNRAS*, 331, 765
- Brocksopp, C., Bandyopadhyay, R. M., & Fender, R. P. 2004, *New Astronomy*, 9, 249
- Brown, E. F. & Ushomirsky, G. 2000, *ApJ*, 536, 915
- Brugmans, F. 1983, *Earth Surface Processes and Landforms* 8, 527
- Bulik, T., Gondek-Rosińska, D., & Kluźniak, W. L. 1999, *A&A*, 344, L71
- Bulik, T., Kluźniak, W. & Zhang, W. 2000, *A&A*, 361, 153
- Bussard, R. W., Weisskopf, M. C., Elsner, R. F., & Shibasaki, N. 1988, *ApJ*, 327, 284
- Campana, S. 2000, *ApJ*, 534, L79
- Campana, S., Stella, L., Belloni, T., Israel, G. L., Santangelo, A., et al. 2002, *A&A*, 384, 163
- Canizares, C. R., Clark, G. W., Li, F. K., Murthy, G. T., Bardas, D., et al. 1975, *ApJ*, 197, 457
- Cannizzo, J. K. 1997, *ApJ*, 482, 178
- Carpenter, G. F., Eyles, C. J., Skinner, G. K., Willmore, A. P., et al. 1976, *MNRAS*, 176, 397
- Chagelishvili, G. D., Lominadze, J. G., & Rogava, A. D. 1989, *ApJ*, 347, 1100
- Chakrabarti, S. K. & Manickam, S. G. 2000, *ApJ*, 531, L41
- Chakrabarty, D., Morgan, E. H., Muno, M. P., Galloway, D. K., et al. 2003, *Nature*, 424, 42
- Chaput, C., Bloom, E., Cominsky, L., Godfrey, G., Hertz, P., Scargle, J., et al. 2000, *ApJ*, 541, 1026
- Chen, X. & Taam, R. E. 1994, *ApJ*, 431, 732
- Chen, X. & Taam, R. E. 1995, *ApJ*, 441, 354
- Chen, X., Swank, J. H., & Taam, R. E. 1997, *ApJ*, 477, L41
- Chiappetti, L., et al. 1990, *ApJ*, 361, 596
- Churazov, E., Gilfanov, M., & Revnivtsev, M. 2001, *MNRAS*, 321, 759
- Corbet, R. H. D., Smale, A. P., Charles, P. A., Lewin, W. H. G., et al. 1989, *MNRAS*, 239, 533
- Cowley, A. P., et al. 1991, *ApJ*, 381, 526
- Crary, D. J., Kouveliotou, C., van Paradijs, J., van der Hooft, F., et al. 1996, *ApJ*, 462, L71
- Cropper, M., Soria, R., Mushotzky, R. F., Wu, K., Markwardt, C. B., et al. 2004, *MNRAS*, 349, 39
- Cui, W. 1999, *ApJ*, 524, L59
- Cui, W. 2000, *ApJ*, 534, L31
- Cui, W., Heindl, W. A., Rothschild, R. E., Zhang, S. N., Jahoda, K., & Focke, W. 1997a, *ApJ*, 474, L57
- Cui, W., Zhang, S. N., Focke, W., & Swank, J. H. 1997b, *ApJ*, 484, 383
- Cui, W., Heindl, W. A., Swank, J. H., Smith, D. M., Morgan, E. H., et al. 1997c, *ApJ*, 487, L73
- Cui, W., Barret, D., Zhang, S.N., Chen, W., Boirin, L., Swank, J. 1998a, *ApJ*, 502, L49

- Cui, W., Zhang, S. N., & Chen, W. 1998b, *ApJ*, 492, L53
 Cui, W., Zhang, S. N., Chen, W., & Morgan, E. H. 1999, *ApJ*, 512, L43
 Cui, W., Zhang, S. N., & Chen, W. 2000a, *ApJ*, 531, L45
 Cui, W., Shrader, C. R., Haswell, C. A., & Hynes, R. I. 2000b, *ApJ*, 535, L123
 Cullen, J. 2000, *Publications of the Astronomical Society of Australia*, 17, 48
 Cunningham, C. T. & Bardeen, J. M. 1972, *ApJ*, 173, L137
 Czerny, B., Niłakajuk, M., Piasecki, M., & Kuraszkiewicz, J. 2001, *MNRAS*, 325, 865
 dal Fiume, D., Robba, N. R., Frontera, F., & Stella, L. 1990, *Nuovo Cimento C*, 13, 463
 Damen, E., Wijers, R. A. M. J., van Paradijs, J., Penninx, W., et al. 1990, *A&A*, 233, 121
 Das, T. K., Rao, A. R., & Vadawale, S. V. 2003, *MNRAS*, 343, 443
 Datta, B., Thampan, A. V., & Bombaci, I. 1998, *A&A*, 334, 943
 Datta, B., Thampan, A. V., & Bombaci, I. 2000, *A&A*, 355, L19
 Deeter, J. E. 1984, *ApJ*, 281, 482
 DeDeo, S. & Psaltis, D. 2004, astro-ph/0405067
 den Hartog, P. R., in't Zand, J. J. M., Kuulkers, E., Cornelisse, R., Heise, J., et al. 2003, *A&A*, 400, 633
 Denis, M., Olive, J.-F., Mandrou, P., Roques, J. P., Ballet, J., Goldwurm, A., et al. 1994, *ApJS*, 92, 459
 Dieters, S. W. & van der Klis, M. 2000, *MNRAS*, 311, 201
 Dieters, S. W., Vaughan, B. A., Kuulkers, E., Lamb, F. K., & van der Klis, M. 2000a, *A&A*, 353, 203
 Dieters, S. W., Belloni, T., Kuulkers, E., Woods, P., Cui, W., Zhang, S. N., et al. 2000b, *ApJ*, 538, 307
 di Matteo, T. & Psaltis, D. 1999, *ApJ*, 526, L101
 di Matteo, T., Celotti, A., & Fabian, A. C. 1999, *MNRAS*, 304, 809
 Ding, G. Q., Qu, J. L., & Li, T. P. 2003, *ApJ*, 596, L219
 Di Salvo, T., & Stella, L. 2002, astro-ph/0207219
 Di Salvo, T., Stella, L., Robba, N. R., van der Klis, M., Burderi, L., et al. 2000, *ApJ*, 544, L119
 Di Salvo, T., Méndez, M., van der Klis, M., Ford, E., & Robba, N. R. 2001a, *ApJ*, 546, 1107
 Di Salvo, T., Robba, N. R., Iaria, R., Stella, L., Burderi, L., & Israel, G. L. 2001b, *ApJ*, 554, 49
 Di Salvo, T., Farinelli, R., Burderi, L., Frontera, F., Kuulkers, E., et al. 2002, *A&A*, 386, 535
 Di Salvo, T., Méndez, M., & van der Klis, M. 2003, *A&A*, 406, 177
 Doi, K. 1978, *Nature*, 275, 197
 Done, C. & Gierliński, M. 2003, *MNRAS*, 342, 1041
 Done, C., Zych, P. T., & Smith, D. A. 2002, *MNRAS*, 331, 453
 Dotani, T., Mitsuda, K., Makishima, K., & Jones, M. H. 1989, *PASJ*, 41, 577
 Dotani, T., Mitsuda, K., Inoue, H., Tanaka, Y., Kawai, N., Tawara, Y., et al. 1990, *ApJ*, 350, 395
 Dubus, G., Kern, B., Esin, A. A., Rutledge, R. E., & Martin, C. 2003, astro-ph/0310615
 Ebisawa, K., Mitsuda, K., & Inoue, H. 1989, *PASJ*, 41, 519
 Ebisawa, K., Ogawa, M., Aoki, T., Dotani, T., Takizawa, M., Tanaka, Y., et al. 1994, *PASJ*, 46, 375
 Edelson, R. & Nandra, K. 1999, *ApJ*, 514, 682
 Elsner, R. F., Weisskopf, M. C., Darbro, W., Ramsey, B. D., Williams, A. C., et al. 1986, *ApJ*, 308, 655
 Elsner, R. F., Shibasaki, N., & Weisskopf, M. C. 1987, *ApJ*, 320, 527
 Elsner, R. F., Shibasaki, N., & Weisskopf, M. C. 1988, *ApJ*, 327, 742
 Epstein, R. I. 1988, *ApJ*, 333, 880
 Esin, A. A., McClintock, J. E., & Narayan, R. 1997, *ApJ*, 489, 865
 Esin, A. A., Kuulkers, E., McClintock, J. E., & Narayan, R. 2000, *ApJ*, 532, 1069
 Esin, A. A., McClintock, J. E., Drake, J. J., Garcia, M. R., Haswell, C. A., et al. 2001, *ApJ*, 555, 483
 Fabian, A. C., Iwasawa, K., Reynolds, C. S., & Young, A. J. 2000, *PASP*, 112, 1145
 Farinelli, R., Frontera, F., Masetti, N., Amati, L., Guidorzi, C., et al. 2003, *A&A*, 402, 1021
 Feng, Y. X., Li, T. P., & Chen, L. 1999, *ApJ*, 514, 373
 Feroci, M., Matt, G., Pooley, G., Costa, E., Tavani, M., & Belloni, T. 1999, *A&A*, 351, 985
 Finger, M. H., Wilson, R. B., & Harmon, B. A. 1996, *ApJ*, 459, 288
 Focke, W. B. 1996, *ApJ*, 470, L127
 Ford, E. C., & van der Klis, M. 1998, *ApJ*, 506, L39
 Ford, E., Kaaret, P., Tavani, M., Barret, D., Bloser, P., Grindlay, J., et al. 1997a, *ApJ*, 475, L123
 Ford, E. C., Kaaret, P., Chen, K., Tavani, M., Barret, D., Bloser, P., et al. 1997b, *ApJ*, 486, L47
 Ford, E. C., van der Klis, M., & Kaaret, P. 1998a, *ApJ*, 498 L41
 Ford, E. C., van der Klis, M., van Paradijs, J., Méndez, M., Wijands, R., et al. 1998b, *ApJ*, 508, L155
 Ford, E. C., van der Klis, M., Méndez, M., van Paradijs, J., & Kaaret, P. 1999, *ApJ*, 512, L31
 Ford, E. C., van der Klis, M., Méndez, M., Wijnands, R., Homan, J., et al. 2000, *ApJ*, 537, 368
 Fortner, B., Lamb, F. K., & Miller, G. S. 1989, *Nature*, 342, 775
 Fox, D. W., Lewin, W.H.G., Rutledge, R.E., Morgan, E.H., Guerriero, R., et al. 2001, *MNRAS*, 321, 776
 Fragile, P. C., Mathews, G. J., & Wilson, J. R. 2001, *ApJ*, 553, 955
 Franco, L. M. 2001, *ApJ*, 554, 340
 Frontera, F., dal Fiume, D., Robba, N. R., Manzo, G., Re, S., & Costa, E. 1987, *ApJ*, 320, L127
 Frontera, F., Palazzi, E., Zdziarski, A. A., Haardt, F., Perola, G. C., et al. 2001, *ApJ*, 546, 1027
 Frontera, F., Amati, L., Zdziarski, A. A., Belloni, T., Del Sordo, S., et al. 2003, *ApJ*, 592, 1110
 Fukue, J. & Okada, R. 1990, *PASJ*, 42, 533
 Galeev, A. A., Rosner, R., & Vaiana, G. S. 1979, *ApJ*, 229, 318
 Galloway, D. K., Chakrabarty, D., Munro, M. P., & Savov, P. 2001, *ApJ*, 549, L85
 Galloway, D. K., Chakrabarty, D., Morgan, E. H., & Remillard, R. A. 2002, *ApJ*, 576, L137
 Gierliński, M. & Done, C. 2002a, *MNRAS*, 337, 1373
 Gierliński, M. & Done, C. 2002b, *MNRAS*, 331, L47
 Gierliński, M. & Done, C. 2003, *MNRAS*, 342, 1083

- Gierliński, M. & Zdziarski, A. A. 2003, *MNRAS*, 343, L84
 Gierliński, M., Zdziarski, A. A., Poutanen, J., Coppi, P. S., et al. 1999, *MNRAS*, 309, 496
 Gierliński, M., Done, C., & Barret, D. 2002, *MNRAS*, 331, 141
 Giles, A. B. 1981, *MNRAS*, 195, 721
 Gilfanov, M., Churazov, E., & Revnivtsev, M. 1999, *A&A*, 352, 182
 Gilfanov, M., Churazov, E., & Revnivtsev, M. 2000, *MNRAS*, 316, 923
 Gilfanov, M., Revnivtsev, M., & Molkov, S. 2003, *A&A*, 410, 217
 Gilfanov, M., Churazov, E., & Revnivtsev, M. 2004, in Rossi and beyond, AIP Conf. Proc. 714, 97; astro-ph/0312445
 Gleissner, T., Wilms, J., Pottschmidt, K., Uttley, P., Nowak, M. A., et al. 2004, *A&A*, 414, 1091
 Glendenning, N. K. & Weber, F. 2001, *ApJ*, 559, L119
 Gnedin, Y. N. & Kiiakov, S. O. 2001, *Astronomy Letters*, 27, 507
 Gondek-Rosińska, D., Stergioulas, N., Bulik, T., Kluźniak, W., & Gourgoulhon, E. 2001, *A&A*, 380, 190
 Grebenev, S. A., Syunyaev, R. A., Pavlinskii, M. N., et al. 1991, *Soviet Astronomy Letters*, 17, 413
 Grindlay, J. E., Band, D., Seward, F., Leahy, D., Weisskopf, M. C., et al. 1984, *ApJ*, 277, 286
 Grove, J. E., Strickman, M. S., Matz, S. M., Hua, X.-M., Kazanas, D., et al. 1998, *ApJ*, 502, L45
 Gruzinov, A. 1999, astro-ph/9910335
 Haardt, F., Maraschi, L., & Ghisellini, G. 1994, *ApJ*, 432, L95
 Haardt, F., Galli, M. R., Treves, A., Chiappetti, L., Dal Fiume, D., et al. 2001, *ApJS*, 133, 187
 Halpern, J. P., Leighly, K. M., & Marshall, H. L. 2003, *ApJ*, 585, 665
 Hameury, J.-M., King, A. R., & Lasota, J.-P. 1985, *Nature*, 317, 597
 Hanami, H. 1988, *MNRAS*, 233, 423
 Hanawa, T., Hirotani, K., & Kawai, N. 1989, *ApJ*, 336, 920
 Hartle, J. B. & Thorne, K. S. 1968, *ApJ*, 153, 807
 Hasinger, G. 1987, in The origin and evolution of neutron stars, IAU Symp. 125, 333
 Hasinger, G. 1988, in Physics of Neutron Stars and Black Holes, Tokyo, Tanaka (ed.), p. 97
 Hasinger, G., & van der Klis, M. 1989, *A&A*, 225, 79
 Hasinger, G., Langmeier, A., Sztajno, M., Truemper, J., & Lewin, W. H. G. 1986, *Nature*, 319, 469
 Hasinger, G., Priedhorsky, W. C., & Middleditch, J. 1989, *ApJ*, 337, 843
 Hasinger, G., van der Klis, M., Ebisawa, K., Dotani, T., & Mitsuda, K. 1990, *A&A*, 235, 131
 Hawley, J. F. & Krolik, J. H. 2001, *ApJ*, 548, 348
 Hawley, J. F. & Krolik, J. H. 2002, *ApJ*, 566, 164
 Heiselberg, H., & Hjorth-Jensen, M. 1999, *ApJ*, 525, L45
 Hertz, P., Vaughan, B., Wood, K. S., Norris, J. P., Mitsuda, K., et al. 1992, *ApJ*, 396, 201
 Hirano, A., Kitamoto, S., Yamada, T. T., Mineshige, S., & Fukue, J. 1995, *ApJ*, 446, 350
 Hjellming, R. M., Han, X. H., Cordova, F. A., & Hasinger, G. 1990a, *A&A*, 235, 147
 Hjellming, R. M., Stewart, R. T., White, G. L., Strom, R., Lewin, W. H. G., et al. 1990b, *ApJ*, 365, 681
 Homan, J. & van der Klis, M. 2000, *ApJ*, 539, 847
 Homan, J., van der Klis, M., Wijnands, R., Vaughan, B., & Kuulkers, E. 1998, *ApJ*, 499, L41
 Homan, J., Méndez, M., Wijnands, R., van der Klis, M., & van Paradijs, J. 1999a, *ApJ*, 513, L119
 Homan, J., Jonker, P. G., Wijnands, R., van der Klis, M., & van Paradijs, J. 1999b, *ApJ*, 516, L91
 Homan, J., Wijnands, R., van der Klis, M., Belloni, T., van Paradijs, J., et al. 2001, *ApJS*, 132, 377
 Homan, J., van der Klis, M., Jonker, P. G., Wijnands, R., Kuulkers, E., et al. 2002, *ApJ*, 568, 878
 Homan, J., Miller, J. M., Wijnands, R., Steeghs, D., Belloni, T., et al. 2003a, *ATel*, 162, 1
 Homan, J., Klein-Wolt, M., Rossi, S., Miller, J. M., Wijnands, R., et al. 2003b, *ApJ*, 586, 1262
 Homan, J., Wijnands, R., Rupen, M. P., Fender, R., Hjellming, R. M., et al. 2004, *A&A*, 418, 255
 Hoshino, M. & Takeshima, T. 1993, *ApJ*, 411, L79
 Hua, X. & Titarchuk, L. 1996, *ApJ*, 469, 280
 Hua, X., Kazanas, D., & Titarchuk, L. 1997, *ApJ*, 482, L57
 Hua, X., Kazanas, D., & Cui, W. 1999, *ApJ*, 512, 793
 Hynes, R. I., O'Brien, K., Horne, K., Chen, W., & Haswell, C. A. 1998, *MNRAS*, 299, L37
 Hynes, R. I., Charles, P. A., Casares, J., Haswell, C. A., et al. 2003a, *MNRAS*, 340, 447
 Hynes, R. I., Haswell, C. A., Cui, W., Shrader, C. R., O'Brien, K., et al. 2003b, *MNRAS*, 345, 292
 Iaria, R., Di Salvo, T., Robba, N. R., Burderi, L., Stella, L., Frontera, F., et al. 2004, *ApJ*, 600, 358
 Ikegami, T. 1986, PhD thesis, University of Tokyo
 Illovaisky, S. A., Chevalier, C., White, N. E., Mason, K. O., Sanford, P. W., et al. 1980, *MNRAS*, 191, 81
 Imamura, J. N., Kristian, J., Middleditch, J., & Steiman-Cameron, T. Y. 1990, *ApJ*, 365, 312
 Inogamov, N. A. & Sunyaev, R. A. 1999, *Astronomy Letters*, 25, 269
 in 't Zand, J. J. M., Verbunt, F., Strohmayer, T. E., Bazzano, A., et al. 1999a, *A&A*, 345, 100
 in 't Zand, J. J. M., Heise, J., Kuulkers, E., Bazzano, A., Cocchi, M., et al. 1999b, *A&A*, 347, 891
 in 't Zand, J. J. M., Bazzano, A., Cocchi, M., Cornelisse, R., Heise, J., et al. 2000, *A&A*, 355, 145
 in 't Zand, J. J. M., Cornelisse, R., Kuulkers, E., Heise, J., Kuiper, L., et al. 2001, *A&A*, 372, 916
 in 't Zand, J. J. M., Markwardt, C. B., Bazzano, A., Cocchi, M., et al. 2002, *A&A*, 390, 597
 Ipser, J. R. 1996, *ApJ*, 458, 508
 Israel, G. L., Mereghetti, S., & Stella, L. 1994, *ApJ*, 433, L25
 Jernigan, J. G., Klein, R. I., & Arons, J. 2000, *ApJ*, 530, 875
 Ji, J. F., Zhang, S. N., Qu, J. L., & Li, T. 2003, *ApJ*, 584, L23
 Jones, C., Giacconi, R., Forman, W., & Tananbaum, H. 1974, *ApJ*, 191, L71
 Jonker, P. G., Wijnands, R., van der Klis, M., Psaltis, D., Kuulkers, E., et al. 1998, *ApJ*, 499, L191
 Jonker, P. G., van der Klis, M., & Wijnands, R. 1999, *ApJ*, 511, L41
 Jonker, P. G., van der Klis, M., Wijnands, R., Homan, J., van Paradijs, J., et al. 2000a, *ApJ*, 537, 374

- Jonker, P. G., Méndez, M., & van der Klis, M. 2000b, *ApJ*, 540, L29
 Jonker, P. G., van der Klis, M., Homan, J., Wijnands, R., van Paradijs, J., et al. 2000c, *ApJ*, 531, 453
 Jonker, P. G., van der Klis, M., Homan, J., Méndez, M., van Paradijs, J., et al. 2001, *ApJ*, 553, 335
 Jonker, P. G., van der Klis, M., Homan, J., Méndez, M., et al. 2002a, *MNRAS*, 333, 665
 Jonker, P. G., Méndez, M., & van der Klis, M. 2002b, *MNRAS*, 336, L1
 Jonker, P. G., Méndez, M., Nelemans, G., Wijnands, R., & van der Klis, M. 2003, *MNRAS*, 341, 823
 Kaaret, P. 2000, in Stellar endpoints, AIP-Conf. Proc. 599, 406; astro-ph/0008424
 Kaaret, P., Ford, E., & Chen, K. 1997, *ApJ*, 480, L27
 Kaaret, P., Yu, W., Ford, E.C., & Zhang, S.N. 1998, *ApJ*, 497, L93
 Kaaret, P., Piraino, S., Ford, E.C., & Santangelo, A. 1999a, *ApJ*, 514, L31
 Kaaret, P., Piraino, S., Bloser, P.F., Ford, E.C., Grindlay, J.E., et al. 1999b, *ApJ*, 520, L37
 Kaaret, P., Zand, J. J. M. i., Heise, J., & Tomsick, J. A. 2002, *ApJ*, 575, 1018
 Kaaret, P., Zand, J. J. M. i., Heise, J., & Tomsick, J. A. 2003, *ApJ*, 598, 481
 Kahn, S. M. & Blissett, R. J. 1980, *ApJ*, 238, 417
 Kalemci, E., Tomsick, J. A., Rothschild, R. E., Pottschmidt, K., & Kaaret, P. 2001, *ApJ*, 563, 239
 Kalemci, E., Tomsick, J. A., Rothschild, R. E., Pottschmidt, K., Corbel, S., et al. 2003, *ApJ*, 586, 419
 Kalemci, E., Tomsick, J. A., Rothschild, R. E., Pottschmidt, K., & Kaaret, P. 2004, *ApJ*, 603, 231
 Kallman, T., Boroson, B., & Vrtilek, S. D. 1998, *ApJ*, 502, 441
 Kalogera, V. & Psaltis, D. 2000, *Phys. Rev. D*, 61, 024009
 Kamado, Y., Kitamoto, S., & Miyamoto, S. 1997, *PASJ*, 49, 589
 Kanbach, G., Straubmeier, C., Spruit, H. C., & Belloni, T. 2001, *Nature*, 414, 180
 Karas, V. 1999a, *ApJ*, 526, 953
 Karas, V. 1999b, *PASJ*, 51, 317
 Kato, S. 1989, *PASJ*, 41, 745
 Kato, S. 1990, *PASJ*, 42, 99
 Kato, S. 2001, *PASJ*, 53, L37
 Kato, S., Fukue, J., & Mineshige, S. 1998, in Black-hole accretion disks, Kyoto University Press
 Kato, Y., Hayashi, M. R., Miyaji, S., & Matsumoto, R. 2001, Advances in Space Research, 28, 505
 Kawaguchi, T., Mineshige, S., Machida, M., Matsumoto, R., & Shibata, K. 2000, *PASJ*, 52, L1
 Kawai, N., Matsuoka, M., Inoue, H., Ogawara, Y., Tanaka, Y., Kunieda, H., et al. 1990, *PASJ*, 42, 115
 Kazanas, D. & Hua, X. 1999, *ApJ*, 519, 750
 Kazanas, D., Hua, X., & Titarchuk, L. 1997, *ApJ*, 480, 735
 King, A. R., Pringle, J. E., West, R. G., & Livio, M. 2004, *MNRAS*, 348, 111
 Kitamoto, S., Tsunemi, H., & Roussel-Dupre, D. 1992, *ApJ*, 391, 220
 Klein, R. I., Arons, J., Jernigan, G., & Hsu, J. J.-L. 1996a, *ApJ*, 457, L85
 Klein, R. I., Jernigan, J. G., Arons, J., Morgan, E. H., & Zhang, W. 1996b, *ApJ*, 469, L119
 Klein-Wolt, M., Homan, J., & van der Klis, M. 2004a, PhD thesis, Univ. of Amsterdam, p. 113
 Klein-Wolt, M., van Straaten, S., & van der Klis, M. 2004b, PhD thesis, Univ. of Amsterdam, p. 165
 Kluźniak, W. 1998, *ApJ*, 509, L37
 Kluźniak, W. & Abramowicz, M. A. 2001, astro-ph/0105057
 Kluźniak, W. & Abramowicz, M. A. 2002, astro-ph/0203314
 Kluźniak, W. & Abramowicz, M. A. 2003, astro-ph/0304345
 Kluźniak, W. & Wagoner, R. V. 1985, *ApJ*, 297, 548
 Kluźniak, W., Michelson, P., & Wagoner, R. V. 1990, *ApJ*, 358, 538
 Kluźniak, W., Abramowicz, M. A., Kato, S., Lee, W. H., & Stergioulas, N. 2004, *ApJ*, 603, L89
 Kommers, J. M., Fox, D. W., Lewin, W. H. G., Rutledge, R. E., et al. 1997, *ApJ*, 482, L53
 Kommers, J. M., Chakrabarty, D., & Lewin, W. H. G. 1998, *ApJ*, 497, L33
 Kong, A. K. H., Charles, P. A., Kuulkers, E., & Kitamoto, S. 2002, *MNRAS*, 329, 588
 Körding, E. & Falcke, H. 2004, *A&A*, 414, 795
 Kotov, O., Churazov, E., & Gilfanov, M. 2001, *MNRAS*, 327, 799
 Krishan, V., Ramadurai, S., & Wiita, P. J. 2003, *A&A*, 398, 819
 Krolik, J. H. & Hawley, J. F. 2002, *ApJ*, 573, 754
 Kubota, A. & Done, C. 2004, *MNRAS*, 353, 980
 Kubota, A. & Makishima, K. 2004, *ApJ*, 601, 428
 Kuulkers, E. 1995, PhD thesis, Univ. of Amsterdam
 Kuulkers, E. 1998, New Astronomy Review, 42, 1
 Kuulkers, E. & van der Klis, M. 1995, *A&A*, 303, 801
 Kuulkers, E., & van der Klis, M. 1998, *A&A*, 332, 845
 Kuulkers, E., van der Klis, M., Oosterbroek, T., Asai, K., Dotani, T., et al. 1994, *A&A*, 289, 795
 Kuulkers, E., van der Klis, M., & van Paradijs, J. 1995, *ApJ*, 450, 748
 Kuulkers, E., van der Klis, M., & Vaughan, B. A. 1996, *A&A*, 311, 197
 Kuulkers, E., van der Klis, M., Oosterbroek, T., et al. 1997a, *MNRAS*, 287, 495
 Kuulkers, E., van der Klis, M., & Parmar, A. N. 1997b, *ApJ*, 474, L47
 Kuulkers, E., Wijnands, R., & van der Klis, M. 1999, *MNRAS*, 308, 485
 Kuulkers, E., Homan, J., van der Klis, M., Lewin, W. H. G., & Méndez, M. 2002, *A&A*, 382, 947
 Kuznetsov, S. I. 2001, *Astronomy Letters*, 27, 790
 Kuznetsov, S. I. 2002a, *Astronomy Letters*, 28, 73
 Kuznetsov, S. I. 2002b, *Astronomy Letters*, 28, 811
 Kylafis, N. D. & Klimis, G. S. 1987, *ApJ*, 323, 678
 Lai, D. 1998, *ApJ*, 502, 721
 Lai, D. 1999, *ApJ*, 524, 1030

- Lamb, F. K. 2003, in Jan van Paradijs memorial meeting, ASP Conf. Series 308, 221
- Lamb, F. K. & Miller, M. C. 2001, *ApJ*, 554, 1210
- Lamb, F. K. & Miller, M. C. 2003, astro-ph/0308179
- Lamb, F. K., Shibasaki, N., Alpar, M. A., & Shaham, J. 1985, *Nature*, 317, 681
- Langmeier, A., Sztajno, M., Hasinger, G., Truemper, J., & Gottwald, M. 1987, *ApJ*, 323, 288
- Langmeier, A., Hasinger, G., & Truemper, J. 1989, *ApJ*, 340, L21
- Langmeier, A., Hasinger, G., & Truemper, J. 1990, *A&A*, 228, 89
- Laurent, P. & Titarchuk, L. 2001, *ApJ*, 562, L67
- Lazzati, D. & Stella, L. 1997, *ApJ*, 476, 267
- Lee, H. C. & Miller, G. S. 1998, *MNRAS*, 299, 479
- Lee, H. C., Misra, R., & Taam, R. E. 2001, *ApJ*, 549, L229
- Lee, W. H., Abramowicz, M. A., & Kluźniak, W. 2004, *ApJ*, 603, L93
- Lense, J., & Thirring, H. 1918, *Phys. Z.* 19, 156
- Levin, Y. 1999, *ApJ*, 517, 328
- Lewin, W. H. G., et al. 1987, *MNRAS*, 226, 383
- Lewin, W. H. G., van Paradijs, J., & van der Klis, M. 1988, *Space Science Reviews*, 46, 273
- Lewin, W. H. G., Lubin, L. M., Tan, J., van der Klis, M., et al. 1992, *MNRAS*, 256, 545
- Lewin, W. H. G., van Paradijs, J., & Taam, R. E. 1993, *Space Science Reviews*, 62, 223
- Lewin, W.H.G., van Paradijs, J., & van den Heuvel, E.P.J. 1995, X-ray binaries, CUP
- Lewin, W. H. G., Rutledge, R. E., Komers, J. M., van Paradijs, J., et al. 1996, *ApJ*, 462, L39
- Li, F. K., McClintock, J. E., Rappaport, S., Wright, E. L., & Joss, P. C. 1980, *ApJ*, 240, 628
- Li, X., Ray, S., Dey, J., Dey, M., & Bombaci, I. 1999, *ApJ*, 527, L51
- Li, T. P. & Muraki, Y. 2002, *ApJ*, 578, 374
- Li, L. & Narayan, R. 2004, *ApJ*, 601, 414
- Liang, E. P. T. & Thompson, K. A. 1980, *ApJ*, 240, 271
- Lin, D., Smith, I. A., Böttcher, M., & Liang, E. P. 2000a, *ApJ*, 531, 963
- Lin, D., Smith, I. A., Liang, E. P., Bridgman, T., Smith, D. M., et al. 2000b, *ApJ*, 532, 548
- Lin, D., Smith, I. A., Liang, E. P., & Böttcher, M. 2000c, *ApJ*, 543, L141
- Ling, J. C., Mahoney, W. A., Wheaton, W. A., Jacobson, A. S., & Kaluzienski, L. 1983, *ApJ*, 275, 307
- Lochner, J. C., Swank, J. H., & Szymkowiak, A. E. 1989, *ApJ*, 337, 823
- Lochner, J. C., Swank, J. H., & Szymkowiak, A. E. 1991, *ApJ*, 376, 295
- Lubin, L. M., Lewin, W. H. G., Tan, J., Stella, L., & van Paradijs, J. 1991, *MNRAS*, 249, 300
- Lubin, L. M., Lewin, W. H. G., Dotani, T., Oosterbroek, T., et al. 1992a, *MNRAS*, 256, 624
- Lubin, L. M., Lewin, W. H. G., Rutledge, R. E., van Paradijs, J., et al. 1992b, *MNRAS*, 258, 759
- Lubin, L. M., Lewin, W. H. G., van Paradijs, J., & van der Klis, M. 1993, *MNRAS*, 261, 149
- Luo, C. & Liang, E. P. 1994, *MNRAS*, 266, 386
- Lutovinov, A. A. & Revnivtsev, M. G. 2003, *Astronomy Letters*, 29, 719
- Lyubarskii, Y. E. 1997, *MNRAS*, 292, 679
- Maccarone, T. J. & Coppi, P. S. 2002a, *MNRAS*, 335, 465
- Maccarone, T. J. & Coppi, P. S. 2002b, *MNRAS*, 336, 817
- Maccarone, T. J. & Coppi, P. S. 2003, *MNRAS*, 338, 189
- Maccarone, T. J., Coppi, P. S., & Poutanen, J. 2000, *ApJ*, 537, L107
- Maejima, Y., Makishima, K., Matsuoka, M., Ogawara, Y., Oda, M., et al. 1984, *ApJ*, 285, 712
- Main, D. S., Smith, D. M., Heindl, W. A., Swank, J., Leventhal, M., et al. 1999, *ApJ*, 525, 901
- Makino, Y. 1993, PhD thesis, University of Tokyo
- Makishima, K., Mitsuda, K., Inoue, H., Koyama, K., Matsuoka, M., et al. 1983, *ApJ*, 267, 310
- Makishima, K., Maejima, Y., Mitsuda, K., Bradt, H. V., Remillard, R. A., et al. 1986, *ApJ*, 308, 635
- Makishima, K., Ishida, M., Ohashi, T., Dotani, T., Inoue, H., Mitsuda, K., et al. 1989, *PASJ*, 41, 531
- Malzac, J., Belloni, T., Spruit, H. C., & Kanbach, G. 2003, *A&A*, 407, 335
- Manmoto, T., Takeuchi, M., Mineshige, S., Matsumoto, R., & Negoro, H. 1996, *ApJ*, 464, L135
- Marković, D., 2000, astro-ph/0009450
- Marković, D. & Lamb, F. K. 1998, *ApJ*, 507, 316
- Marković, D. & Lamb, F. K. 2000, astro-ph/0009169
- Markowitz, A., Edelson, R., Vaughan, S., Uttley, P., et al. 2003, *ApJ*, 593, 96
- Markwardt, C. 2001, *Astrophysics and Space Science Supplement*, 276, 209
- Markwardt, C. B. & Swank, J. H. 2003, *IAU Circ. No.*, 8144
- Markwardt, C. B., Strohmayer, T. E., & Swank, J. H. 1999a, *ApJ*, 512, L125
- Markwardt, C. B., Swank, J. H., & Taam, R. E. 1999b, *ApJ*, 513, L37
- Markwardt, C. B., Swank, J. H., Strohmayer, T. E., in 't Zand, J. J. M., et al. 2002, *ApJ*, 575, L21
- Markwardt, C. B., Smith, E., & Swank, J. H. 2003, *IAU Circ. No.*, 8080, 2
- Marshall, F.E., & Markwardt, C.B. 1999, *IAU Circ. No.*, 7103
- Matsuba, E., Dotani, T., Mitsuda, K., Asai, K., Lewin, W.H.G., et al. 1995, *PASJ*, 47, 575
- Mauche, C. W. 2002, *ApJ*, 580, 423
- McClintock, J. E., Haswell, C. A., Garcia, M. R., Drake, J. J., Hynes, R. I., et al. 2001, *ApJ*, 555, 477
- McDermott, P. N. & Taam, R. E. 1987, *ApJ*, 318, 278
- McDermott, P. N., van Horn, H. M., & Hansen, C. J. 1988, *ApJ*, 325, 725
- McGowan, K. E., Charles, P. A., O'Donoghue, D., & Smale, A. P. 2003, *MNRAS*, 345, 1039
- McHardy, I. M., Papadakis, I. E., Uttley, P., Page, M. J., & Mason, K. O. 2004, *MNRAS*, 348, 783
- McNamara, B. J., Harrison, T. E., Zavala, R. T., Galvan, E., et al. 2003, *AJ*, 125, 1437
- Meekins, J. F., Wood, K. S., Hedler, R. L., Byram, E. T., Yentis, D. J., et al. 1984, *ApJ*, 278, 288
- Méndez M. 1999, in 19th Texas Symp., Paris; astro-ph/9903469

- Méndez M. 2002a, in Jan van Paradijs memorial meeting, ASP Conf. Proc. 308, 289; astro-ph/0207279
- Méndez, M. 2002b, in The Ninth Marcel Grossmann Meeting, 2319; astro-ph/0207278
- Méndez, M. & van der Klis, M. 1997, *ApJ*, 479, 926
- Méndez, M., & van der Klis, M. 1999, *ApJ*, 517, L51
- Méndez, M. & van der Klis, M. 2000, *MNRAS*, 318, 938
- Méndez, M., van der Klis, M., van Paradijs, J., Lewin, W.H.G., Lamb, F.K., et al. 1997, *ApJ*, 485, L37
- Méndez, M., van der Klis, M., van Paradijs, J., Lewin, W.H.G., et al. 1998a, *ApJ*, 494, L65
- Méndez, M., van der Klis, M., Wijnands, R., Ford, E.C., van Paradijs, J., et al. 1998b, *ApJ*, 505, L23
- Méndez, M., van der Klis, M., & van Paradijs, J. 1998c, *ApJ*, 506, L117
- Méndez, M., Belloni, T., & van der Klis, M. 1998d, *ApJ*, 499, L187
- Méndez, M., van der Klis, M., Ford, E.C., Wijnands, R., & van Paradijs, J. 1999, *ApJ*, 511, L49
- Méndez, M., van der Klis, M., & Ford, E. C. 2001, *ApJ*, 561, 1016
- Méndez, M., Cottam, J., & Paerels, F. 2002, astro-ph/0207277
- Menna, M. T., Burderi, L., Stella, L., Robba, N., & van der Klis, M. 2003, *ApJ*, 589, 503
- Merloni, A., Vietri, M., Stella, L., & Bini, D. 1999, *MNRAS*, 304, 155
- Merloni, A., Di Matteo, T., & Fabian, A. C. 2000, *MNRAS*, 318, L15
- Middleditch, J. & Priedhorsky, W. C. 1986, *ApJ*, 306, 230
- Migliari, S., Fender, R. P., Rupen, M., Jonker, P. G., Klein-Wolt, M., et al. 2003a, *MNRAS*, 342, L67
- Migliari, S., van der Klis, M., & Fender, R. P. 2003b, *MNRAS*, 345, L35
- Migliari, S., Fender, R. P., Rupen, M., Wachter, S., Jonker, P. G. et al. 2004, *MNRAS*, 351, 186
- Miller, M. C. 1995, *ApJ*, 441, 770
- Miller, M. C. 1999, *ApJ*, 520, 256
- Miller, M. C. 2000, *ApJ*, 537, 342
- Miller, M. C. 2003, in Rossi and beyond, AIP Conf. Proc. 714, 365; astro-ph/0312449
- Miller, G. S. & Lamb, F. K. 1992, *ApJ*, 388, 541
- Miller, G. S. & Park, M. 1995, *ApJ*, 440, 771
- Miller, M.C., Lamb, F.K., & Psaltis, D. 1998a, *ApJ*, 508, 791
- Miller, M.C., Lamb, F.K., & Cook, G.B. 1998b, *ApJ*, 509, 793
- Miller, J. M., Wijnands, R., Homan, J., Belloni, T., Pooley, D., et al. 2001, *ApJ*, 563, 928
- Miller, J. M., Fabian, A. C., Wijnands, R., Reynolds, C. S., Ehle, M., et al. 2002, *ApJ*, 570, L69
- Milsom, J. A. & Taam, R. E. 1996, *MNRAS*, 283, 919
- Milsom, J. A. & Taam, R. E. 1997, *MNRAS*, 286, 358
- Mineshige, S., Takeuchi, M., & Nishimori, H. 1994a, *ApJ*, 435, L125
- Mineshige, S., Ouchi, N. B., & Nishimori, H. 1994b, *PASJ*, 46, 97
- Mineshige, S., Kusnose, M., & Matsumoto, R. 1995, *ApJ*, 445, L43
- Misra, R. 2000, *ApJ*, 529, L95
- Mitsuda, K. & Dotani, T. 1989, *PASJ*, 41, 557
- Mitsuda, K., Inoue, H., Nakamura, N., & Tanaka, Y. 1989, *PASJ*, 41, 97
- Mitsuda, K., Dotani, T., Yoshida, A., Vaughan, B., & Norris, J. P. 1991, *PASJ*, 43, 113
- Miyamoto, S., 1994, ISAS RN 548
- Miyamoto, S. & Kitamoto, S. 1989, *Nature*, 342, 773
- Miyamoto, S., Kitamoto, S., Mitsuda, K., & Dotani, T. 1988, *Nature*, 336, 450
- Miyamoto, S., Kimura, K., Kitamoto, S., Dotani, T., & Ebisawa, K. 1991, *ApJ*, 383, 784
- Miyamoto, S., Kitamoto, S., Iga, S., Negoro, H., & Terada, K. 1992, *ApJ*, 391, L21
- Miyamoto, S., Iga, S., Kitamoto, S., & Kamado, Y. 1993, *ApJ*, 403, L39
- Miyamoto, S., Kitamoto, S., Iga, S., Hayashida, K., & Terada, K. 1994, *ApJ*, 435, 398
- Miyamoto, S., Kitamoto, S., Hayashida, K., & Egoshi, W. 1995, *ApJ*, 442, L13
- Moon, D. & Eikenberry, S. S. 2001a, *ApJ*, 549, L225
- Moon, D. & Eikenberry, S. S. 2001b, *ApJ*, 552, L135
- Morgan, E. H., Remillard, R. A., & Greiner, J. 1997, *ApJ*, 482, 993
- Morsink, S. M. & Stella, L. 1999, *ApJ*, 513, 827
- Motch, C., Illovaisky, S. A., & Chevalier, C. 1982, *A&A*, 109, L1
- Motch, C., Ricketts, M. J., Page, C. G., Illovaisky, S. A., & Chevalier, C. 1983, *A&A*, 119, 171
- Mukhopadhyay, B., Ray, S., Dey, J., & Dey, M. 2003, *ApJ*, 584, L83
- Muno, M. P., Morgan, E. H., & Remillard, R. A. 1999, *ApJ*, 527, 321
- Muno, M. P., Remillard, R. A., Morgan, E. H., Waltman, E. B., et al. 2001, *ApJ*, 556, 515
- Muno, M. P., Remillard, R. A., & Chakrabarty, D. 2002, *ApJ*, 568, L35
- Muno, M. P., Galloway, D. K., & Chakrabarty, D. 2004, *ApJ*, 608, 930
- Murdin, P., Jauncey, D. L., Lerche, I., Nicolson, G. D., Kaluzienski, L. J., et al. 1980, *A&A*, 87, 292
- Naik, S. & Rao, A. R. 2000, *A&A*, 362, 691
- Naik, S., Agrawal, P. C., Paul, B., et al. 2000, *Journal of Astrophysics and Astronomy*, 21, 29
- Nandi, A., Manickam, S. G., Rao, A. R., & Chakrabarti, S. K. 2001, *MNRAS*, 324, 267
- Narita, T., Grindlay, J. E., Bloser, P. F., & Chou, Y. 2003, *ApJ*, 593, 1007
- Negoro, H., Miyamoto, S., & Kitamoto, S. 1994, *ApJ*, 423, L127
- Negoro, H., Kitamoto, S., Takeuchi, M., & Mineshige, S. 1995, *ApJ*, 452, L49
- Negoro, H., Kitamoto, S., & Mineshige, S. 2001, *ApJ*, 554, 528
- Nespoli, E., Belloni, T., Homan, J., Miller, J. M., Lewin, W. H. G., et al. 2003, *A&A*, 412, 235
- Nobili, L. 2003, *ApJ*, 582, 954
- Nobili, L., Turolla, R., Zampieri, L., & Belloni, T. 2000, *ApJ*, 538, L137
- Nolan, P. L., Gruber, D. E., Matteson, J. L., Peterson, L. E., Rothschild, R. E., et al. 1981, *ApJ*, 246, 494
- Norris, J. P. & Wood, K. S. 1987, *ApJ*, 312, 732

- Norris, J. P., Hertz, P., Wood, K. S., Vaughan, B. A., Michelson, P. F., et al. 1990, *ApJ*, 361, 514
- Nowak, M. A. 1994, *ApJ*, 422, 688
- Nowak, M. A. 1995, *PASP*, 107, 1207
- Nowak, M. A. 2000, *MNRAS*, 318, 361
- Nowak, M. & Lehr, D. 1998, in *Theory of Black Hole Accretion Disks*, Abramowicz et al. (eds.), Cambridge Univ. Press, 233
- Nowak, M. A. & Vaughan, B. A. 1996, *MNRAS*, 280, 227
- Nowak, M. A. & Wagoner, R. V. 1993, *ApJ*, 418, 187
- Nowak, M. A. & Wilms, J. 1999, *ApJ*, 522, 476
- Nowak, M. A., Wagoner, R. V., Begelman, M. C., & Lehr, D. E. 1997, *ApJ*, 477, L91
- Nowak, M. A., Vaughan, B. A., Wilms, J., Dove, J. B., & Begelman, M. C. 1999a, *ApJ*, 510, 874
- Nowak, M. A., Wilms, J., Vaughan, B. A., Dove, J. B., & Begelman, M. C. 1999b, *ApJ*, 515, 726
- Nowak, M. A., Wilms, J., & Dove, J. B. 1999c, *ApJ*, 517, 355
- Nowak, M. A., Wilms, J., Heindl, W. A., Pottschmidt, K., et al. 2001, *MNRAS*, 320, 316
- Nowak, M. A., Wilms, J., & Dove, J. B. 2002, *MNRAS*, 332, 856
- O'Brien, K., Horne, K., Gomer, R. H., Oke, J. B., & van der Klis, M. 2004, *MNRAS*, 350, 587
- Oda, M., Gorenstein, P., Gursky, H., Kellogg, E., Schreier, E., et al. 1971, *ApJ*, 166, L1
- Ogawara, Y., Doi, K., Matsuoka, M., Miyamoto, S., & Oda, M. 1977, *Nature*, 270, 154
- Okuda, T. & Mineshige, S. 1991, *MNRAS*, 249, 684
- Olive, J. F., Barret, D., Boirin, L., Grindlay, J. E., Swank, J. H., & Smale, A. P. 1998, *A&A*, 333, 942
- Olive, J., Barret, D., & Gierliński, M. 2003, *ApJ*, 583, 416
- O'Neill, P. M., Kuulkers, E., Sood, R. K., & Dotani, T. 2001, *A&A*, 370, 479
- O'Neill, P. M., Kuulkers, E., Sood, R. K., & van der Klis, M. 2002, *MNRAS*, 336, 217
- Oosterbroek, T., Penninx, W., van der Klis, M., van Paradijs, J., & et al. 1991, *A&A*, 250, 389
- Oosterbroek, T., Lewin, W. H. G., van Paradijs, J., van der Klis, M., et al. 1994, *A&A*, 281, 803
- Oosterbroek, T., van der Klis, M., Kuulkers, E., van Paradijs, J., et al. 1995, *A&A*, 297, 141
- Oosterbroek, T., van der Klis, M., Vaughan, B., van Paradijs, J., et al. 1996, *A&A*, 309, 781
- Oosterbroek, T., van der Klis, M., van Paradijs, J., Vaughan, B., et al. 1997, *A&A*, 321, 776
- Oosterbroek, T., Barret, D., Guainazzi, M., & Ford, E. C. 2001, *A&A*, 366, 138
- Orlandini, M. & Boldt, E. 1993, *ApJ*, 419, 776
- Orlandini, M. & Morfill, G. E. 1992, *ApJ*, 386, 703
- Ortega-Rodríguez, M. & Wagoner, R. V. 2000, *ApJ*, 537, 922
- Osherovich, V. & Titarchuk, L. 1999, *ApJ*, 522, L113
- Ouyed, R. 2002, *A&A*, 382, 939
- Paczynski, B. 1987, *Nature*, 327, 303
- Park, S. Q., Miller, J. M., McClintock, J. E., Remillard, R. A., et al. 2003, astro-ph/0308363
- Parmar, A. N., Stella, L., & White, N. E. 1986, *ApJ*, 304, 664
- Parmar, A. N., Angelini, L., Roche, P., & White, N. E. 1993, *A&A*, 279, 179
- Parmar, A. N., Oosterbroek, T., Boirin, L., & Lumb, D. 2002, *A&A*, 386, 910
- Patterson, J. 1979, *ApJ*, 234, 978
- Paul, B., Agrawal, P. C., Rao, A. R., Vahia, M. N., Yadav, J. S., et al. 1997, *A&A*, 320, L37
- Payne, D. G. 1980, *ApJ*, 237, 951
- Penninx, W., Lewin, W. H. G., Zijlstra, A. A., Mitsuda, K., et al. 1988, *Nature*, 336, 146
- Penninx, W., Hasinger, G., Lewin, W. H. G., van Paradijs, J., et al. 1989, *MNRAS*, 238, 851
- Penninx, W., Lewin, W. H. G., Mitsuda, K., van der Klis, M., et al. 1990, *MNRAS*, 243, 114
- Penninx, W., Lewin, W. H. G., Tan, J., Mitsuda, K., van der Klis, M., et al. 1991, *MNRAS*, 249, 113
- Pérez, C. A., Silbergleit, A. S., Wagoner, R. V., & Lehr, D. E. 1997, *ApJ*, 476, 589
- Piraino, S., Santangelo, A., & Kaaret, P. 2000, *A&A*, 360, L35
- Piraino, S., Santangelo, A., & Kaaret, P. 2002, *ApJ*, 567, 1091
- Ponman, T. J., Cooke, B. A., & Stella, L. 1988, *MNRAS*, 231, 999
- Popham, R. & Sunyaev, R. 2001, *ApJ*, 547, 355
- Pottschmidt, K., Koenig, M., Wilms, J., & Staubert, R. 1998, *A&A*, 334, 201
- Pottschmidt, K., Wilms, J., Nowak, M. A., Pooley, G. G., Gleissner, T., et al. 2003, *A&A*, 407, 1039
- Poutanen, J. 2002, *MNRAS*, 332, 257
- Poutanen, J. & Fabian, A. C. 1999, *MNRAS*, 306, L31
- Press, W. H. & Schechter, P. 1974, *ApJ*, 193, 437
- Priedhorsky, W., Garmire, G. P., Rothschild, R., Boldt, E., Serlemitsos, P., et al. 1979, *ApJ*, 233, 350
- Priedhorsky, W., Hasinger, G., Lewin, W. H. G., Middleditch, J., Parmar, A., et al. 1986, *ApJ*, 306, L91
- Pringle, J. E. 1981, *ARA&A*, 19, 137
- Prins, S. & van der Klis, M. 1997, *A&A*, 319, 498
- Psaltis, D. 2000, astro-ph/0010316
- Psaltis, D. 2001, *Advances in Space Research*, 28, 481
- Psaltis, D., & Norman, C. 2000, astro-ph/0001391
- Psaltis, D., Méndez, M., Wijnands, R., Homan, J., Jonker, P. G., et al. 1998, *ApJ*, 501, L95
- Psaltis, D., Belloni, T., & van der Klis, M. 1999a, *ApJ*, 520, 262
- Psaltis, D., Wijnands, R., Homan, J., Jonker, P. G., van der Klis, M., et al. 1999b, *ApJ*, 520, 763
- Pudritz, R. E. & Fahlman, G. G. 1982, *MNRAS*, 198, 689
- Qu, J. L., Yu, W., & Li, T. P. 2001, *ApJ*, 555, 7
- Rao, A. R., Naik, S., Vadawale, S. V., & Chakrabarti, S. K. 2000a, *A&A*, 360, L25
- Rao, A. R., Yadav, J. S., & Paul, B. 2000b, *ApJ*, 544, 443
- Rebusco, P. 2004, *PASJ*, 56, 553

- Rebusco, P. 2004, astro-ph/0403341
- Reerink, T., Schnerr, R., van der Klis, M., & van Straaten, S. 2004, *A&A*, submitted
- Reig, P., Méndez, M., van der Klis, M., & Ford, E. C. 2000a, *ApJ*, 530, 916
- Reig, P., Belloni, T., van der Klis, M., Méndez, M., Kylafis, N. D., & Ford, E. C. 2000b, *ApJ*, 541, 883
- Reig, P., Papadakis, I., & Kylafis, N. D. 2002, *A&A*, 383, 202
- Reig, P., Papadakis, I., & Kylafis, N. D. 2003a, *A&A*, 398, 1103
- Reig, P., Belloni, T., & van der Klis, M. 2003b, *A&A*, 412, 229
- Reig, P., Kylafis, N. D., & Giannios, D. 2003c, *A&A*, 403, L15
- Reig, P., van Straaten, S., & van der Klis, M. 2004, *ApJ*, 602, 918
- Reilly, K. T., Bloom, E. D., Focke, W., Giebels, B., Godfrey, G., et al. 2001, *ApJ*, 561, L183
- Remillard, R. A. & Morgan, E. H. 1998, Nuclear Physics B, (Proc. Suppl.), 69, 316
- Remillard, R. A. & Morgan, E. H. 1999, *BAAS*, 31, 1421
- Remillard, R. A., McClintock, J. E., Sobczak, G. J., Bailyn, C. D., et al. 1999a, *ApJ*, 517, L127
- Remillard, R., Morgan, E., Levine, A., Muno, M., McClintock, J., et al. 1999b, *BAAS*, 31, 731
- Remillard, R. A., Morgan, E. H., McClintock, J. E., Bailyn, C. D., & Orosz, J. A. 1999c, *ApJ*, 522, 397
- Remillard, R. A., Muno, M. P., McClintock, J. E., & Orosz, J. A. 2002a, *ApJ*, 580, 1030
- Remillard, R., Muno, M., McClintock, J. E., & Orosz, J. 2002b, in 4th Microquasars Workshop, Cargèse, 2002, Durouchoux et al. (eds.), p. 49; astro-ph/0208402
- Remillard, R. A., Sobczak, G. J., Muno, M. P., & McClintock, J. E. 2002c, *ApJ*, 564, 962
- Remillard, R. A., Muno, M. P., McClintock, J. E., & Orosz, J. A. 2003, abstract AAS/HEAD 7, 30.03
- Revnivtsev, M., Gilfanov, M., Churazov, E., Sunyaev, R., Borozdin, K., et al. 1998a, *A&A*, 331, 557
- Revnivtsev, M., Gilfanov, M., & Churazov, E. 1998b, *A&A*, 339, 483
- Revnivtsev, M., Borozdin, K., & Emelyanov, A. 1999a, *A&A*, 344, L25
- Revnivtsev, M., Gilfanov, M., & Churazov, E. 1999b, *A&A*, 347, L23
- Revnivtsev, M. G., Borozdin, K. N., Priedhorsky, W. C., & Vikhlinin, A. 2000a, *ApJ*, 530, 955
- Revnivtsev, M., Sunyaev, R., & Borozdin, K. 2000b, *A&A*, 361, L37
- Revnivtsev, M. G., Trudolyubov, S. P., & Borozdin, K. N. 2000c, *MNRAS*, 312, 151 see also 315, 655
- Revnivtsev, M., Churazov, E., Gilfanov, M., & Sunyaev, R. 2001a, *A&A*, 372, 138
- Revnivtsev, M., Gilfanov, M., & Churazov, E. 2001b, *A&A*, 380, 520
- Revnivtsev, M., Gilfanov, M., Churazov, E., & Sunyaev, R. 2002, *A&A*, 391, 1013
- Reynolds, C. S. & Nowak, M. A. 2003, *Phys. Rep.*, 377, 389
- Rezzolla, L., Lamb, F. K., & Shapiro, S. L. 2000, *ApJ*, 531, L139
- Rezzolla, L., Yoshida, S., Maccarone, T. J., & Zanotti, O. 2003, *MNRAS*, 344, L37
- Ricci, D., Israel, G. L., & Stella, L. 1995, *A&A*, 299, 731
- Robinson, E. L. & Warner, B. 1972, *MNRAS*, 157, 85
- Rodriguez, J., Durouchoux, P., Mirabel, I. F., Ueda, Y., Tagger, M., et al. 2002a, *A&A*, 386, 271
- Rodriguez, J., Corbel, S., Kalemci, E., & Tomsick, J. A. 2002b, astro-ph/0205341
- Rodriguez, J., Varnière, P., Tagger, M., & Durouchoux, P. 2002c, *A&A*, 387, 487
- Rodriguez, J., Corbel, S., & Tomsick, J. A. 2003, *ApJ*, 595, 1032
- Rossi, S., Homan, J., Miller, J. M., & Belloni, T. 2004, in The restless high-energy universe, Nuclear Phys. B, 132, 416; astro-ph/0309129
- Rothschild, R. E., Boldt, E. A., Holt, S. S., & Serlemitsos, P. J. 1974, *ApJ*, 189, L13
- Rothschild, R. E., Boldt, E. A., Holt, S. S., & Serlemitsos, P. J. 1977, *ApJ*, 213, 818
- Rutledge, R. E., Lubin, L. M., Lewin, W. H. G., Vaughan, B., et al. 1995, *MNRAS*, 277, 523
- Rutledge, R. E., Lewin, W. H. G., van der Klis, M., van Paradijs, J., et al. 1999, *ApJS*, 124, 265
- Samimi, J., Share, G. H., Wood, K., Yentis, D., Meekins, J., et al. 1979, *Nature*, 278, 434
- Santolamazza, P., Fiore, F., Burderi, L., & Di Salvo, T. 2003, astro-ph/0311382
- Scargle, J. D., Steiman-Cameron, T., Young, K., Donoho, D. L., et al. 1993, *ApJ*, 411, L91
- Schaab, C., & Weigel, M. K. 1999, *MNRAS*, 308, 718
- Schmidtko, P. C., Ponder, A. L., & Cowley, A. P. 1999, *AJ*, 117, 1292
- Schnerr, R. S., Reerink, T., van der Klis, M., Homan, J., Méndez, M., et al. 2003, *A&A*, 406, 221
- Schnerr, R. S., Reerink, T., van der Klis, M., Homan, J., Méndez, M., et al. 2003, astro-ph/0305161
- Schnittman, J. D. & Bertschinger, E. 2004, *ApJ*, 606, 1098
- Schulz, N. S. & Wijers, R. A. M. J. 1993, *A&A*, 273, 123
- Schulz, N. S., Hasinger, G., & Truemper, J. 1989, *A&A*, 225, 48
- Sellmeijer, H. & van der Klis, M. 1999, unpublished
- Shakura, N. I. & Sunyaev, R. A. 1973, *A&A*, 24, 337
- Shakura, N. I. & Sunyaev, R. A. 1976, *MNRAS*, 175, 613
- Shibata, M. & Sasaki, M. 1998, *Phys. Rev. D*, 58, 104011
- Shibazaki, N. & Ebisuzaki, T. 1989, *PASJ*, 41, 641
- Shibazaki, N. & Lamb, F. K. 1987, *ApJ*, 318, 767
- Shibazaki, N., Elsner, R. F., & Weisskopf, M. C. 1987, *ApJ*, 322, 831
- Shibazaki, N., Elsner, R. F., Bussard, R. W., Ebisuzaki, T., & Weisskopf, M. C. 1988, *ApJ*, 331, 247
- Shirakawa, A. & Lai, D. 2002a, *ApJ*, 564, 361
- Shirakawa, A. & Lai, D. 2002b, *ApJ*, 565, 1134
- Shirey, R. E., Bradt, H. V., Levine, A. M., & Morgan, E. H. 1996, *ApJ*, 469, L21
- Shirey, R. E., Bradt, H. V., Levine, A. M., & Morgan, E. H. 1998, *ApJ*, 506, 374
- Shirey, R. E., Bradt, H. V., & Levine, A. M. 1999, *ApJ*, 517, 472
- Shvartsman, V. F. 1971, Soviet Astronomy, 15, 377
- Sibgatullin, N. R. 2002, *Astronomy Letters*, 28, 83
- Silbergleit, A. S., Wagoner, R. V., & Ortega-Rodríguez, M. 2001, *ApJ*, 548, 335

- Singh, K. P. & Apparao, K. M. V. 1994, *ApJ*, 431, 826
- Smale, A. P. 1998, *ApJ*, 498, L141
- Smale, A. P. & Kuulkers, E. 2000, *ApJ*, 528, 702
- Smale, A.P., Zhang, W., & White, N.E. 1997, *ApJ*, 483, L119
- Smale, A. P., Homan, J., & Kuulkers, E. 2003, *ApJ*, 590, 1035
- Smith, I. A. & Liang, E. P. 1999, *ApJ*, 519, 771
- Smith, D. M., Heindl, W. A., Swank, J., Leventhal, M., Mirabel, I. F., et al. 1997, *ApJ*, 489, L51
- Smith, D. M., Heindl, W. A., Markwardt, C. B., & Swank, J. H. 2001, *ApJ*, 554, L41
- Smith, D. M., Heindl, W. A., & Swank, J. H. 2002, *ApJ*, 569, 362
- Sobczak, G. J., McClintock, J. E., Remillard, R. A., Bailyn, C. D., & Orosz, J. A. 1999, *ApJ*, 520, 776
- Sobczak, G. J., McClintock, J. E., Remillard, R. A., Cui, W., Levine, A. M., et al. 2000a, *ApJ*, 531, 537
- Sobczak, G. J., McClintock, J. E., Remillard, R. A., Cui, W., Levine, A. M., et al. 2000b, *ApJ*, 544, 993
- Spruit, H. C. & Kanbach, G. 2002, *A&A*, 391, 225
- Spruit, H. C. & Taam, R. E. 1990, *A&A*, 229, 475
- Srinivasan, G. 2002, *A&A Rev.*, 11, 67
- Steiman-Cameron, T. Y., Scargle, J. D., Imamura, J. N., & Middleditch, J. 1997, *ApJ*, 487, 396
- Stella, L. 1988, Memorie della Societa Astronomica Italiana, 59, 185
- Stella, L. & Vietri, M. 1998, *ApJ*, 492, L59
- Stella, L. & Vietri, M. 1999, Physical Review Letters, 82, 17
- Stella, L., White, N. E., Davelaar, J., Parmar, A. N., Blissett, R. J., et al. 1985, *ApJ*, 288, L45
- Stella, L., Parmar, A. N., & White, N. E. 1987a, *ApJ*, 321, 418
- Stella, L., White, N.E., & Priedhorsky, W., 1987b, *ApJ*, 315, L49
- Stella, L., Haberl, F., Lewin, W. H. G., Parmar, A. N., van der Klis, M., et al. 1988a, *ApJ*, 327, L13
- Stella, L., Haberl, F., Lewin, W. H. G., Parmar, A. N., van Paradijs, J., et al. 1988b, *ApJ*, 324, 379
- Stella, L., Vietri, M., & Morsink, S. M. 1999, *ApJ*, 524, L63
- Stergioulas, N., Klužniak, W., & Bulik, T. 1999, *A&A*, 352, L116
- Stoeger, W. R. 1980, *MNRAS*, 190, 715
- Stollman, G. M., van Paradijs, J., Hasinger, G., Lewin, W. H. G., et al. 1987, *MNRAS*, 227, 7P
- Strohmayer, T. E. 2001a, *ApJ*, 552, L49
- Strohmayer, T. E. 2001b, *ApJ*, 554, L169
- Strohmayer, T. E. & Lee, U. 1996, *ApJ*, 467, 773
- Strohmayer, T.E., Zhang, W., Swank, J.H., Smale, A., Titarchuk, L., & Day, C. 1996, *ApJ*, 469, L9
- Strohmayer, T.E., Jahoda, K., Giles, A.B., & Lee, U. 1997, *ApJ*, 486, 355
- Strohmayer, T. E., Markwardt, C. B., Swank, J. H., & in't Zand, J. 2003, *ApJ*, 596, L67
- Strohmayer, T. E. & Mushotzky, R. F. 2003, *ApJ*, 586, L61
- Sunyaev, R. A. 1973, Soviet Astronomy, 16, 941
- Sunyaev, R. & Revnivtsev, M. 2000, *A&A*, 358, 617
- Sutherland, P. G., Weisskopf, M. C., & Kahn, S. M. 1978, *ApJ*, 219, 1029
- Swank, J., Chen, X., Markwardt, C., & Taam, R. 1998, in Some like it hot, AIP Conf. Proc. 431, 327
- Taam, R. E. & Lin, D. N. C. 1984, *ApJ*, 287, 761
- Takeshima, T. 1992, PhD thesis, Univ. of Tokyo
- Takeshima, T., Dotani, T., Mitsuda, K., & Nagase, F. 1991, *PASJ*, 43, L43
- Takeuchi, M., Mineshige, S., & Negoro, H. 1995, *PASJ*, 47, 617
- Takizawa, M., Dotani, T., Mitsuda, K., Matsuba, E., Ogawa, M., Aoki, T., et al. 1997, *ApJ*, 489, 272
- Tan, J., Lewin, W. H. G., Lubin, L. M., van Paradijs, J., Penninx, W., et al. 1991, *MNRAS*, 251, 1
- Tan, J., Lewin, W. H. G., Hjellming, R. M., Penninx, W., van Paradijs, J., et al. 1992, *ApJ*, 385, 314
- Tanaka, Y. & Tenma team, 1983, IAU Circ. 3891
- Tanaka, Y. 1989, in 23d ESLAB Symp., White et al. (eds.), p. 3
- Tananbaum, H., Gursky, H., Kellogg, E., Giacconi, R., & Jones, C. 1972, *ApJ*, 177, L5
- Tawara, Y., Hayakawa, S., Hunieda, H., Makino, F., & Nagase, F. 1982, *Nature*, 299, 38
- Taylor, J. H., Wolszczan, A., Damour, T., & Weisberg, J. M. 1992, *Nature*, 355, 132
- Tennant, A. F. 1987, *MNRAS*, 226, 971
- Tennant, A. F. 1988, *MNRAS*, 230, 403
- Tennant, A. F., Fabian, A. C., & Shafer, R. A. 1986, *MNRAS*, 219, 871
- Terada, K., Kitamoto, S., Negoro, H., & Iga, S. 2002, *PASJ*, 54, 609
- Terrell, N. J. J. 1972, *ApJ*, 174, L35
- Thampan, A.V., Bhattacharya, D., & Datta, B. 1999, *MNRAS*, 302, L69
- Thorne, K. S. & Price, R. H. 1975, *ApJ*, 195, L101
- Timmer, J., Schwarz, U., Voss, H. U., Wardinski, I., Belloni, T., et al. 2000, Phys. Rev. E, 61, 1342
- Titarchuk, L. 2002, *ApJ*, 578, L71
- Titarchuk, L. 2003, *ApJ*, 591, 354
- Titarchuk, L. & Osherovich, V. 1999, *ApJ*, 518, L95
- Titarchuk, L. & Osherovich, V. 2000, *ApJ*, 542, L111
- Titarchuk, L. & Shrader, C. R. 2002, *ApJ*, 567, 1057
- Titarchuk, L. & Wood, K. 2002, *ApJ*, 577, L23
- Titarchuk, L., Lapidus, I., & Muslimov, A. 1998, *ApJ*, 499, 315
- Titarchuk, L., Osherovich, V., & Kuznetsov, S. 1999, *ApJ*, 525, L129
- Tomsick, J. A. & Kaaret, P. 2000, *ApJ*, 537, 448
- Tomsick, J. A. & Kaaret, P. 2001, *ApJ*, 548, 401
- Tomsick, J.A., Halpern, J.P., Kemp, J., & Kaaret, P. 1999, *ApJ*, 521, 341
- Tomsick, J. A., Kalemci, E., & Kaaret, P. 2004, *ApJ*, 601, 439

- Treves, A., Belloni, T., Corbet, R. H. D., Ebisawa, K., Falomo, R., et al. 1990, *ApJ*, 364, 266
- Trudolyubov, S. P. 2001, *ApJ*, 558, 276
- Trudolyubov, S. P., Churazov, E. M., & Gilfanov, M. R. 1999a, *Astronomy Letters*, 25, 718
- Trudolyubov, S., Churazov, E., & Gilfanov, M. 1999b, *A&A*, 351, L15
- Trudolyubov, S. P., Borozdin, K. N., & Priedhorsky, W. C. 2001, *MNRAS*, 322, 309
- Ubertini, P., Bazzano, A., Cocchi, M., Natalucci, L., Heise, J., et al. 1999, *ApJ*, 514, L27
- Uemura, M., Kato, T., Ishioka, R., Tanabe, K., Kiyota, S., Monard, B., et al. 2002, *PASJ*, 54, L79
- Uemura, M., Kato, T., Ishioka, R., Tanabe, K., Torii, K., Santallo, R., et al. 2004, *PASJ*, 56, 61
- Unno, W., Yoneyama, T., Urata, K., Masaki, I., Kondo, M., & Inoue, H. 1990, *PASJ*, 42, 269
- Ushomirsky, G., Cutler, C., & Bildsten, L. 2000, *MNRAS*, 319, 902
- Uttley, P. 2004, *MNRAS*, 347, L61
- Uttley, P. & McHardy, I. M. 2001, *MNRAS*, 323, L26
- Uttley, P., McHardy, I. M., & Papadakis, I. E. 2002, *MNRAS*, 332, 231
- van der Hooft, F., et al. 1996, *ApJ*, 458, L75
- van der Hooft, F., et al. 1999a, *ApJ*, 513, 477
- van der Hooft, F., et al. 1999b, *ApJ*, 519, 332
- van der Klis, M. 1986, in *The physics of accretion onto compact objects*, Lect. Notes Phys. 266, 157
- van der Klis, M. 1989a, *ARA&A*, 27, 517
- van der Klis, M. 1989b, in *Timing Neutron Stars*, NATO ASI C262, p. 27
- van der Klis, M. 1994a, *ApJS*, 92, 511
- van der Klis, M. 1994b, *A&A*, 283, 469
- van der Klis, M. 1995a, in *X-ray binaries*, Lewin et al. (eds.), Cambridge Univ. Press, p. 252
- van der Klis, M. 1995b, in *The lives of the neutron stars*, NATO ASI C450, p. 301
- van der Klis, M. 1997, in *Astronomical Time Series*, ASSL 218, 121
- van der Klis, M. 1998, in *The Many Faces of Neutron Stars*, NATO ASI C Proc. 515, p. 337
- van der Klis, M. 1999, in *Stellar endpoints*, AIP Conf. Proc. 599, 406
- van der Klis, M. 2000, *ARA&A*, 38, 717
- van der Klis, M. 2001, *ApJ*, 561, 943
- van der Klis, M. 2002, in *XEUS - studying the evolution of the hot universe*, MPE rep. 281, 354
- van der Klis, M. & Jansen, F. A. 1985, *Nature*, 313, 768
- van der Klis, M., Jansen, F., van Paradijs, J., Lewin, W. H. G., et al. 1985, *Nature*, 316, 225
- van der Klis, M., Jansen, F., van Paradijs, J., Lewin, W. H. G., Sztajno, M., et al. 1987a, *ApJ*, 313, L19
- van der Klis, M., Stella, L., White, N., Jansen, F., & Parmar, A. N. 1987b, *ApJ*, 316, 411
- van der Klis, M., Hasinger, G., Stella, L., Langmeier, A., et al. 1987c, *ApJ*, 319, L13
- van der Klis, M., Hasinger, G., Damen, E., Penninx, W., et al. 1990, *ApJ*, 360, L19
- van der Klis, M., Kitamoto, S., Tsunemi, H., & Miyamoto, S. 1991, *MNRAS*, 248, 751
- van der Klis, M., Swank, J.H., Zhang, W., Jahoda, K., Morgan, E.H., et al. 1996, *ApJ*, 469, L1
- van der Klis, M., Wijnands, R.A.D., Horne, K., & Chen, W. 1997, *ApJ*, 481, L97
- van der Klis, M., Chakrabarty, D., Lee, J. C., Morgan, E. H., et al. 2000, *IAU Circ. No.*, 7358, 3
- van Paradijs, J., Hasinger, G., Lewin, W. H. G., et al. 1988a, *MNRAS*, 231, 379
- van Paradijs, J., Penninx, W., Lewin, W. H. G., Sztajno, M., & Truemper, J. 1988b, *A&A*, 192, 147
- van Straaten, S., Ford, E. C., van der Klis, M., Méndez, M., & Kaaret, P. 2000, *ApJ*, 540, 1049
- van Straaten, S., van der Klis, M., Kuulkers, E., & Méndez, M. 2001, *ApJ*, 551, 907
- van Straaten, S., van der Klis, M., Di Salvo, T., & Belloni, T. 2002, *ApJ*, 568, 912
- van Straaten, S., van der Klis, M., & Méndez, M. 2003, *ApJ*, 596, 1155
- van Straaten, S., van der Klis, M., & Wijnands, R. 2004, *ApJ* in press
- Varnière, P., Rodriguez, J., & Tagger, M. 2002, *A&A*, 387, 497
- Vasiliev, L., Trudolyubov, S., & Revnivtsev, M. 2000, *A&A*, 362, L53
- Vaughan, B. A. & Nowak, M. A. 1997, *ApJ*, 474, L43
- Vaughan, B., van der Klis, M., Lewin, W. H. G., Wijers, R. A. M. J., et al. 1994, *ApJ*, 421, 738
- Vaughan, B.A., van der Klis, M., Méndez, M., van Paradijs, J., et al. 1997, *ApJ*, 483, L115
- Vaughan, B.A., van der Klis, M., Méndez, M., van Paradijs, J., et al. 1998, *ApJ*, 509, L145
- Vaughan, B. A., van der Klis, M., Lewin, W. H. G., van Paradijs, J., et al. 1999, *A&A*, 343, 197
- Vietri, M. & Stella, L. 1998, *ApJ*, 503, 350
- Vignarca, F., Migliari, S., Belloni, T., Psaltis, D., & van der Klis, M. 2003, *A&A*, 397, 729
- Vikhlinin, A. 1999, *ApJ*, 521, L45
- Vikhlinin, A., Churazov, E., & Gilfanov, M. 1994, *A&A*, 287, 73
- Vikhlinin, A., Churazov, E., Gilfanov, M., Sunyaev, R., et al. 1995, *ApJ*, 441, 779
- Vrtilek, S. D., Raymond, J. C., Garcia, M. R., Verbunt, F., Hasinger, G., et al. 1990, *A&A*, 235, 162
- Vrtilek, S. D., Penninx, W., Raymond, J. C., Verbunt, F., Hertz, P., et al. 1991, *ApJ*, 376, 278
- Vrtilek, S. D., Raymond, J. C., Boroson, B., McCray, R., Smale, A., et al. 2003, *PASP*, 115, 1124
- Wagoner, R. W. 1999, *Phys. Rep.*, 311, 259
- Wagoner, R. V. 2002, *ApJ*, 578, L63
- Wallinder, F. H. 1995, *MNRAS*, 273, 1133
- Wang, Y.-M. & Schlickeiser, R. 1987, *ApJ*, 313, 200
- Wang, D., Ma, R., Lei, W., & Yao, G. 2003, *MNRAS*, 344, 473
- Warner, B. & Woudt, P. A. 2002, *MNRAS*, 335, 84
- Watarai, K. & Mineshige, S. 2003a, *PASJ*, 55, 959
- Watarai, K. & Mineshige, S. 2003b, *ApJ*, 596, 421
- Weinberg, N., Miller, M. C., & Lamb, D. Q. 2001, *ApJ*, 546, 1098
- Weisskopf, M. C. & Sutherland, P. G. 1978, *ApJ*, 221, 228

- Weisskopf, M. C., Kahn, S. M., & Sutherland, P. G. 1975, *ApJ*, 199, L147
 Wen, L., Cui, W., & Bradt, H. V. 2001, *ApJ*, 546, L105
 Wheeler, J. C. 1977, *ApJ*, 214, 560
 White, N. E. & Marshall, F. E. 1984, *ApJ*, 281, 354
 White, N.E., & Zhang, W. 1997, *ApJ*, 490, L87
 White, N. E., Peacock, A., & Taylor, B. G. 1985, *ApJ*, 296, 475
 Wijers, R. A. M. J., van Paradijs, J., & Lewin, W. H. G. 1987, *MNRAS*, 228, 17P
 Wijnands, R. 2004, in Rossi and beyond, AIP Conf. Proc. 714, 97; astro-ph/0403409
 Wijnands, R. & Homan, J. 2003, ATel, 165, 1
 Wijnands, R. & Miller, J. M. 2002, *ApJ*, 564, 974
 Wijnands, R.A.D., & van der Klis, M. 1997, *ApJ*, 482, L65
 Wijnands, R. & van der Klis, M. 1998a, *ApJ*, 507, L63
 Wijnands, R. & van der Klis, M. 1998b, *Nature*, 394, 344
 Wijnands, R. & van der Klis, M. 1999a, *ApJ*, 514, 939
 Wijnands, R. & van der Klis, M. 1999b, *A&A*, 345, L35
 Wijnands, R. & van der Klis, M. 1999c, *ApJ*, 522, 965
 Wijnands, R. & van der Klis, M. 2000, *ApJ*, 528, L93
 Wijnands, R. & van der Klis, M. 2001, *MNRAS*, 321, 537
 Wijnands, R. A. D., van der Klis, M., Psaltis, D., Lamb, F. K., Kuulkers, E., et al. 1996, *ApJ*, 469, L5
 Wijnands, R.A.D., van der Klis, M., van Paradijs, J., Lewin, W.H.G., et al. 1997a, *ApJ*, 479, L141
 Wijnands, R., Homan, J., van der Klis, M., Méndez, M., Kuulkers, E., et al. 1997b, *ApJ*, 490, L157
 Wijnands, R. A. D., van der Klis, M., Kuulkers, E., Asai, K., & Hasinger, G. 1997c, *A&A*, 323, 399
 Wijnands, R., Homan, J., van der Klis, M., Kuulkers, E., van Paradijs, J., et al. 1998a, *ApJ*, 493, L87
 Wijnands, R.A.D., van der Klis, M., Méndez, M., van Paradijs, J., et al. 1998b, *ApJ*, 495, L39
 Wijnands, R., Méndez, M., van der Klis, M., Psaltis, D., Kuulkers, E., et al. 1998c, *ApJ*, 504, 35
 Wijnands, R., van der Klis, M., & Rijkhorst, E. 1999a, *ApJ*, 512, L39
 Wijnands, R., Homan, J., & van der Klis, M. 1999b, *ApJ*, 526, L33
 Wijnands, R., Méndez, M., Miller, J. M., & Homan, J. 2001a, *MNRAS*, 328, 451
 Wijnands, R., Strohmayer, T., & Franco, L. M. 2001b, *ApJ*, 549, L71
 Wijnands, R., Miller, J. M., & van der Klis, M. 2002a, *MNRAS*, 331, 60
 Wijnands, R., Munro, M. P., Miller, J. M., Franco, L. M., Strohmayer, T., et al. 2002b, *ApJ*, 566, 1060
 Wijnands, R., van der Klis, M., Homan, J., Chakrabarty, D., et al. 2003, *Nature*, 424, 44
 Wilms, J., Nowak, M. A., Pottschmidt, K., Heindl, W. A., et al. 2001, *MNRAS*, 320, 327
 Wood, K. S., Ray, P. S., Bandyopadhyay, R. M., Wolff, M. T., et al. 2000, *ApJ*, 544, L45
 Woods, P. M., Kouveliotou, C., Finger, M. H., Gogus, E., Swank, J., et al. 2002, *IAU Circ. No.*, 7856, 1
 Xiong, Y., Witte, P. J., & Bao, G. 2000, *PASJ*, 52, 1097
 Yamaoka, K., Ueda, Y., Inoue, H., Nagase, F., Ebisawa, K., et al. 2001, *PASJ*, 53, 179
 Yoshida, S. & Lee, U. 2001, *ApJ*, 546, 1121
 Yoshida, K., Mitsuda, K., Ebisawa, K., Ueda, Y., Fujimoto, R., et al. 1993, *PASJ*, 45, 605
 Yu, W. & van der Klis, M. 2002, *ApJ*, 567, L67
 Yu, W., Zhang, S.N., Harmon, B.A., Paciesas, W.S., Robinson, C.R., et al. 1997, *ApJ*, 490, L153
 Yu, W., Li, T.P., Zhang, W., & Zhang, S.N. 1999, *ApJ*, 512, L35
 Yu, W., van der Klis, M., & Jonker, P. G. 2001, *ApJ*, 559, L29
 Yu, W., Klein-Wolt, M., Fender, R., & van der Klis, M. 2003, *ApJ*, 589, L33
 Zdziunik, J. L., Haensel, P., Gondek-Rosińska, D., & Gourgoulhon, E. 2000, *A&A*, 356, 612
 Zdziarski, A. A., Poutanen, J., Paciesas, W. S., & Wen, L. 2002, *ApJ*, 578, 357
 Zhang, W., Lapidus, I., White, N.E., & Titarchuk, L. 1996a, *ApJ*, 469, L17
 Zhang, W., Lapidus, I., White, N.E., & Titarchuk, L. 1996b, *ApJ*, 473, L135
 Zhang, W., Morgan, E. H., Jahoda, K., Swank, J. H., Strohmayer, T. E., et al. 1996c, *ApJ*, 469, L29
 Zhang, S. N., Cui, W., Harmon, B. A., Paciesas, W. S., Remillard, R. E., et al. 1997a, *ApJ*, 477, L95
 Zhang, W., Strohmayer, T.E., & Swank, J.H. 1997b, *ApJ*, 482, L167
 Zhang, S. N., Ebisawa, K., Sunyaev, R., Ueda, Y., Harmon, B. A., et al. 1997c, *ApJ*, 479, 381
 Zhang, W., Strohmayer, T.E., & Swank, J.H. 1998a, *ApJ*, 500, L167
 Zhang, W., Smale, A.P., Strohmayer, T.E., & Swank, J.H. 1998b, *ApJ*, 500, L171
 Zhang, W., Jahoda, K., Kelley, R.L., Strohmayer, T.E., Swank, J.H., & Zhang, S.N. 1998c, *ApJ*, 495, L9
 Źycki, P. T. 2002, *MNRAS*, 333, 800
 Źycki, P. T. 2003, *MNRAS*, 340, 639
 Źycki, P. T., Done, C., & Smith, D. A. 1999a, *MNRAS*, 305, 231
 Źycki, P. T., Done, C., & Smith, D. A. 1999b, *MNRAS*, 309, 561